# Structure and Function of the Mammalian Circadian Clock

Shannon Noël Nangle

A dissertation
submitted in partial fulfillment of the
requirements for the degree of

Doctor of Philosophy

University of Washington

2015

Reading Committee:

Ning Zheng, Chair

Joseph Beavo

Edith Wang

Program Authorized to Offer Degree:
Pharmacology

University of Washington

**Abstract**

Structure and Function of the Mammalian Circadian Clock

Shannon Noël Nangle

Chair of the Supervisory Committee:
Professor Ning Zheng
Pharmacology

Circadian clocks are essential in all kingdoms of life to maintain appropriate synchronization with their environment. Robust, 24-hr rhythms in eukaryotes are generated by a transcription-translation negative feedback loop. Proper oscillation of the mammalian clock depends on the complex formation and periodic turnover of the Period (PER) and Cryptochrome (CRY) proteins, which together inhibit their own transcriptional activator complex, CLOCK-BMAL1. While these four proteins form the core of the clock, post-translational modifications are essential for generating the oscillations. Phosphorylation and ubiquitination are necessary for localization, complex formation, and degradation of each component. Ubiquitin ligase FBXL3 is required for the nuclear degradation of CRY and competes with both PER and a novel clock-modulating compound KL001 for CRY binding. We present the mechanism of action of this small molecule showing that it occupies the same pocket as FBXL3 thereby stabilizing CRY and lengthening the circadian period. We also report structural and functional evidence for the diverse roles of PERs with respect to CRYs. Briefly, the PER CRY-binding domain adopts a highly-extended conformation, embracing CRY2 with a sinuous binding mode. Unexpectedly, a strictly-conserved intermolecular zinc finger, whose integrity is important for rhythmicity, stabilizes PER-CRY. This work has provided the foundation to explore the assemblies of the core clock machinery. Preliminary progress has been made in establishing the CRY-CLOCK-BMAL1 repression complex.

# TABLE OF CONTENTS

# LIST OF FIGURES

# LIST OF TABLES

# GLOSSARY

CRY: Cryptochrome. Two paralogs CRY1–2. Core clock transcriptional repressor.

PER: Period. Three paralogs PER1–3. Core clock transcriptional repressor.

CLOCK: Circadian Locomotor Output Cycles Kaput. Core clock transcription factor.

BMAL1: Brain and Muscle Arnt-like protein-1. Core clock transcription factor.

PL: Photolyase. Light-sensitive DNA repair enzyme.

PHR: Photolyase Homology Domain. Core globular region of CRYs which contain the $\alpha/\beta$-domain and the $\alpha$-helical domain.

CBD: CRY-binding domain. Necessary and sufficient CRY binding region on PERs.

FAD: Flavin adenine diphosphate. Primary chromophore found in all PLs and Type I CRYs.

FBXL3: F-box and leucine-rich repeat protein 3. The E3 substrate receptor for mammalian CRYs.

KL001: Clock-modulating small molecule that binds to the FAD-binding pocket to stabilize CRY and dose-dependently lengthen the circadian period.

CT: Circadian time. Standard of time based on free-running period (under constant light or dark conditions) of an organism. The onset of activity in diurnal organisms is CT 0 and the onset of nocturnal organism activity is CT 12.

ZT: Zeitgeber time. Standard of time based on the period of a zeitgeber (entrainment signal). In standard light-dark cycles, for diurnal organisms lights on is ZT 0 for diurnal organisms and and lights off is ZT 12 for nocturnal organisms.

$F_O$-$F_C$: The Fourier difference map. The difference between the observed structure factors and calculated structure factors from the current model. Used to demonstrate the quality of the positive electron density maps before refinement.

# ACKNOWLEDGMENTS

I wish to express sincere appreciation to my advisor Ning Zheng, without whom none of this would be possible. I am eternally grateful for being a part of his lab as well as his patience in teaching me structure biology, a field I was essentially oblivious to before grad school. His enthusiasm for and fascination with science is something that I will take with me in all my future endeavors, like Frodo and the Star of Elendil. I will greatly miss our marathon discussions about chaos theory, transhumanism, philosophy, and pretty much any other topic I was curious about. I have difficulty imagining a more supportive mentor. I would also like to thank Joe Beavo for his encouragement and guidance throughout my graduate schooling. Ron Stenkamp for showing me the beauty of reciprocal space (twice) and the exceedingly helpful visualizations of space group symmetry relationships with plastic severed baby arms. My very excellent, but too brief of a bay-neighbor Vivian Tran, whose pipets I will always defend to the death and rainbows I will always treasure. She was replaced by the also excellent Heng Li, whose 5 M NaCl has saved my buffers on myriad evenings. The venerable Tom 'One-Eye' Hinds for all his help with SEC-MALS, the Octet, and AlphaScreen. I will miss our discussions about space, spacecraft engine design, and old movies. I also want to express gratitude to Peter Hsu for his insight and data while he was helping me with the CLOCK-BMAL1 project as well as his general moral and experimental support. Nitzan Shabek for always being available for all sorts of troubleshooting advice, exceptional flask-cleaning skills, and occasional Hebrew help, תודה רבה. Ken Garbutt for fixing everything I broke and unparalleled competent cell production. Xiaobo Tang for answering all my inane general lab questions and her seamless transition into a fantastic lab manager. And of course the rest of the Zheng lab. Thank you to the Pharmacology

Department and all its administrative staff, especially Diane Schulstad.

My everlasting gratitude to all my dear friends. Brian Zoltowski for consenting to the mind meld, competitively reading *Infinite Jest* with me, and commenting on early drafts of this dissertation, which despite the obstacles, reached a broad consensus about the text's central theme and, to a lesser degree, its point. Teresa Swanson for her unconditional love as well as reminding, and occasionally forcing, me to eat and sleep (Soylent and barbiturates though an oral gavage when necessary). Chris Kleinknecht for his decade-long patronage, love, and therapeutic pictures of Kitty. Scott B. Weingart for letting me see through his eyes and being the crystal goblet and—somehow—the wine. Jon 'NR' Bauman for masterful TEX(t) support, high quality inter-writing interval foot massages, and unprecedented emotional stanchioning. And Deniz Top for being the Luke to my Han, the Riker to my Picard, the Simon to my River, and his valiant, but futile, effort to dissuade me from doing a postdoc.

Finally, to my Dad, who made me the person I am today (cf. Tom Lehrer's *Lobachevsky*).

# DEDICATION

To exploring strange new worlds. To seeking out new life and new civilizations. To tackling the ineluctable itself to see whether it can be elucted after all. To boldly going where no one has gone before. Oh yeah, and to my Dad.

# Chapter 1

# INTRODUCTION

## *1.1 Co-evolution of UV/Blue-Light Photoreception and Circadian Clocks*

The daily rotation of the Earth, and consequent light and dark cycles, has instilled unrelenting rhythms into life. Organisms in all kingdoms have adapted mechanisms to coordinate their molecular, physiological, and behavioral processes around this enduring cycle; this internal clockwork is almost as ancient as life itself. Billions of years ago, before the Earth had a protective ozone, intense UV radiation (100–400 nm) bombarded its surface. Emerging lifeforms were subject to extreme selective pressure to repair and protect their genomes in response to light (Cockell and Raven, 2007). Because the land temperature of late-Hadean Earth was incompatible with life, early archaeans and prokaryotes could only survive under the protective filter of water. Even so, they were forced to evolve mechanisms to not only sense light, but to use it as a catalyst for UV-induced DNA damage repair. Since the only region of visible spectrum that can penetrate to significant depths of water (200 m) is in the blue range (450–495 nm), it is the wavelength of choice for detecting sunlight and coincident UV radiation. In addition to repair, these early cells could also protect their DNA by coordinating especially sensitive and vital processes, such as replication, during the night and moving towards to light during the day for energy harvesting and genome maintenance (Gehring and Rosbash, 2003; Cushing, 1951; Klugh, 1930). These rudimentary behaviors formed the basis for the first and most basic form of a circadian rhythm. It is therefore not coincidental that blue-light detection evolved with early aquatic life and was readily coupled with circadian clock pathways (Gehring and Rosbash, 2003).

### *1.1.1 Photolyase Evolution and Function*

Two particularly deleterious types of DNA damage directly caused by UV radiation are the cyclobutane pyrimidine dimers (CBD) and (6-4) photoproducts. These lesions result from a UV-catalyzed covalent linkage between two adjacent pyrimidine bases, prohibit polymerase processivity, and ultimately replication (Sancar, 2008). One of the earliest innovations that is still extant today is a family of UV- and blue light-activated (300–500 nm) DNA damage repair photoreceptor enzymes that transduce light energy, via electron transfer, into cleavage of the DNA photoproduct (Sancar, 1994). These proteins, photolyases, together with cryptchromes, constitute a large but surprisingly well-conserved family of flavoproteins and have an extensive and complex evolutionary past (Sancar, 2003).

Photoreactivation, the recovery from DNA damage caused by UV-C (180–290 nm) and/or UV-B radiation (290–320 nm) with concurrent or subsequent administration of longer wavelength light (e.g., blue), was discovered in the 1940s when lethal doses of UV radiation on bacteria could be abrogated when the culture was also exposed to visible light (Kelner, 1949). Later work by Rupert and colleagues, determined that after irradiating DNA from a strain lacking an endogenous photoreactivation mechanism (*H. influenzae*) then mixing it with one that did (*E. coli*), the overall survival rate of *H. influenzae* was increased in a light-dependent manner (Rupert et al., 1958). These observations led to the hypothesis that *E. coli* possessed a light-sensitive DNA damage repair pathway that *H. influenzae* did not, and eventually to the discovery of photolyases.

Photolyases, the more ancient of the two subfamilies, are present in all domains of life. A gene duplication of a common ancestor led to the first specialization of UV/blue light-dependent DNA damage repair proteins: the CBD and (6-4) photolyases (Sancar, 2008). As flavoproteins, all known photolyases contain FAD as the primary catalytic cofactor. While not essential for enzymatic activity, they also bind a second, or antenna, cofactor that compensates for the low light absorption capacity of FAD and enhances repair activity (Jorns et al., 1984; Johnson et al., 1988; Eker et al., 1988). The antenna cofactor is generally

a folate (methenyltetrahydrofolate, MTHF) but in other cases can be a flavin derivative (e.g., 5-deazaflavin, 8-hydroxy-5-deazariboflavin, flavin mononucleotide, or FAD itself (Ueda et al., 2005; Fujihashi et al., 2007). The antenna cofactor tranduces the photon energy to the adjacent catalytically active anionic semiquinone $FADH^-$ by Föster resonance energy transfer (Sancar, 2003). The excited $FADH^{\bullet -}$ then transfers an electron to the pyrimidine photolesion and returns to its catalytically competent state (Table 1.1). The repaired DNA can no longer maintain a high affinity interaction with the photolyase and is released. Despite their frequent use of flavins, photolyases lack any obvious sequence homology with other flavoproteins and nucleotide binding proteins (Sancar, 2008) and maintain a unique photolyase/cryptochrome fold (Figure 1.1).

Photolyases have persisted largely unchanged for billions of years, they patrol the genome for deleterious lesions in almost all life from archaebacteria to marsupials and even some viruses (Afonso et al., 1999; Willer et al., 1999). There is, however, a key exception: placental mammals. While many species contains both photolyases and cryptochromes, placental mammals only have cryptochromes, and must resolve their DNA photoproducts solely with the less efficient nucleotide excision repair (Sancar, 1996; Wood, 1997). The evolution of circadian gene-expression regulators from DNA-binding blue-light photoreceptors is a testament to how natural selection co-opts existing traits into novel ones (Cashmore et al., 1999).

### *1.1.2 Cryptochrome Evolution and Function*

During the Neoproterozoic Era (1000–541 Mya) (Mei and Dvornyk, 2015), the first cryptochromes emerged as circadian clock components. Several hundred million years later, following two whole genome duplications, two CRYs diverged (under a yellow sun) from a common ancestor (Amores et al., 1998; Glasauer and Neuhauss, 2014), which coincided with increased climatic stabilization and ozonic protection from damaging UV radiation (Canfield, 2005). Although mammals have only two CRY paralogs (CRY1 and CRY2), some species of amphibians and fishes have additional copies, the most existing in cavefish, a close relative

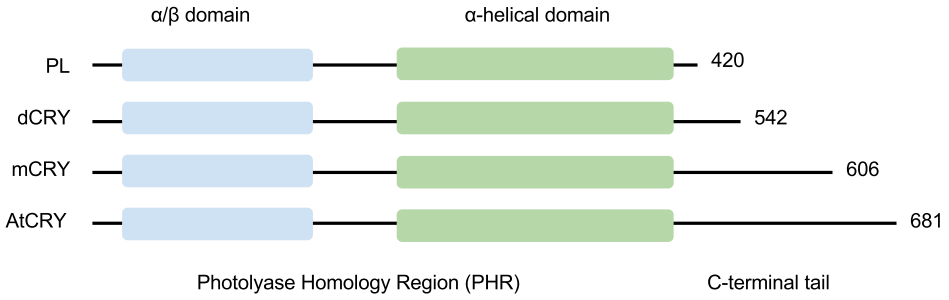


Figure 1.1: **Schematic of the Basic Secondary Structure Elements of the CRY/PL Family** The N-terminal $\alpha/\beta$ photolyase fold is the most evolutionarily conserved domain. It is linked to the $\alpha$-helical domain throught a large, flexible loop. The $\alpha$-helical domain houses the FAD-binding pocket and is the primary locus for protein–protein interactions. CRYs are most divergent in their C-terminal tails (CTT), of which PLs have the shortest. dCRY uses its CTT to seal in the FAD chromophore in the light-activated state, mCRYs fine-tune circadian period and amplitude with post-translational modifications to their CTT, and plants disengage their CTT upon illumination as the sole interaction region for many of their binding partners. PL, *Drosophila* (6-4) photolyase; dCRY, *Drosophila* CRY; mCRY, murine CRY1; AtCRY, *Arabidopsis* CRY1.

to zebrafish, which have seven CRYs as well as an active photolyase (Cavallari et al., 2011).

Even though CRYs are the direct evolutionary progeny of photolyases, they only maintain 25–50% sequence identity, and as their name suggests (from κρυπτός , meaning "hidden"), their identification was non-trivial. Initiated by Darwin (Darwin and Darwin, 1880), a search lasting more than a century was dedicated to revealing the proteins responsible for blue-light detection, photoperiodism, and photomorphogenesis in plants. Forty years after the discovery of photolyases, plant biology finally described the first blue-light photoreceptor in plants, as the HY4 allele (Koornneef et al., 1980). It was later sequenced and characterized as member of the photolyase/cryptochrome protein family in 1993 (Banerjee and Batschauer, 2005; Ahmad and Cashmore, 1993). After this initial breakthrough, homologous sequences were readily uncovered in animals and functionally implicated in the circadian clocks of both plants and animals (Li et al., 1993; Lin and Todo, 2005). For example, genetic ablation of murine *Cry2* showed a 1 hr longer circadian period and amplified phase shifts in response to light. A *Cry1–2* double knock-out was created in 1999 and demonstrated complete arrhythmicity (Van Der Horst et al., 1999) arguing that not only the two CRY paralogs share some overlapping functions but they are indispensable components of the mammalian circadian clockwork.

While extant in plants as crucial photoreceptors and circadian regulators, all subsequent discussion of cryptochromes will be in reference to the animal types. There are two forms of animal cryptochromes, Type I and Type II. Type I, as exemplified by *Drosophila* CRY, are light-sensitive and serve as the primary entrainment proteins for the circadian clock (Zoltowski et al., 2011). Type II, or the vertebrate type, have lost photoreception, FAD as a constitutively-bound prosthetic group, and have been co-opted exclusively as a circadian clock regulator, functioning as the core repressor (Reppert and Weaver, 2002; Xing et al., 2013) (Table 1.1, Table 1.2). Interestingly, Type II CRYs are more homologous in sequence to animal (6-4) photolyases than to plant or Type I CRYs (Xing et al., 2013).

| Protein | Ground state | Signaling state | Antenna cofactor | Activation | Functional oligomer |
|---|---|---|---|---|---|
| (6-4) Photolyase | $FADH^-$ | $FADH^-$ | MTHF, 8-HDF | UV-A/Blue | monomer |
| Type I CRY | FAD | $FAD^-$ | none | Blue | likely monomer |
| Type II CRY | $FAD^\dagger$ | unknown | none | light-inactive | likely monomer |

Table 1.1: **Photoactivity within the Photolyase/Cryptochrome Family**. Comparison of the mechanisms of light activation between PLs and CRYs. $^\dagger$ FAD has not been shown to co-purify with recombinant mammalian CRY PHR, it can however bind to FAD with low affinity and may serve a signaling role *in vivo* (Xing et al., 2013).

## *1.2 Evolution of Circadian Clockwork*

### *1.2.1 General Clock Paradigm*

Life has evolved a self-sustaining molecular timing system that synchronizes cellular activities with the solar day. At the most fundamental level, a circadian clock is an oscillating system that receives input from specific environmental stimuli (e.g., light, temperature, nutrients) and generates synchronized biochemical output to regulate gene expression, metabolism, and behavior. This tripartite model is an oversimplification, as even in the most basic of circadian clocks, the signaling network more resembles a Gordian knot than a road map (Lakin-Thomas and Brody, 2004).

Circadian clocks offer extrinsic adaptive value in variable environments; as such, competitive advantage is lost when organisms are kept under constant conditions (Woelfle et al., 2004). Although clocks continue a self-sustaining cycle in constant conditions, which is one of their defining characteristics, they must also be able to respond to external stimuli that align, or entrain, the organism to the environmental conditions. It is important to note that these zeitgebers ("time givers")—light being the most effective—do not generate the rhythms, they only serve to synchronize the clocks enabling them to predict and prepare for periodic environmental fluctuations. Another necessary characteristic is compensation for

ambient temperature changes while remaining malleable to large periodic changes in temperature (i.e., seasonal) (Bass and Takahashi, 2010; Pittendrigh, 1993; Buhr et al., 2010). Although endothermic mammals rarely entrain to temperature cycles, the heat shock response pathway remains able to reset clocks to thermal zeitgebers and compensate for small fluctuations, which augments internal synchrony (Buhr et al., 2010). Proposed sixty years ago (Hastings and Sweeney, 1957), the molecular mechanisms required for this paradoxical ability for circadian clocks to maintain constant rhythms in conditions when typical biochemical reaction rates would change dramatically are still unresolved (Buhr et al., 2010; Zhou et al., 2015). The persistence of circadian clocks in ostensibly all species of life indicate their significance; however, unraveling the interconnected biochemical pathways has only recently been productive.

### *1.2.2 Evolution of the Metazoan Circadian Clock*

All metazoan clocks are based upon a transcription-translation auto-regulatory negative feedback loop. Two transcription factors bind to E-box elements and promote the transcription of all clock-controlled genes. Of these genes are two negative components whose localization and levels are regulated by a variety of post-transcriptional and post-translational modifications. The cycle is restarted when the negative elements inhibit the transcriptional activity of the positive elements. These interactions generate a cell-autonomous 24-hr oscillation.

The elaborate evolutionary history of CRYs is mirrored in the organization of the clock itself. There are currently three kinds of metazoan clocks: those with only Type I or II or those with both Type I and II. The Type I system is organized around CRY as the central photo-entrainment protein. These CRYs light-dependently binds a transcriptional co-repressor, Timeless (TIM) to stimulate the ubiquitination and degradation by Jetlag (JET), whose effect is to release the inhibition of a PER-driven repression of Clock-Cycle (CLK-CYC) heterodimeric transcription factors. CRY is also degraded by JET but on longer timescales (Zoltowski et al., 2011; Lin and Todo, 2005). Analogously, in the Type II system, CLOCK and BMAL1 function as the core transcriptional activators with Periods

(PERs) and CRYs as the transcriptional repressors. Lepidopterans contain the dual, and likely the ancestral, clock scheme. They use Type I CRYs to entrain their cellular clocks like *Drosophila* but use the Type II CRYs to orchestrate repression (q.v., Table 1.2 for functional equivalences of the proteins found in the Type I- and Type II-based clocks).

### *1.3 Mechanisms of the Mammalian Circadian Clockwork*

In contrast to all other clocks, vertebrate (i.e., mammalian) cells are not transparent to light and so require a more sophisticated mechanism of entrainment and peripheral tissue synchronization. When light enters the retina, melanopsin photoreceptors in intrinsically photosensitive retinal ganglion cells transduce the stimulus to the master pacemaker, the suprachiasmatic nucleus (SCN) via the retinothalamic tract, which coordinates the entire circadian program (Reppert and Weaver, 2002). All cell types peripheral to the SCN are considered slave oscillators and rely on it to maintain 24-hr rhythms (Balsalobre et al., 1998; Yamazaki et al., 2000). The synchronized slave oscillators are then able to coordinate their local rhythms, which underlie physiology and behavior (Figure 1.2). This hierarchical multicellular system ensures precise control over the phase and period of a largely distributed network of oscillators (Pando et al., 2002). The mechanism that determines the dominance of SCN master clock over the slaves as well as how it synchronizes the peripheral oscillators is unknown (Gerber et al., 2013). However, since no unique elements have been discovered in only the SCN, it is more likely that differences in protein abundance and kinetics are responsible for these differences.

At the molecular level, the mammalian circadian clock is generated by a negative feedback loop composed of four core components: the transcriptional activator proteins, CLOCK and BMAL1, and the transcriptional repressors, Periods (PERs) and Cryptochromes (CRYs). The heterodimeric CLOCK and BMAL1 complex acts as the positive arm of the loop by recognizing E-box elements and promoting the expression of clock-controlled genes, including *Per1*, *Per2*, *Cry1*, and *Cry2*. The PER and CRY proteins function as the negative arm of the loop by blocking the activity of CLOCK-BMAL1 and inhibiting the transcription of

their own and all other clock-controlled genes. The cyclic accumulation, localization, and degradation of the PER and CRY proteins are necessary to manifest a 24-hr rhythm (Lowrey and Takahashi, 2011).

The canonical clock mechanism, which was established on genetic studies, suggested that CRYs are the predominant inhibitors of CLOCK-BMAL1 (Griffin et al., 1999; Kume et al., 1999). Independent of PERs, over-expressed CRY1 and CRY2 can each potently inhibit the CLOCK-BMAL1-induced transcription of a luciferase reporter gene in cultured cells (Griffin et al., 1999; Kume et al., 1999). This transcriptional repression activity of CRYs likely occurs through their direct interactions with BMAL1 (Griffin et al., 1999; Xu et al., 2015; Kiyohara et al., 2006) and CLOCK (Zhao et al., 2007; Huang et al., 2012). Later biochemical investigation revealed that despite the important repressor function of CRYs, the PER proteins have been suggested as the rate-limiting factor in the rhythmic negative feedback loop (Lee et al., 2001). Contingent upon its tightly regulated phosphorylation and ubiquitination states during the circadian cycle, PERs mediate the formation of the PER-CRY complexes and their nuclear localization (Lee et al., 2001), regulate epigenetic modifications of clock genes (Duong et al., 2011), stabilize CRY in the nucleus (Busino et al., 2007; Siepka et al., 2007), and control the dynamic formation of core clock machinery on and off chromatin (Ye et al., 2014) (Figure 1.3).

Periodic degradation of PERs and CRYs represents another crucial step in the negative feedback loop. β-TrCP and FBXL3, two F-box protein members of the Skp-Cullin-F-box (SCF) E3 ubiquitin ligase complex, have been discovered as the key substrate receptors that promote the polyubiquitination of PERs and CRYs, respectively (Busino et al., 2007; Siepka et al., 2007; Reischl et al., 2007; Shirogane et al., 2005; Godinho et al., 2007). Phosphorylation of a degron sequence serves as the signal for PER ubiquitination by β-TrCP (Shirogane et al., 2005), whereas recognition of CRYs by FBXL3 is made through a large protein-interaction interface without the involvement of a canonical degron motif or any post-translational modification (Xing et al., 2013). In our recombinant system, the CRY-FBXL3 interface is susceptible to disruption by both the CRY cofactor FAD and the PER

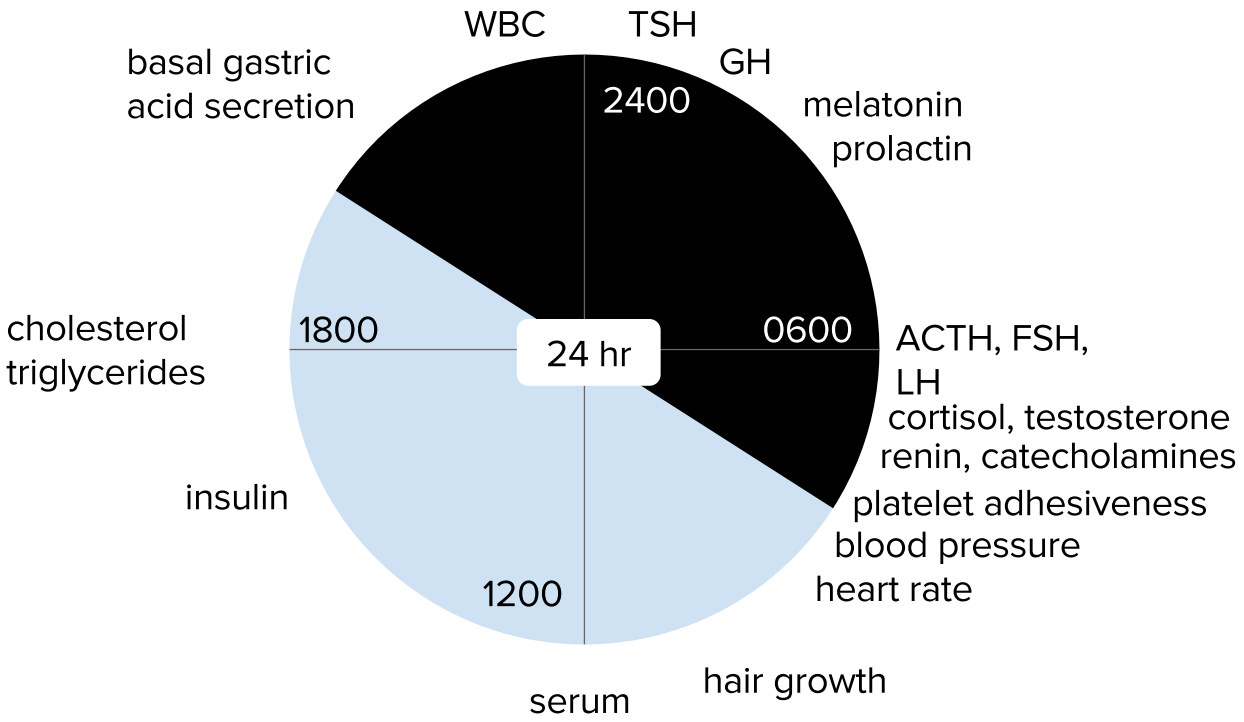


Figure 1.2: **Time of Peak Function of Circadian-controlled Processes.** In the morning, circadian rhythms promote platelet aggregation and an increase in blood catecholamine levels as well as a variety of cardiovascular processes including blood pressure, heart rate, and vascular resistance. These combined features contribute to a higher incidence of acute coronary syndrome during the early morning (Willich et al., 1998). Hair growth reaches its peak in the mid-morning, which is why radiation therapy administered in the evening results in significant reduction of hair loss relative to the morning (Plikus et al., 2013). During the afternoon, serum iron and hemoglobin peak. Mid- to late-afternoon coincides with peak rhythms of respiration rate, and key metabolic products including blood insulin levels, cholesterol, and triglycerides. Neutrophil levels and basal gastric acid production peak late in the day while white blood cell count, thyroid stimulating hormone (TSH), growth hormone (GH), prolactin, and the sleep hormone melatonin peak in the hours between the onset of sleep and early morning. During times of deep sleep, blood levels of adrenocorticaltropic hormone (ACTH), follicle stimulating hormone (FSH), luteinizing hormone (LH), testosterone, cortisol, catecholamines, renin, aldosterone, and angiotensin all peak near the termination of sleep and start of the day. (Approximate times). These processes are used to exemplify the diverse functions regulated by the circadian rhythm as well as to call attention to the myriad ways pharmacological intervention can be optimized to work with rather than against to the endogenous clockwork. Adapted from (Smolensky and Peppas, 2007).

proteins, which have been suggested to control the stability of CRYs by directly competing with FBXL3.

Understandably, alterations to the clock mechanism (e.g., jet lag, social jet lag, shift work, Western diet, and poor sleep hygiene) are implicated in a number of disorders including cancer, metabolic syndrome, diabetes, cardiovascular disease, and sleep disorders (Green et al., 2008; Bass and Takahashi, 2010; Asher and Schibler, 2011). Given the pervasiveness of the clock in physiological processes, identification of circadian modulators may become therapeutically useful to reset dysregulation in a highly coordinated manner. Understanding the fundamental mechanisms of the circadian clock is critical to consolidating a functional description of this ubiquitous system.

## *1.4 Structural Biology of Circadian Clock Components*

### *1.4.1 Cryptochrome/Photolyase Family*

Despite a low degree of sequence conservation of 5.6% and homology of 42%, the overall architecture across the cryptochromes and photolyases remain quite similar with a total root mean square deviation of 1.9 Å (Figure 1.4). The overall conformation of the core region (photolyase homology region, PHR) of CRY and PL proteins is remarkably similar (Figure 1.1). Divided into two lobes, the N-terminal domain of the PHR, the α/β photolyase domain is composed of five parallel β-sheets enveloped by six α-helices that alternate between the β-sheets in a repeating βα pattern along the backbone (Figure 3.3). The second half, aptly named the α-helical domain, is linked to the α/β domain via a long meandering loop, is composed only of α-helices and contains the FAD-binding pocket. On the opposite side of the protein, at the junction of the α/β and α-helical domains, another large surface pocket—9 Å away—abuts the FAD-binding pocket. In photolyases, this pocket binds the antenna cofactor. Interestingly, despite its superficial similarity to the canonical nucleotide binding motif, the Rossmann fold, the helix-sheet packing in the α/β fold is a coincidental product of convergent evolution and favorable entropy rather than ancestry (Chothia et al.,

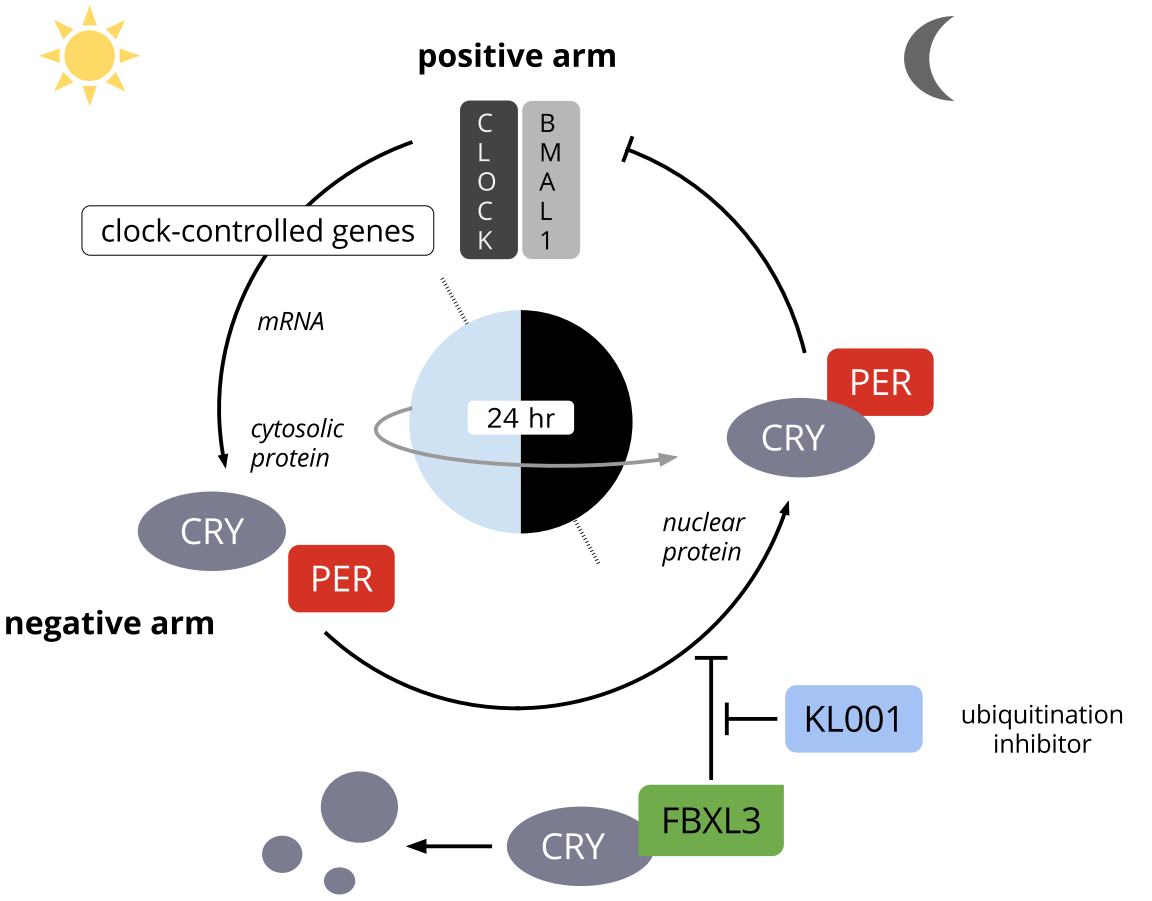


Figure 1.3: **Molecular Mechanisms of the Mammalian Circadian Auto-regulatory Negative Feedback Loop.** The circadian rhythm is maintained by a 24-hr molecular timing system that relies on a transcription-translation negative feedback mechanism of four proteins. Two transcription factors, CLOCK and BMAL1 drive the positive arm of the loop by promoting the expression of clock-controlled genes, along with the components of the negative arm, PERs and CRYs. The PER and CRY proteins block the activity of CLOCK-BMAL1 and inhibiting the transcription of their own and all other clock-controlled genes. The periodic accumulation, localization, and degradation of the PER and CRY proteins are necessary to manifest a robust daily oscillation. CRY ubiquitin ligase, FBXL3, which in addition to an extensive interface, embeds a completely conserved tryptophan at its extreme C-terminus into a large hydrophobic pocket of CRY. The same pocket that binds the first direct clock-modulating small molecule KL001, which directly competes with FBXL3 to promote CRY stability and dose-dependently lengthens the circadian period.

1977). In contrast to the FAD pocket, the maintenance of the antenna cofactor pocket throughout evolutionary history is less straight-forward. Since only photolyases are known to bind and use antenna cofactors (Zoltowski et al., 2011; Glas et al., 2009), it remains unclear why all cryptochromes still contain this pocket, flexibility of a nearby framing loop, and key 8-HDF-interacting residues. The most plausible explanation is that the two globular domains arose from genetic fusion of two functionally distinct proteins. And evolution of the monomer maintained a structural interdependence and might explain the persistence of a non-functional second cofactor binding site. Nevertheless, the conjecture that an unknown cofactor can bind involves no impossibility, but it has no positive support, and little intrinsic probability (Craigie et al., 2015). Rather, as is seen in many other homologous structures this pocket has been exapted for another regulatory role.

Despite the striking three-dimensional homology between photolyases and CRYs, one key divergent structural feature is the presence of a long C-terminal tail (CTT) (Figure 1.1). Type I CRYs require their CTT for phototransduction. Structurally, the dCRY CTT, upon illumination, doubles back on top of the FAD-binding pocket and nestles into a groove along a homologous C-terminal helix, which in photolyases, interfaces with the DNA helix (Zoltowski et al., 2011; Czarna et al., 2013). The CTT of Type II CRYs are dispensable for basic maintenance of the circadian oscillation. However, it is required for fine-tuning the circadian amplitude and period through the modification of several phosphorylation sites as well as a nuclear localization signal (Khan et al., 2012; Chaves et al., 2006; Partch et al., 2005; Kurabayashi et al., 2010; Gao et al., 2013; Zhu et al., 2003). Due to the high degree of disorder in the vertebrate CRY CTT, all solved structures have been only of the PHR (Xing et al., 2013; Nangle et al., 2013, 2014; Czarna et al., 2013; Schmalen et al., 2014).

Also in contrast to photolyases and Type I CRYs, mammalian CRYs do not co-purify with FAD despite containing a highly-conserved binding pocket (Xing et al., 2013). On closer inspection, the FAD-binding pocket lacks several crucial interfaces that normally lock FAD into the center of photosensitive CRYs. Two loops—used by photolyases—that flank the top of the adenine diphosphate groups are disengaged. One, the phosphate-binding loop,

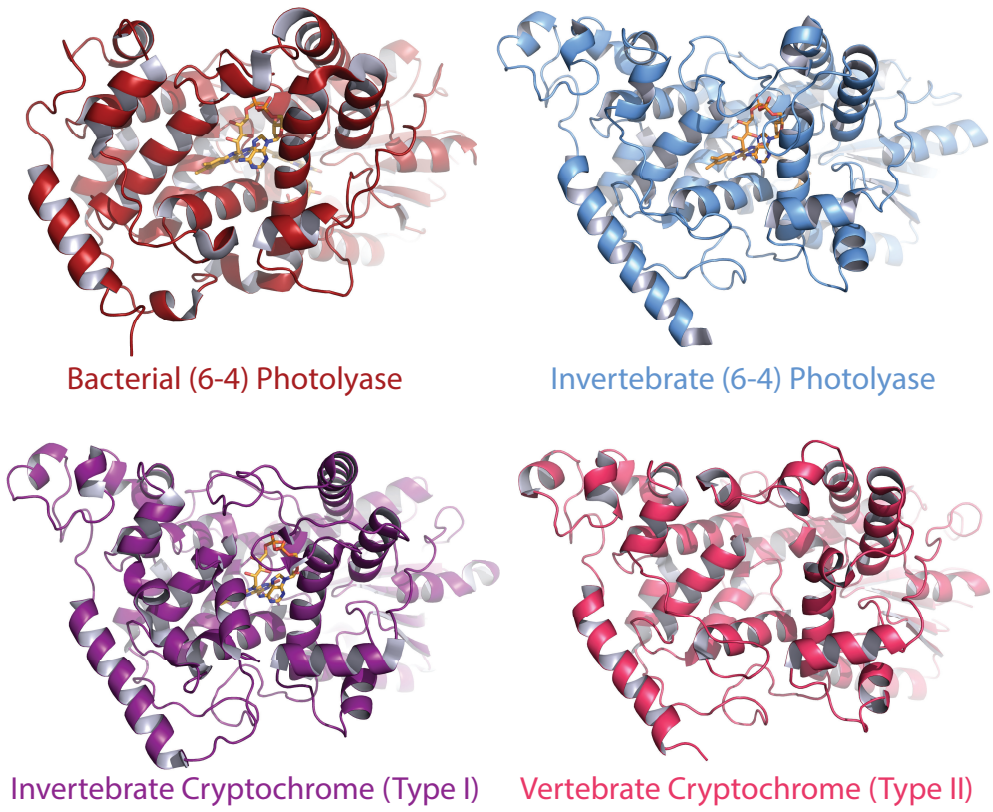


Figure 1.4: **General Structural Comparison of CRY/PL Family.** Four representative proteins are shown to highlight the degree of structural homology maintained within the PL/CRY family. Note the persistence of the the FAD cofactor and corresponding binding pocket as well as the long C-terminal helix, which is responsible for a variety of biochemical processes. For example: interfacing with DNA, in the case of the photolyase and key circadian proteins (e.g., FBXL3, PER CRY-binding domain, and BMAL1 C-terminal tail), in the case of vertebrate CRYs. Bacterial (6-4) photolyase (PDB:1IQR), invertebrate (6-4) photolyase (PBD:3CVV), invertebrate Type I CRY (PDB:4GU5), vertebrate Type II CRY (PDB:4MLP).

which would normally coordinate a hydrogen bond between one of its lysines and the N7 on the adenine ring, not only lacks this residue but is completely disordered. The second, the protrusion loop, which rather than moving inward and occluding the flavin pocket, is shifted outwards, removed from the FAD binding site entirely (Xing et al., 2013). The third conformational difference is the lack of a C-terminal tail, which in dCRY occludes the chormophore. The combination of these three structural differences result in a mostly open pocket conformation. That said, FAD is still able to bind mCRY, albeit at a low affinity (40 μM), and adopts a nearly identical binding mode to all other photolyases and CRYs. One particularly intriguing hypothesis is that FAD can in fact bind CRYs *in vivo* but only in combination with other binding partner(s) and ostensibly functions as a signaling molecule and/or coincidence detector.

Two exapted interfaces critical for circadian functionality are a long C-terminal helix and a highly-conserved stretch of hydrophobic residues framing the outer wall of the FAD-binding pocket called the interface loop. These two features are used in photolyases to engage the DNA helix and in dCRY to secure the CTT. In vertebrates, these sites are required for a variety of protein-protein interactions. For example, FBXL3 forms its extensive binding surface around the CRY C-terminal helix and substantially rearranges the interface loop to engage its C-terminal Trp into the FAD-binding pocket. Mutation of one of the hydrophobic residues (F428D) on this loop abolishes both FBXL3 binding and significantly inhibits the degradation of CRY (Xing et al., 2013). Additionally, the point mutation (*after-hours*) that led to the discovery of FBXL3 and results in circadian periods ranging from 25.3 to 27.6-hr, is mapped to a cysteine residue (C358S) within the hydrophobic core of one of the leucine-rich repeats (Xing et al., 2013)). The CRY C-terminal helix also interacts with the extreme C-terminus of BMAL1 transactivation domain (TAD) (Chaves et al., 2006; Kiyohara et al., 2006; Xu et al., 2015). *In vivo* experiments have demonstrated that mutations to either the TAD-CRY-binding region (TAD-CBR) or CRY C-terminal helix lead to an increase in circadian amplitude owning to decreased repression by CRY (Kiyohara et al., 2006; Sato et al., 2006). Additionally, PERs are also known to bind at this site, as Arg501 and Lys503

in the CRY2 have been documented to be important for PER2 binding (Ozber et al., 2010).

Overall, CRY proteins are highly versatile in both structure and function. Recent work as well as what is described here has only started to shed light on their diverse roles and to reveal the rich landscape of regulation of these ancient proteins.

### *1.4.2 The Period Proteins*

The CRY co-repressor, Period (PER1–3), is another core clock component. Where CRY predominately functions to bind CLOCK-BMAL1 on E-boxes and repress transcription, PERs largely regulate circadian rhythmicity and recruitment of CRY to the transcription activation complex (Ye et al., 2014). Post-translational modifications exert nuanced control over the localization and stability of PERs and their various complexed forms (Lee et al., 2001; Duong et al., 2011). PERs provide the primary force for translocating CRYs into the nucleus and once there, protect them from degradation by FBXL3 (Yagita et al., 2002). Although CRY has its own NLS, its translocation is less efficient, more unstable, and ostensibly remains in the cytoplasm in the absence of PERs (John et al., 2014). The critical role of PERs in driving the molecular clock is underscored by the complete loss of circadian rhythmicity upon constitutive over-expression of PERs, but not CRY1, *in vitro* and *in vivo* (Ye et al., 2011; Chen et al., 2009; McCarthy et al., 2009)

Compared to CRYs, little is known about PERs structurally. Of their ∼1250 amino acids only about 350 are well-folded to form tandem PAS (PER-ARNT-SIM) domains. The remainder of the protein is intrinsically disordered (Kucera et al., 2012). Structures of the PAS domains have been determined as homodimers and have been verified to homo- and heterodimerize *in vivo* (Kucera et al., 2012; Yagita et al., 2000). The dimer interface, in contrast the ouroboroid head-to-tail *Drosophila* PER tandem PAS conformation (Yildiz et al., 2005), mammalian PERs are intertwined along their PAS-B domains. Functional evaluation with the full-length proteins show that mutations to this PAS-B dimer interface affects protein localization indicating that dimer formation is necessary for proper clock function (Kucera et al., 2012). N-terminal to the PER PAS-A domain is a phosphodegron

motif that is targeted by β-TrCP for ubiquitination. While protein turnover is a necessary part of circadian rhythmicity, total PER levels cannot completely explain the generation of robust cycling (Chen et al., 2009). Several hundred residues C-terminal of the degron sequence is a serine-rich region that is regulated primarily by casein kinase 1 (CK1δ/ϵ) phosphorylation. While over-expression of CK1ϵ does not significantly disrupt rhythms, loss or mutation of either CK1 can lead to highly deleterious consequences (Toh et al., 2001). In animal models, CK1δ and CK1ϵ genetic ablation leads to 0.5-hr shorter period (Xu et al., 2005) and 4-hr shorter period (Lowrey et al., 2000), respectively.

The most common circadian-dependent sleep disorder, delayed sleep phase syndrome (DSPS) (Sack et al., 2007), is characterized by sleep onset in the early morning (0300–0600 hr) and arousal in the early afternoon (1100–1400 hr). While the exact genetic mechanism is unresolved, two studies have reported mutations in the *Per3* gene in association with this syndrome. One is a missense mutation (G647V) (Ebisawa et al., 2001), which is in the CK1 binding domain (Toh et al., 2001), another is a variable number tandem repeat within the coding sequence (Archer et al., 2003). Conversely, a single nucleotide polymorphism in the 5'-UTR of the *Per2* gene as well as an amino acid substitution (S408N) in CK1ϵ are associated with morning preference and serve a protective role against phase shifts (Takano et al., 2004). Another sleep disorder related to PER function, familial advanced sleep phase syndrome (FASPS), is the only clearly described Mendelian circadian disorder that presents with early times of sleep (1800–2000 hr) and wake (0300–0600 hr) onset. Both forms of FASPS that have been described correlate with PER phosphorylation states. One has been mapped to a putative priming serine of PER2 (S662G) also within the CK1 binding domain, which leads to the hyperphosphorylation of PERs (Toh et al., 2001; Shanware et al., 2011). The other is in CK1δ itself (T44A) and compromises its phosphorylation activity (Xu et al., 2005). The prevalence of dysregulation of PER phosphorylation in circadian disorders highlights the importance of its precise regulation. Because the biochemical and structural mechanisms of PER are not well-delineated, it is difficult to make any conclusions about how these mutations lead to sleep disorders. However, phosphorylation is known to regulate nucleocytoplasmic

shuttling (Öllinger et al., 2014), β-TrCP-dependent degradation (Reischl et al., 2007), and possibly CLOCK-BMAL1 binding (Lee et al., 2001), all of which could be affected by these mutations.

Binding of PERs to CRYs, CLOCK, and BMAL1 have been detected both *in vivo* and *in vitro* (Ye et al., 2011; Kiyohara et al., 2006; Partch et al., 2014). However, the role of PER2 in coordinating the repression complex assembly is controversial. Although interactions with CLOCK-BMAL1 have been mapped to the PER PAS domains by co-immunoprecipitation (Chen et al., 2009), *in vitro* binding assays with recombinant proteins fail to show this interaction (Ye et al., 2011). Specifically, in an electrophoretic mobility shift assay (EMSA), CRY can form a complex with E-box associated CLOCK-BMAL1, however, PER cannot bind CLOCK-BMAL1 on DNA with or without CRY (Ye et al., 2011). Because these are insect cell purified proteins, they may not have the requisite modifications that ensure complex formation. Conversely, while co-immunoprecipitation experiments are more able to reflect the physiologically relevant complexes, they are unable to reveal direct protein-protein interactions.

PERs are extremely dynamic and complex proteins; one compelling hypothesis suggests that highly disordered proteins are more thermodynamically malleable and can undergo a myriad highly specific modifications and binding events at lower energetic costs (Fuxreiter et al., 2008; Cortese et al., 2008). The molecular and biochemical processes involved in how PER coordinates the repressive complex on and off DNA remains one of the largest unresolved questions in the field (Partch et al., 2014).

### *1.4.3 The CLOCK-BMAL1 Heterodimeric Complex*

CLOCK-BMAL1 are basic helix-loop-helix PER-ARNT-SIM (bHLH-PAS) transcription factors responsible for the majority of circadian clock gene transcription, about 10% of the human transcriptome (Ueda et al., 2002; Panda et al., 2002; Storch et al., 2002). They are a part of a larger family of transcription factors that are involved in diverse cellular function: including hypoxia (HIF-α and ARNT), toxic metabolites (Aryl hydrocarbon receptor, AHR),

synaptic plasticity (NPAS1–4), and neurogenesis (SIM1). Like other bHLH transcription factors, they bind to E-box promoter elements whose ideal consensus sequence is CACGTG. The structure of the heterodimeric bHLH-PAS domains have been determined and reveal a highly intertwined complex with each of the three domains (N-terminal bHLH, PAS-A, and PAS-B) involved in the dimer interface (Figure 1.5) (Huang et al., 2012). In combination with their extensive enmeshment, both monomers contain numerous long, strictly-conserved flexible loops that failed to resolve in the crystal structure but may be involved in coordinating other protein–protein interactions. There is also a marked asymmetry of the complex. CLOCK is overall negatively charged (pI = 5.86) whereas BMAL1 is electrostatically positive (overall pI = 9). Additionally, while the primary sequence of the three domains are similar, the binding mode of the each monomer is notably divergent. CLOCK is hinged at a loop connecting PAS-A and PAS-B which leads to a 'C'-shaped conformation while BMAL1 remains ostensibly linear, with each domain stacked on top of the preceding. These asymmetries may serve as a diverse landscape for potential core clock protein interactions (Etchegaray et al., 2003; Huang et al., 2012).

Although both CRY and CLOCK-BMAL1 structures have been determined, the binding mode of the ternary complex is not intuitive. Yeast two-hybrid data suggests that CRY binding is diminished when two amino acid substitutions are made on the solvent-exposed CLOCK HI loop in the PAS-B domain (Q361P and W362R) (Zhao et al., 2007) and nearby point mutations (G332E, E367K, and H360Y) show derepression phenotypes in a circadian transcriptional reporter assay (Sato et al., 2006). The Trp362 residue corresponds to the BMAL1 Trp427, which tucks into the a hydrophobic cleft of CLOCK PAS-B (Figure 1.5). The intriguing prevalence of interfacial tryptophans suggest that the surface-exposed CLOCK W362 serves a functional role. Additional CRY interfaces on BMAL1 have been mapped to its C-terminal TAD, specifically the last 43 amino acids, which are necessary for transcriptional repression by CRY1 (Kiyohara et al., 2006) (Figure 1.5).

The CLOCK-BMAL1 structure has confirmed a variety of putative functions of specific side chains and provides a framework from which to extrapolate likely interactions with other

clock proteins and delineate a sophisticated circadian clock mechanism.

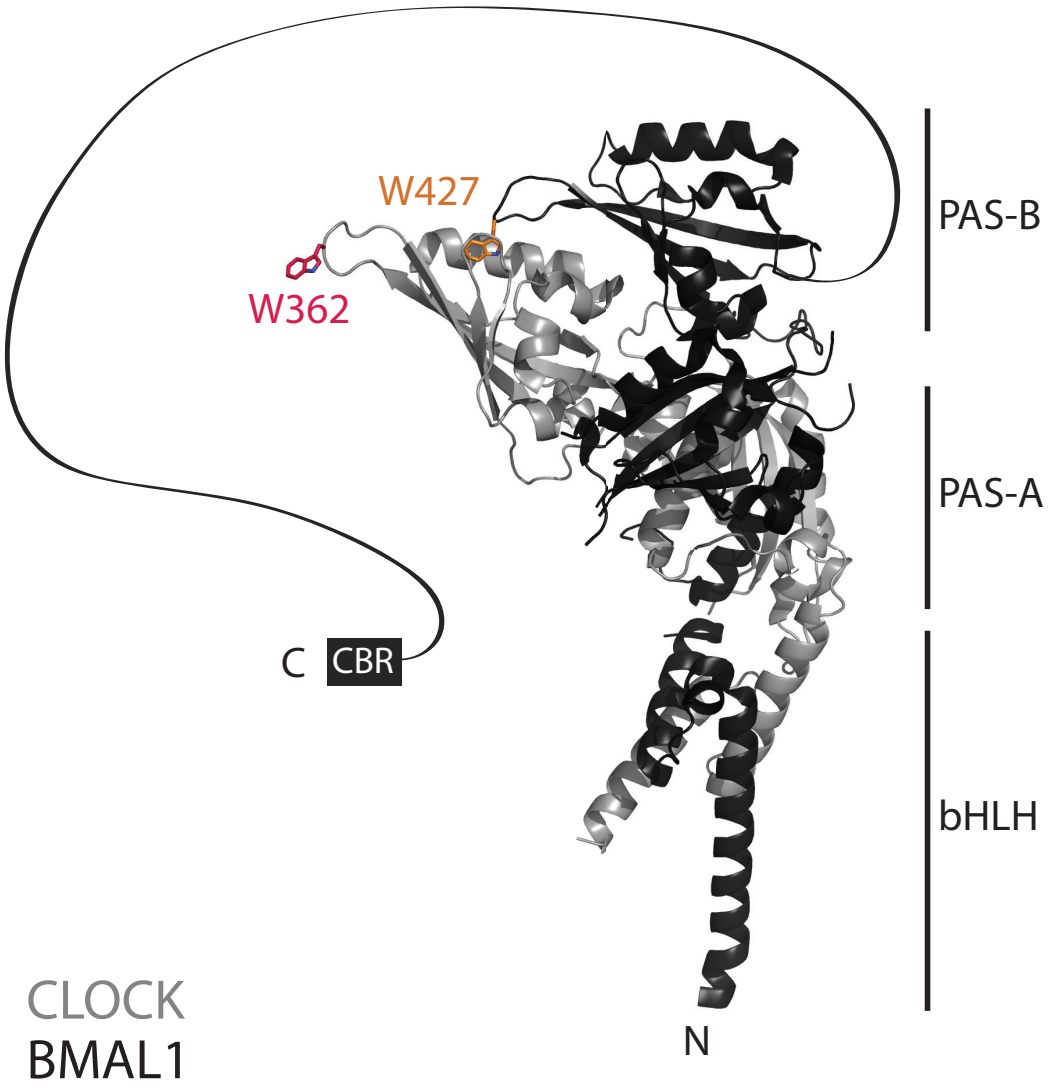


Figure 1.5: **Global Structure of the CLOCK-BMAL1 Complex.** Overall architecture of the CLOCK-BMAL1 heterodimer. CLOCK (gray) adopts a bent conformation around relatively linear BMAL1 (black). N-terminal bHLH domains are linked via long, disordered loops to the PAS-A domains. BMAL1 W427 (orange) inserts into a hydrophobic pocket on CLOCK PAS-B domain. The corresponding Trp on CLOCK W362 (pink) is solvent exposed and together with surrounding residues (the HI loop) is a putative CRY binding site. CRY-binding region (CBR) of the transactivation domain (TAD) is at the BMAL1 extreme C-terminus following a long and non-conserved stretch of amino acids. (PDB:4F3L).

| Protein Type | Primary Function | Mammalian Name | {Drosophila} Name |
|---|---|---|---|
| bHLH Transcription Factors | Binds to E-box elements and promotes the transcription of clock-control genes | CLOCK | CLOCK (CLK) |
| | | BMAL1 | CYCLE (CYC) |
| Primary Transcriptional Repressor | Binds to transcription factor heterodimeric complex to repress transcription | Cryptochrome (CRY1–2) | Period (PER) |
| Co-repressor | Binds primary repressor and facilitates trafficking, stability, and repression complex organization. | Period (PER1–2) | Timeless (TIM) |
| Ubiquitin Ligase SCF F-box | Promotes the ubiqtuination of PERs | β-TrCP | SLIMB |
| Ubiquitin Ligase SCF F-box | Promotes the ubiqtuination of CRYs | FBXL3 | Jetlag (JET) |
| Kinase | Phosphorylates PERs, which regulates localization, function, and stability | Casein Kinase 1 (CK1 δ–ϵ | Doubletime (DBT) |
| Light-sensitive flavoprotein | Primary entrainment photoreceptor | N/A | Cryptochrome (CRY) |

Table 1.2: **Functional Equivalences Between Mammalian and *Drosophila* Clock Proteins.** Although invertebrate and vertebrate clocks diverged millions of years ago, the core clock components remain strikingly homologous. Both CLOCK-BMAL1 and Clock-Cycle are bHLH tandem PAS transcription factors that bind to E-box DNA elements (the ideal consensus sequence being CACGTG) and regulate the majority of clock-controlled genes. While dPER is more structurally homologous to mPER, it serves as the primary repressor by binding to the transcription factors as mCRY does in the Type I paradigm. dCRY, which has high structural homology to mCRY has no functional homolog in the vertebrate clock. Post-translational modification proteins are also highly homologous between systems suggesting a high degree of importance of these mechanisms for the generation of a robust rhythm.

# Chapter 2

# STRUCTURAL MECHANISM OF A CLOCK-MODULATING SMALL MOLECULE

## *2.1 Introduction*

Perturbations to the clock mechanism are implicated in a number of disorders including cancer, metabolic syndrome, diabetes, cardiovascular disease, and sleep disorders (Green et al., 2008; Bass and Takahashi, 2010; Asher and Schibler, 2011). Given the pervasiveness of the clock in physiological processes, identification of circadian modulators may become therapeutically useful to reset dysregulation in a highly coordinated manner.

A recent cell-based screen of small-molecule circadian modulators identified three carbazole derivatives that are characterized by their common dose-dependent circadian period-lengthening activity (Hirota et al., 2012). Further analyses have shown that a representative compound, KL001, acts by directly interacting with CRYs and protects them from FBXL3-mediated ubiquitination and subsequent degradation. Its pharmacological activity results in CRY stabilization, which increases the duration of transcriptional repression and lengthens the circadian period in cell culture. We show that KL001 exerts if function through binding to the FAD-binding pocket and antagonizing FBXL3-dependent ubiquitination.

### *2.1.1 Flavin Interactions with Cryptochromes*

While vertebrate CRYs evolved from light-sensitive flavoproteins, they no longer retain FAD binding or photoreception. In Type I CRYs, blue-light exposure promotes the conversion of the oxidized FAD to the catalytically-active anionic semiquinone $FAD^{\bullet -}$. Interestingly, the light-induced conformational change of the dCRY C-terminal tail (CTT) completely seals in FAD at the center of the protein by folding back on itself (Zoltowski et al., 2011; Czarna

et al., 2013). It is this flavin-dependent conformational switching that regulates complex formation with ubiquitin ligase Jetlag (JET) and co-repressor Timeless (TIM).

Despite loss of conserved function, the key structural elements have exapted to suit different demands. CRY1 and CRY2 cannot be co-purified with FAD, unlike all other known cryptochromes and photolyases. However, the FAD-binding pocket remains remarkably conserved (Xing et al., 2013). Previous work in the lab demonstrated that while FAD is not used as a catalytic cofactor, FAD is able to bind CRY2 PHR with low affinity (40 μM). Its modest affinity is attributed primarily to the absence of a lid-like seal above by CRY C-terminus and the relative openness of the surrounding outer cavity around the diphosphate arch. When visualized crystallographically from soaked CRY2 crystals, FAD occupies the conserved binding pocket identically to how it is seen in *Drosophila* CRY (Xing et al., 2013). The physiological significance or even possibility of FAD binding to vertebrate CRYs is still unknown. Although the determination of the free FAD concentration in cells is challenging and remains to be rigorously determined, estimates are 0.1–3 μM (Xing et al., 2013; Tu and Weissman, 2002). This is at least ten-fold lower than the $K_d$ of FAD for CRY2 PHR. As such, the ability of vertebrate CRYs to bind FAD may require the presence of an intermediary binding partner to increase the affinity of the FAD-CRY interaction or, more simply, be a evolutionary relic with no physiological significance.

### *2.1.2 Exaptation of the Flavin Pocket to Bind Ubiquitin Ligases*

Although the function of FAD in vertebrate CRYs is unclear, the biological importance of the FAD-binding pocket itself is less enigmatic. Recent work from the lab has explored the structural and biochemical role of the FAD-binding pocket at the interface between FBXL3 ubiquitin ligase and CRY2. Unlike all previously described F-box protein and substrate complexes which recognize a short, phosophorylated degron sequence on the substrate, FBXL3 exploits the cavernous and hydrophobic FAD-binding pocket to insert a C-terminal tryptophan (Xing et al., 2013). Despite their extensive functional divergence, the majority of CRYs are directly coupled to coordinating signalling via ubiquitination and proteosomal degrada-

tion specifically in circadian clockwork. For example, Type I CRYs serve as the primary entrainment photoreceptor in flies; whereupon blue-range illumination dCRY facilitates the degradation of TIM via its ubiquitin ligase JET to release repression and restart the circadian cycle (Koh et al., 2006). In plants, cryptochromes inhibit COP1 ubiquitin ligase to promote photomorphogenesis (Wang et al., 2001). The FBXL3 ubiquitin ligase complex regulates the clock by promoting the ubiquitination and degradation of CRYs (Busino et al., 2007; Godinho et al., 2007; Siepka et al., 2007).

### *2.1.3 Discovery and Function of the Core Clock Modulator KL001*

Using a luciferase reporter system to evaluate clock function, Hirota et al. (2012) revealed several clock-modulating compounds from a high-throughput 60,000 compound screen. One compound KL001, most effectively dose-dependently lengthened the period and attenuated the amplitude. Immunoprecipitation anaylsis showed that an agarose-conjugated compound could purify CRY proteins from cell lines. Further structure-activity relationship assays determined that administration of KL001 could stabilize CRY by inhibiting FBXL3-dependent ubiquitination and subsequent degradation, presumably the cause of the longer period length. CRYs are known to repress the glucagon-dependent up-regulation of several important gluconeogenetic enzymes: phosphoenolpyruvate carboxykinase 1 (PCK1) and glucose-6-phosphatase (G6PC), whose catalysis is the final step of gluconeogenesis and glycogenolysis. To investigate the possible therapeutic applications of this compound, glucagon-induced gluconeogenesis was targeted for obvious links to metabolic syndromes and diabetes. KL001 was ablw to repressed gluconeogenesis in primary hepatocytes suggesting that compounds that bind to core clock proteins can be useful therapies for certain physiological disorders (Hirota et al., 2012).

## *2.2 Structure of CRY2 Bound to KL001*

Part of the material in this chapter is published in: Nangle, S., Xing, W., Zheng, N. (2013), Crystal structure of mammalian cryptochrome in complex with a small molecule competitor

of its ubiquitin ligase. *Cell Research*.

Our recent studies have shown that CRY2-FBXL3 complex formation depends on the insertion of the FBXL3 C-terminal tail into the FAD-binding pocket (Xing et al., 2013). Because FAD can compete with both KL001 and FBXL3 for binding CRYs (Xing et al., 2013; Hirota et al., 2012), we postulated that KL001 might inhibit CRY ubiquitination by occupying its cofactor pocket and impairing its association with FBXL3. It is, however, also possible that the small molecule binds at an allosteric site on CRYs.

To unravel the binding mode of KL001, we co-purified and crystallized murine CRY2 PHR (1–512) with KL001 and determined the complex structure at 1.94 Å resolution (Figure 2.1, Table 2.1) (Nangle et al., 2013). In the crystal, CRY2 adopts an overall structure nearly identical to its apo, FAD-bound, and FBXL3-complexed forms (Xing et al., 2013). The largest conformational differences are limited to two local structural elements: the phosphate-binding loop and the interface loop (Figure 2.6). KL001 can be readily located in the FAD-binding pocket of CRY2. Clear density is found for the majority of the molecule except its furan moiety, which likely has a flexible conformation (Figure 2.2).

The CRY2 cofactor pocket can be subdivided into three parts: an inner cleft accommodating the FAD isoalloxazine moiety, an outer crater occupied by the ribityl and ADP moieties of FAD, and an auxiliary cleft, which is empty (Figure 2.4). KL001 buries its carbazole ring deep into the inner cleft, indicating that the compound targets the clock protein as a cofactor mimic. Despite their analogous tricyclic scaffolds (Figure 2.3), the KL001 carbazole group sterically imitates the outer dimethylbenzene and central pyrazine moieties of the FAD isoalloxazine ring instead of its entire tricyclic system (Figure 2.5).

Associated with this lateral shift of the carbazole ring, the rest of KL001 significantly deviates from the FAD cofactor. Instead of interacting with the outer crater, the methanesulfonamide group of KL001 is anchored at an outer vestibule of the FAD-binding pocket, where the FBXL3 C-terminal tail enters in the FBXL3-CRY2 structure (Figure 2.5). Overall, the clock-modulating small molecule represents a molecular chimera—one half of it resembles

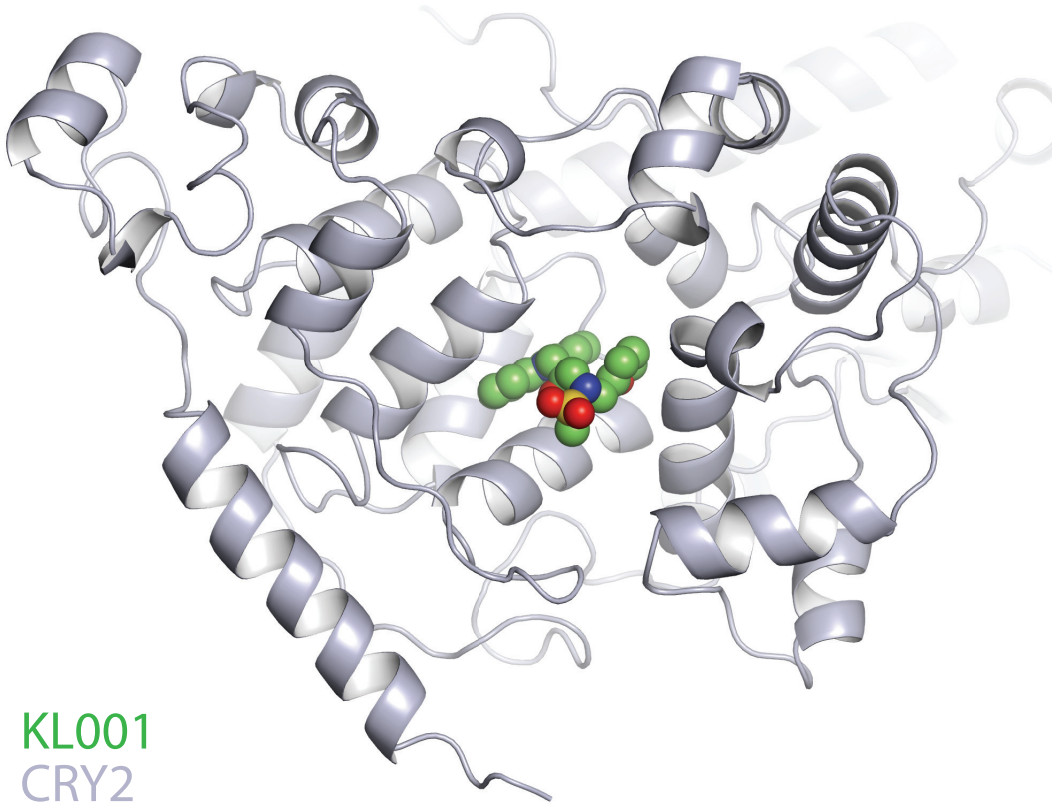


Figure 2.1: **Clock-modulating compound KL001 binds to CRY FAD-binding pocket.** Overall structure of CRY2 shows the binding mode of KL001 occupying the large flavin pocket.

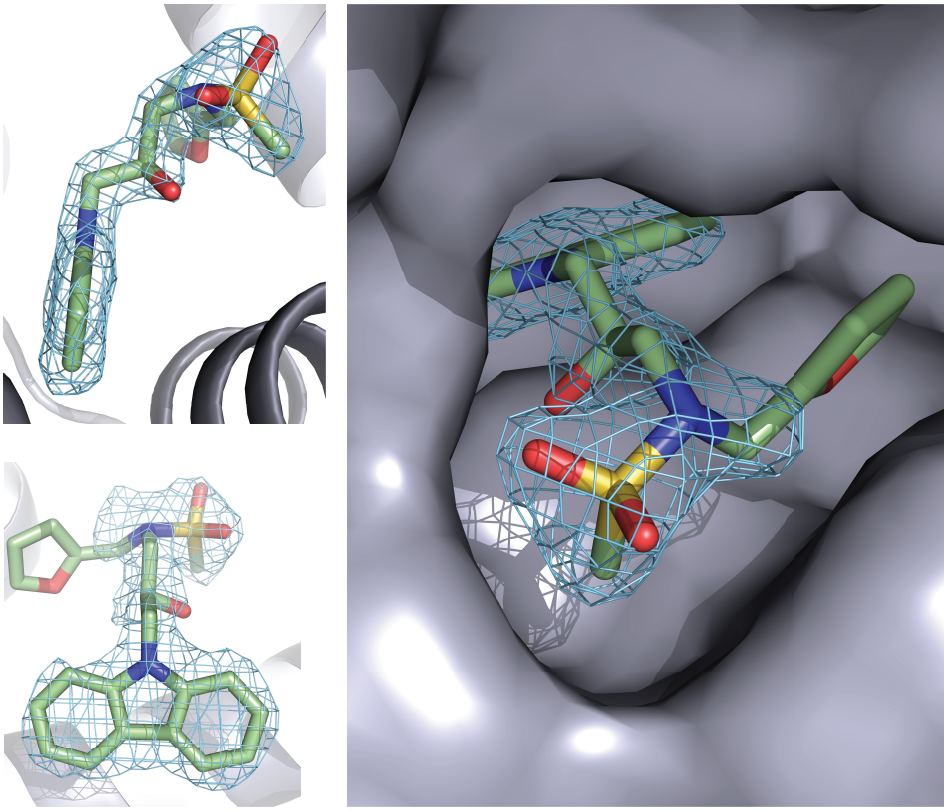

Figure 2.2: ***Fo-Fc* Difference Map of KL001.** Three close-up views of KL001 bound to CRY2 with *Fo-Fc* electron density contoured at 3.5 σ and calculated before the compound was built.

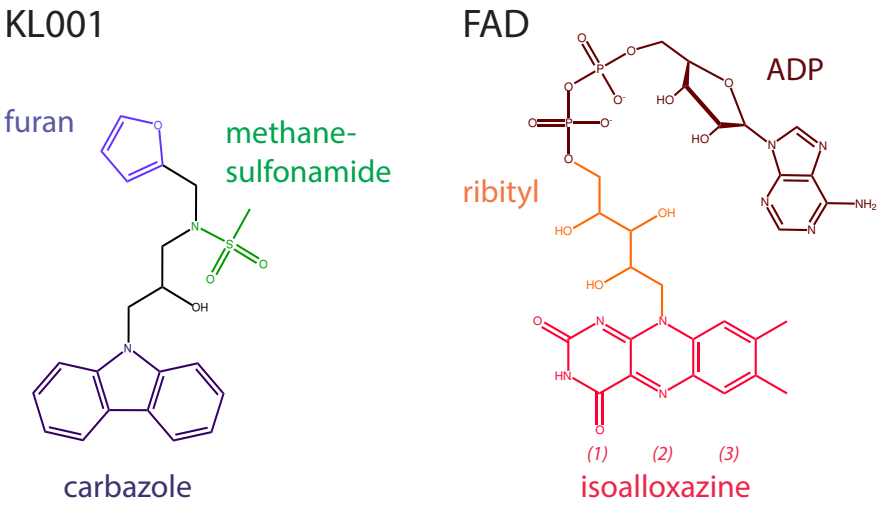


Figure 2.3: **Structural Homology Between FAD and KL001.** FAD and KL001 with their functional groups labeled. Subdivisions of the isoalloxazine ring: (1) pyrimidine, (2) pyrazine, (3) dimethylbenzene.

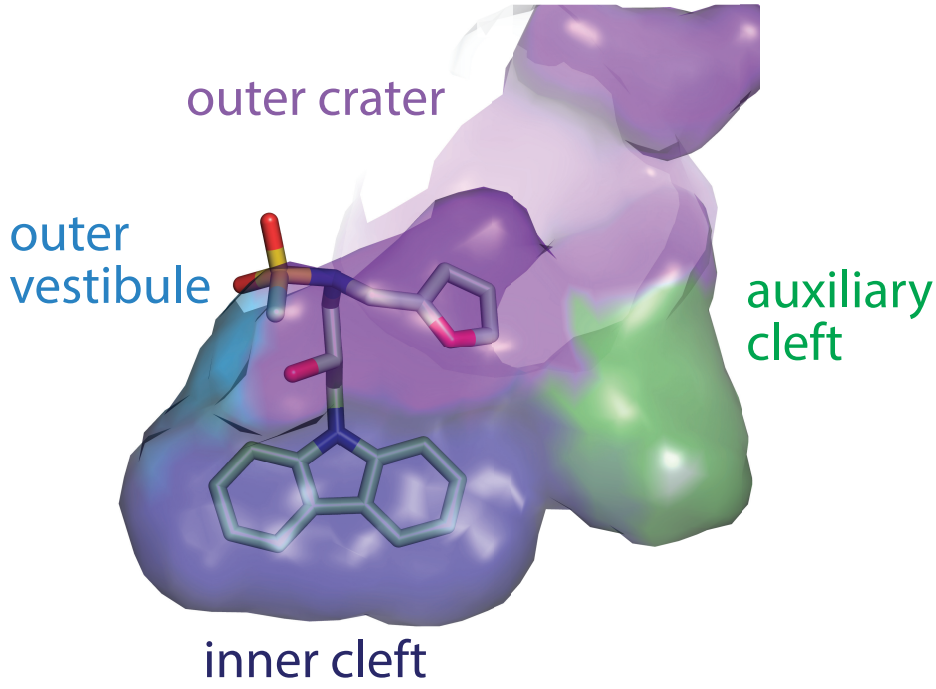


Figure 2.4: **Subdivisions of the FAD-binding Pocket.** Docking of the KL001 carbazole ring at the inner cleft (blue) of the FAD-binding pocket with the nearby auxiliary cleft (green), the outer crater (purple) and part of the outer vestibule shown.

part of the FAD cofactor and the other half sterically imitates the tail of the ubiquitin ligase. Consistent with previous studies showing that both free FAD and point mutations of two inner cleft residues in CRY1, D387N and N393D (D405 and N411 in CRY2), are each capable of abolishing KL001-CRY1 interaction (Hirota et al., 2012) and highlight the carbazole moiety as a critical moiety for CRY binding.

By stabilizing CRYs, KL001 has been shown to inhibit glucagon-induced gluconeogenesis in hepatocytes, suggesting a therapeutic potential for diabetes (Hirota et al., 2012). The CRY2-KL001 complex structure provides structural basis for further improving its potency. For example, functional groups can be introduced to exchange out the methanesulfonamide and/or to one end of its carbazole ring, which would mimic the pyrimidine portion of the FAD isoalloxazine ring that forms two hydrogen bonds with CRY2 (Figure 2.5A). Such modifications can be further extended to exploit the nearby auxiliary cleft of the FAD-binding pocket, which is enriched in polar amino acids.

### *2.3 Structural Features of the Phosphate-binding Loop*

Distinct from non-vertebrate CRYs and their closely related photolyases, mammalian CRYs feature an open and dynamic FAD-binding pocket characterized by a flexible phosphate-binding loop and a moderate affinity of FAD binding (Xing et al., 2013). Unexpectedly, our structure reveals an ordered phosphate-binding loop, which adopts a well-defined conformation in the crystal (Figure 2.6A). When modeled onto the structure of FAD-bound CRY2, this ordered loop is still well-removed from the cofactor ($>$ 5.3 Å) and the FAD-binding pocket remains largely open to the solvent (Figure 2.6B). In contrast, the same loop in *Drosophila* (6-4)photolyase, which shares a sequence identity of 53% with CRY2, folds into a lid and traps the cofactor within the pocket as a prosthetic group (Figure 2.7) (Maul et al., 2008).

Because the phosphate-binding loop is located at the opposite end of the FAD-binding pocket to KL001 (Figure 2.6), its ordered structure is likely attributable to crystal packing instead of compound binding. Indeed, crystal analysis shows that the phosphate-binding loop

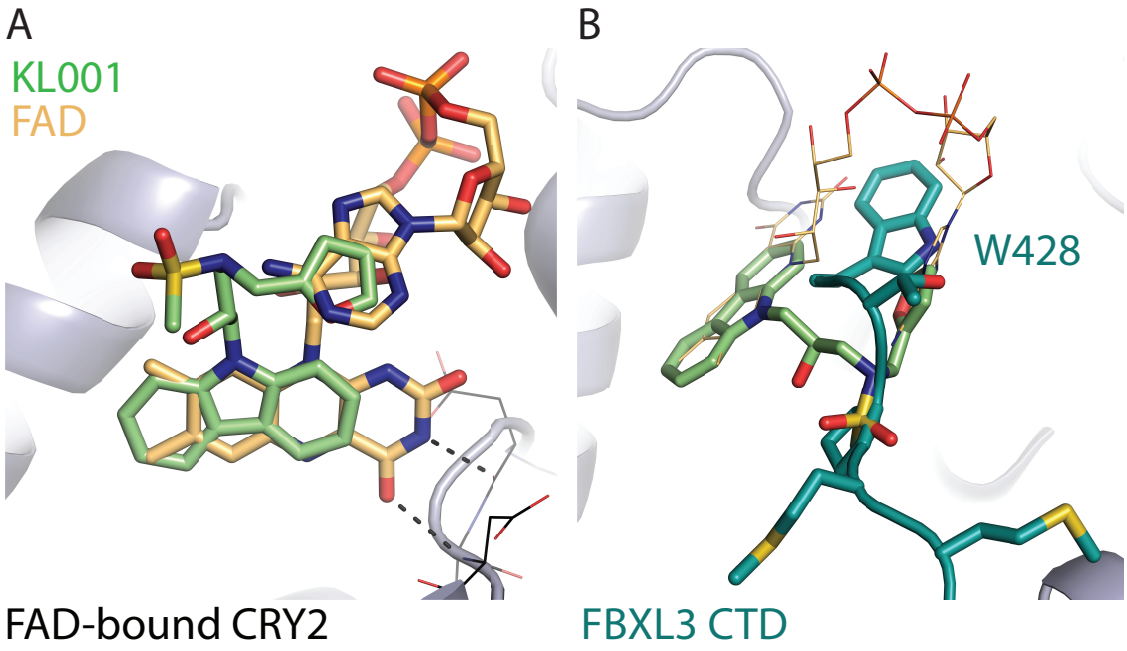


Figure 2.5: **KL001 Structurally Mimics FAD and FBXL3 C-terminus.** A. A comparison of KL001 and FAD bound to CRY2. FAD is modeled onto the KL001-bound CRY2 (ribbon diagram) by CRY2 superposition. Two hydrogen bonds formed between the backbone of FAD-bound CRY2 (line representation) and the pyrimidine moiety of the FAD isoalloxazine ring are shown. B. Another view of CRY2-bound KL001 in comparison with FAD (line representation) and the C-terminal tail of FBXL3 (teal).

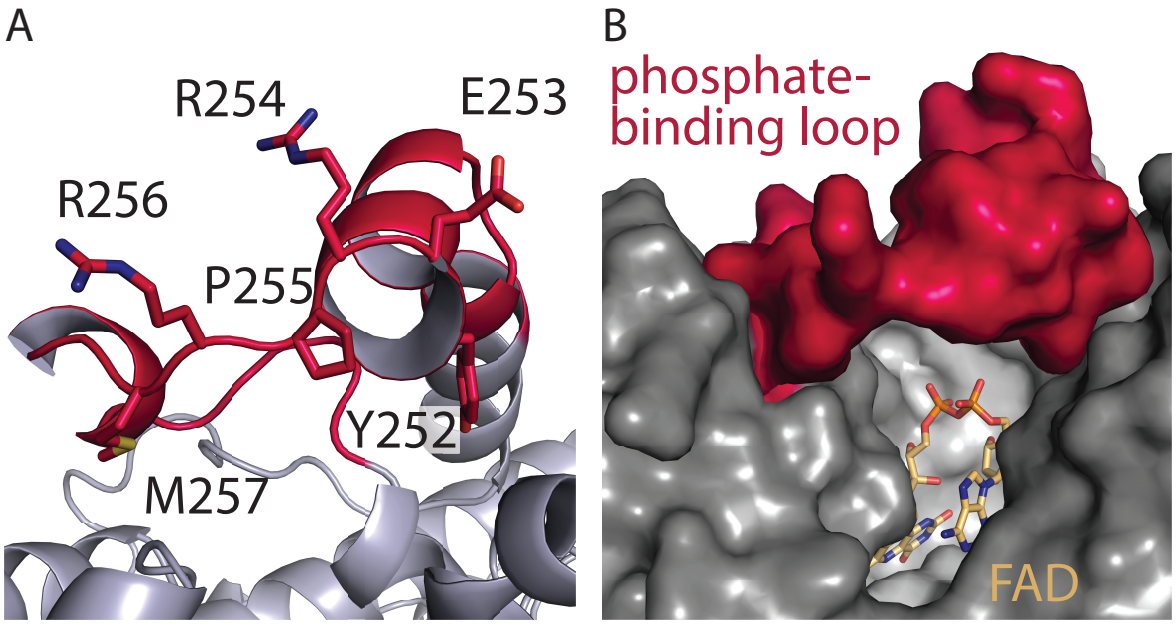


Figure 2.6: **Stabilization of the Phosphate-binding Loop.** A. Conformation of the ordered phosphate-binding loop of CRY2 with highly conserved but solvent-exposed residues. B. A model of FAD-bound CRY2 with an ordered phosphate-binding loop showing an open cofactor pocket.

is in close contact with a C-terminal tyrosine residue from an adjacent molecule, which approaches the FAD-binding pocket under the loop. In conjunction with its strictly-conserved sequence among vertebrate orthologs, the structural sensitivity of the phosphate-binding loop to its immediate environment implicates an important role in protein–protein interactions. We speculate that these interactions might increase the affinity of FAD and enable the cofactor to regulate the activity, and possibly stability, of CRYs in a manner analogous to the function of the dCRY C-terminal tail (Zoltowski et al., 2011).

### *2.4 Conclusions*

KL001 is the first-in-class cryptochrome-targeting circadian modulator and substrate-targeting ubiquitination antagonist. The crystal structure of the CRY2-KL001 complex not only reveals its novel mechanism of action as a cofactor-mimicking interfacial inhibitor but also makes further development possible to realize its full therapeutic potential.

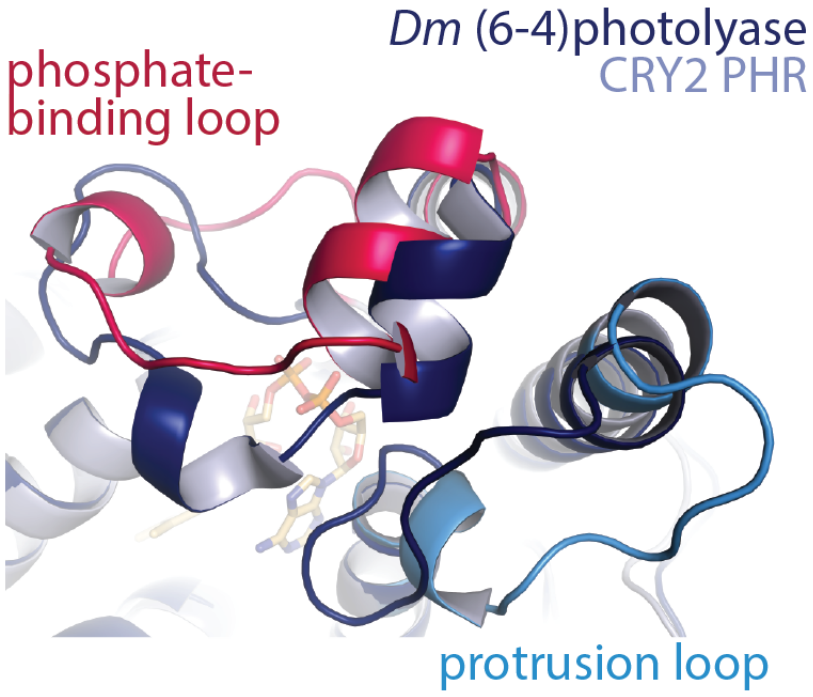


Figure 2.7: **Comparison of Loops in Vertebrate CRY and Invertebrate Photolyase.** A structural comparison between KL001-bound murine CRY2 (grey) and *Drosophila* (6-4)photolyase (dark blue) showing the phosphate-binding loop (pink in CRY2) and its nearby protrusion loop (light blue in CRY2). FAD is modeled in to replace KL001.

| | CRY2-KL001 |
|---|---|
| Data collection | |
| Space group | P1 |
| Cell dimensions: | |
| a, b, c (Å) | 48.1, 93.8, 141.6 |
| $\alpha$, $\beta$, $\gamma$ (°) | 90.1, 90.0, 90.3 |
| Resolution (Å) | 50–1.94 (1.98–1.94) |
| $R_{sym}$ / $R_{merge}$ | 0.079 (0.601) |
| I/$\sigma$I | 32.2 (3.6) |
| Completeness (%) | 97.1 (95.1) |
| Redundancy | 3.7 (3.8) |
| | |
| Refinement: | |
| Resolution (Å) | 1.94 |
| No. reflections | 170540 |
| $R_{work}$ / $R_{free}$ | 0.180 / 0.217 |
| No. atoms | |
| Protein | 16060 |
| Ligand/ion | 112 |
| Water | 1557 |
| B-factors | |
| Protein | 32.37 |
| Ligand/ion | 32.25 |
| Water | 36.97 |
| R.m.s. deviations | |
| Bond lengths (Å) | 0.007 |
| Bond angles (°) | 1.087 |

Table 2.1: Data collection and refinement statistics for CRY2-KL001. Values in parentheses are for highest-resolution shell.

# Chapter 3

# ARCHITECTURE OF THE CO-REPRESSOR COMPLEX

## *3.1 Introduction*

Proper oscillation of the clock depends on the complex formation and periodic turnover of the Period and Cryptochrome proteins, which together inhibit their own transcriptional activator complex, CLOCK-BMAL1. We determined the crystal structure of the CRY-binding domain (CBD) of PER2 in complex with CRY2 at 2.8 Å resolution. PER2-CBD adopts an meandering conformation around CRY2. Its N-terminus tucks into CRY near the antenna cofactor binding pocket, which we rename the repression pocket as it is critical for CLOCK-BMAL1 binding. The CBD C-terminal half winds around to flank the CRY2 C-terminal helix and sterically hinders the recognition of CRY2 by FBXL3. Unexpectedly, a strictly conserved intermolecular zinc finger, whose integrity is important for clock rhythmicity, further stabilizes the complex. Our structure-guided analyses show that these interspersed CRY-interacting regions represent multiple functional modules of PERs at the CRY-binding interface.

The canonical clock mechanism, which was established on genetic studies, suggested that CRYs are the predominant inhibitors of CLOCK-BMAL1 (Griffin et al., 1999; Kume et al., 1999). Independent of PERs, over-expressed CRY1 and CRY2 can each potently inhibit the CLOCK-BMAL1-induced transcription of a luciferase reporter gene in cultured cells (Griffin et al., 1999; Kume et al., 1999). This transcriptional repression activity of CRYs likely occurs through their direct interactions with BMAL1 (Griffin et al., 1999; Shearman et al., 2000; Partch et al., 2014) and CLOCK (Huang et al., 2012). Later biochemical investigation revealed that despite the important repressor function of CRYs, the PER proteins have been suggested as the rate-limiting factor of the rhythmic negative feedback loop (Lee et al., 2001).

Contingent upon its tightly regulated phosphorylation and ubiquitination states during the circadian cycle, PERs mediate diverse circadian mechanisms, including: the formation of the PER-CRY complexes and their nuclear localization (Lee et al., 2001), epigenetic regulation of clock genes (Duong et al., 2011), stabilization of CRY in the nucleus (Busino et al., 2007; Siepka et al., 2007), and dynamic control of the formation of core clock machinery on and off chromatin (Ye et al., 2014).

### *3.1.1 PER-mediated Nuclear Translocation of CRY*

Each core clock component undergoes rhythmic changes throughout the day. However of the four, PERs exhibit the most striking circadian changes in modification, sub-cellular localization, and function. And timing of nuclear localization is essential to create rhythms (Öllinger et al., 2014). Recent live-cell imaging studies show PER2 as a critical shuttling component and putative scaffold upon which the negative clock elements assemble and whose import is accelerated by association with CRY1 (Öllinger et al., 2014). Both PERs are hyperphosphorylated by CK1 in the cytoplasm, which appears to facilitate complex formation with CRYs and nuclear shuttling (Lee et al., 2001; Yagita et al., 2002). While CRY levels remain relatively stable in the cytoplasm, their nuclear localization is correlated to increases in phosphorylation and subsequent translocation of PERs with peak levels of both in mid-evening (CT 18). This indicates that there is a cytoplasmic pool of CRYs and PERs are rate-limiting. Both PER levels and phosphorylation state are critical for maintaining robust rhythms. Over-expression of the primary PER kinase CK1$\epsilon$ does not significantly change PER activity or rhythms. Rather, it is PER levels that limit phosphorylation and abolish rhythms when constitutively over-expressed (Lee et al., 2001; Chen et al., 2009; McCarthy et al., 2009). Phosphorylation of PERs is integrated in many facets of its function. While the details are not largely well understood, consistent data relates PER phosphorylation to nucleocytoplasmic shuttling. Indeed, these phosphorylation events are so critical that there is evidence that CK1$\epsilon$ migrates with the PER-CRY complex into the nucleus (Lee et al., 2001; Öllinger et al., 2014; Vanselow and Kramer, 2007).

### *3.1.2 Epigenetic Regulation of Clock Genes*

Once in the nucleus, PERs might physically bridge CRYs and other repression proteins and CLOCK-BMAL1 and promote their interactions (Chen et al., 2009). PER rhythmically assembles with CLOCK-BMAL1 in a large chromatin-bound complex and is able to recruit the histone deacetylating SIN3-HDAC complex, which facilitates the subsequent recruitment of transcriptional repression proteins (Duong et al., 2011). SIN3-HDAC is conserved in almost all eukaryotes and its ancestors may have played a crucial role in the origins of the transcription-translation-based feedback circadian clock pathways. Additionally, PER can also inhibit RNA termination by antagonizing SETX, a termination helicase, at the 3 termination site (Padmanabhan et al., 2012). PER therefore exerts transcriptional control across two venues; at both transcription initiation and termination.

### *3.1.3 PER-dependent Stabilization of CRY*

Cyclic degradation of PERs and CRYs represents another crucial step in the negative feedback loop. The F-box proteins β-TrCP and FBXL3 have been discovered as the key ubiquitin ligases, responsible for promoting the polyubiquitination of PERs and CRYs, respectively (Busino et al., 2007; Siepka et al., 2007; Reischl et al., 2007; Shirogane et al., 2005; Godinho et al., 2007). Phosphorylation of a degron sequence serves as the signal for PER ubiquitination by β-TrCP (Shirogane et al., 2005), whereas recognition of CRYs by FBXL3 is made through a large protein interface without the involvement of a canonical degron motif or any post-translational modification (Xing et al., 2013). While there is *in vivo* evidence for CRY phosphorylation by AMPK at solvent-exposed Ser71 and to a lesser degree buried Ser280 in CRY1 (Ser89 and Ser298 in CRY2), which leads to increased FBXL3 binding and subsequent degradation of CRY (Lamia et al., 2009), the structure of this complex does not inform a possible mechanism. Not only is a high affinity complex formed between FBXL3 and CRY without any detectable phosphorylation at these sites, but both serines are quite distant from the binding interface 14.5 Å for Ser89 53 Å for Ser298, for the shortest distances to

FBXL3 (Xing et al., 2013). It remains possible that these phosphorylation sites regulate CRY stability independent of FBXL3 or act in combination with other proteins in ways that are non-obvious from the structure. These residues have also been implicated in PER binding. Phosphomimetic mutant in CRY1 (S71D) abolished PER2 binding in co-IP suggesting overlapping interface surfaces. Nevertheless, in our *in vitro* recombinant system, the CRY-FBXL3 interface is susceptible to disruption by both the CRY cofactor FAD and the PER proteins (Xing et al., 2013). Importantly, nuclear PER protects CRY from ubiquitination and consequent degradation by competing directly with FBXL3 for CRY binding (Czarna et al., 2013; Xing et al., 2013; Yoo et al., 2013; Hirano et al., 2013).

### *3.1.4 Dynamic Remodelling of Circadian Repression Complexes*

Although genetic studies have firmly established a central role of PERs in clock regulation, the molecular mechanisms by which PERs orchestrate the dynamic clock protein network remain elusive. Binding of PERs to CRYs, CLOCK, and BMAL1 have been detected both *in vivo* and *in vitro* (Ye et al., 2011; Kiyohara et al., 2006; Partch et al., 2014). However, the role of PER2 in coordinating the repression complex assembly is controversial. In addition, how PER-CRY interaction might interfere with FBXL3 for CRY binding also remains unclear.

CRY has also been demonstrated to bind and repress the transcriptional activity of CLOCK-BMAL1 independent of PERs on and off E-box DNA (Koike et al., 2012; John et al., 2014). In contrast, PERs alone cannot affect CLOCK-BMAL1 binding to chromatin or transcriptional activity in a CRY1–2 DKO cell line (Ye et al., 2014). They can, however, disrupt the CRY-CLOCK-BMAL1 complex on E-box DNA and chromatin *in vitro* and *in vivo*, respectively (Ye et al., 2011, 2014). Taken together, CRYs can inhibit CLOCK-BMAL1-mediated transcription on chromatin, perhaps by directly competing with transcriptional co-activators (e.g., CREB-binding protein, p300-CBP) (Partch et al., 2014). PERs can also exert comparable repressional control over the clock it does so by dislodging CRY-CLOCK-BMAL1 pre-formed complex from chromatin (Figure 3.1) (Ye et al., 2014). Here, we report the crystal structure of a PER2-CRY2 complex, which provides a missing structural

framework for understanding the multiple functions of PERs in driving the molecular clock.

In an effort to resolve these biochemical discrepancies and to start assembling the core clock machinery, we purified a representative PER2-CBD-CRY2-PHR complex and determined its crystal structure at a resolution of 2.8 Å (Figure 3.2, Table 3.1) (Nangle et al., 2014).

### *3.2 The PER CRY-binding Domain*

Mammalian PER1 and PER2 share 50% sequence identity and a common domain architecture comprised of tandem N-terminal PER-ARNT-SIM (PAS) domains, a central CK1δ/ε-binding region, and a ∼100 amino acid-long C-terminal CRY-binding domain (CBD), which is necessary and sufficient for CRY binding (Yagita et al., 2002). The isolated PER2 CBD can stabilize CRY1/2 *in vivo* and compete with FBXL3 for CRY1/2 binding *in vitro* (Xing et al., 2013; Chen et al., 2009). In mouse embryonic fibroblasts (MEFs), over-expression of PER2-CBD alone was able to completely disrupt the circadian bioluminescence rhythm of the luciferase activity of a $Per^{Luc}$ reporter gene (Chen et al., 2009). To first characterize the PER-CRY interaction, we performed an alanine-scanning mutagenic analysis of PER2-CBD. We initially targeted stretches of residues strictly conserved among vertebrate PER1–2 orthologs (Figure 3.4A). Surprisingly, none of the 10 single mutants, which were distributed along the length of the CBD, showed any detectable defect in CRY1 binding. The PER2-CRY1 interaction was only abolished when alanine mutations were simultaneously introduced to two adjacent stretches of residues in the C-terminal, but not N-terminal half of PER2-CBD (Figure 3.2B-C). These results suggesting an unusual binding mode of PER2-CBD onto CRYs and the importance of the C-terminal half of the CBD in complex formation.

### *3.3 Overall Architecture of CRY2-PER2 Complex*

Part of the material in this chapter is published in: Nangle, S.N., Rosensweig, C., Koike, N., Tei, H., Takahashi, J. S., Green, C. B., & Zheng, N. (2014), Molecular Assembly of the

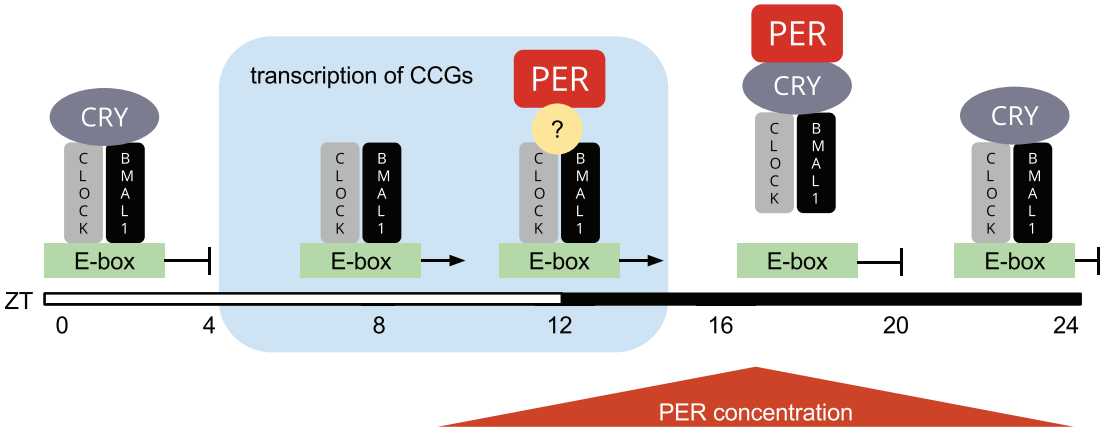


Figure 3.1: **Model of Molecular Timing in the Mammalian Clock.** A semi-quantitative schematic based on protein expression and ChIP data in liver, which seeks to reconcile seemingly conflicting biochemical data. At ZT 0, CRY levels are high and bound to CLOCK-BMAL1 on chromatin, repressing transcription. As their levels begin to decrease as a result of low PER levels and increased degradation, CLOCK-BMAL1 are able to activate the transcriptional program. Their activity peaks around ZT 8 when nuclear CRY levels are at their nadir. As PER levels start increasing they (in)directly interact with CLOCK-BMAL1 on DNA but cannot repress transcription alone, instead it primes the transcription activation complex for eventual CRY recruitment and displacement from chromatin around ZT 18. Later, as PER levels decline, CRY alone is bound to CLOCK-BMAL1 and renews the cycle. Adapted from (Ye et al., 2014).

Period-Cryptochrome Circadian Transcriptional Repressor Complex. *eLife*.

Mammalian CRY1 and CRY2 paralogs contain a highly similar photolyase-homology region (PHR) and a more diverse cryptochrome C-terminal extension (CCE) sequence (Figure 3.3). Their PER-binding activity has previously been mapped to the PHR, which is made of an $\alpha/\beta$ photolyase domain and an $\alpha$-helical domain (Figure 3.2). Consistent with their high sequence homology (86%), the crystal structures of CRY1-PHR and CRY2-PHR can be superimposed with a root-mean-square deviation (RMSD) of 0.43 Å out of 377 aligned C$\alpha$ atoms.

The PER2-CBD adopts a highly extended structure, which is devoid of a hydrophobic core. It folds into five $\alpha$-helices of variable length, which are dispersed along an otherwise linear polypeptide (Figure 3.2). In the crystal, PER2-CBD meanders along one side of CRY2-PHR and sinuously wraps around the region. With nearly half of the PER2 residues involved in binding, the two proteins bury a total 2800 Å$^2$ of solvent accessible surface area at the interface, which stretches over a distance of approximately 215 Å. This unusually extensive interface provides a plausible explanation for the high-affinity binding between the two clock proteins and their insensitivity to mutational disruption (Figure 3.4B).

In comparison to its FBXL3-, KL001-, and FAD-complexed forms, CRY2 adopts the same global fold when bound to PER2-CBD (Figure 3.18). The largest structural variations take place in two local regions: the interface loop next to the FAD-binding pocket and a serine-rich loop neighboring a back pocket. The majority of PER2-contacting residues on CRY2 (85%) are strictly conserved between mammalian CRY1 and CRY2, suggesting that the two cryptochrome proteins share a common PER2 binding mode.

### *3.4 Interactions at the CRY2 C-terminal Helix*

The two stretches of residues, whose alanine mutations abrogated CRY1 binding, are mapped to a loop flanked by two $\alpha$-helical regions in the C-terminal half of PER2 (Figure 3.2C). The PER2-CBD $\alpha$3 helix preceding this loop packs against the long CRY2 C-terminal helix at an

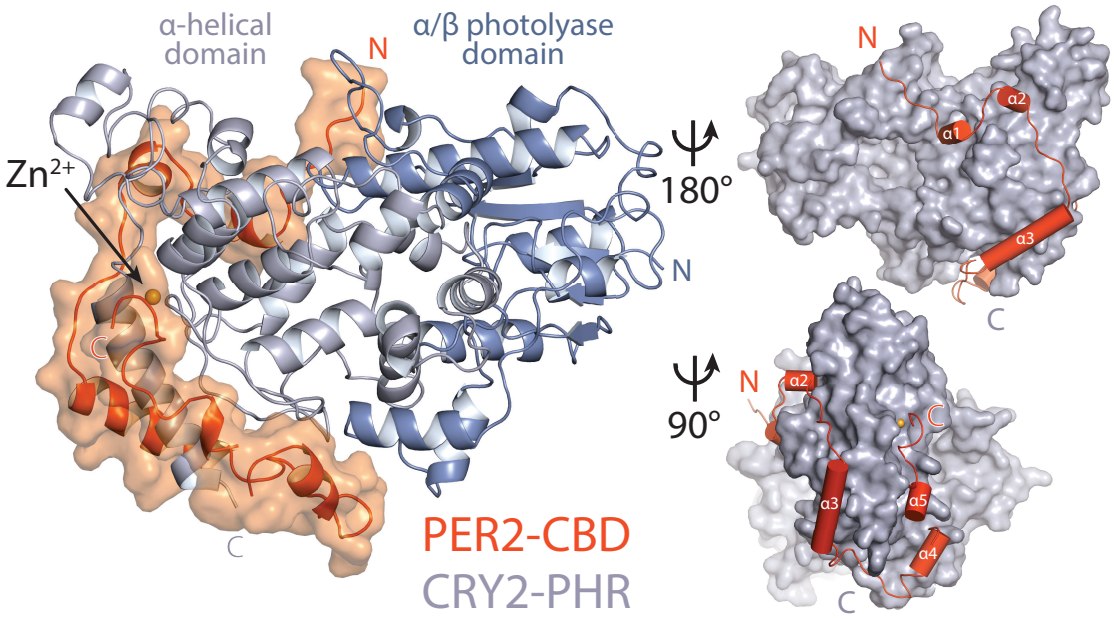


Figure 3.2: **Architecture of PER2-CRY2 Complex.** CRY2 PHR (gray) adopts an overall fold identical to its apo and complexed forms (e.g., FAD, FBXL3, and KL001). PER2 CRY-binding domain (CBD) (orange) shows a highly extended binding mode around CRY2. PER2 flanks the CRY2 C-terminal helix and coordinates a zinc ion with CRY2 within a CCCH-type intermolecular zinc finger motif.

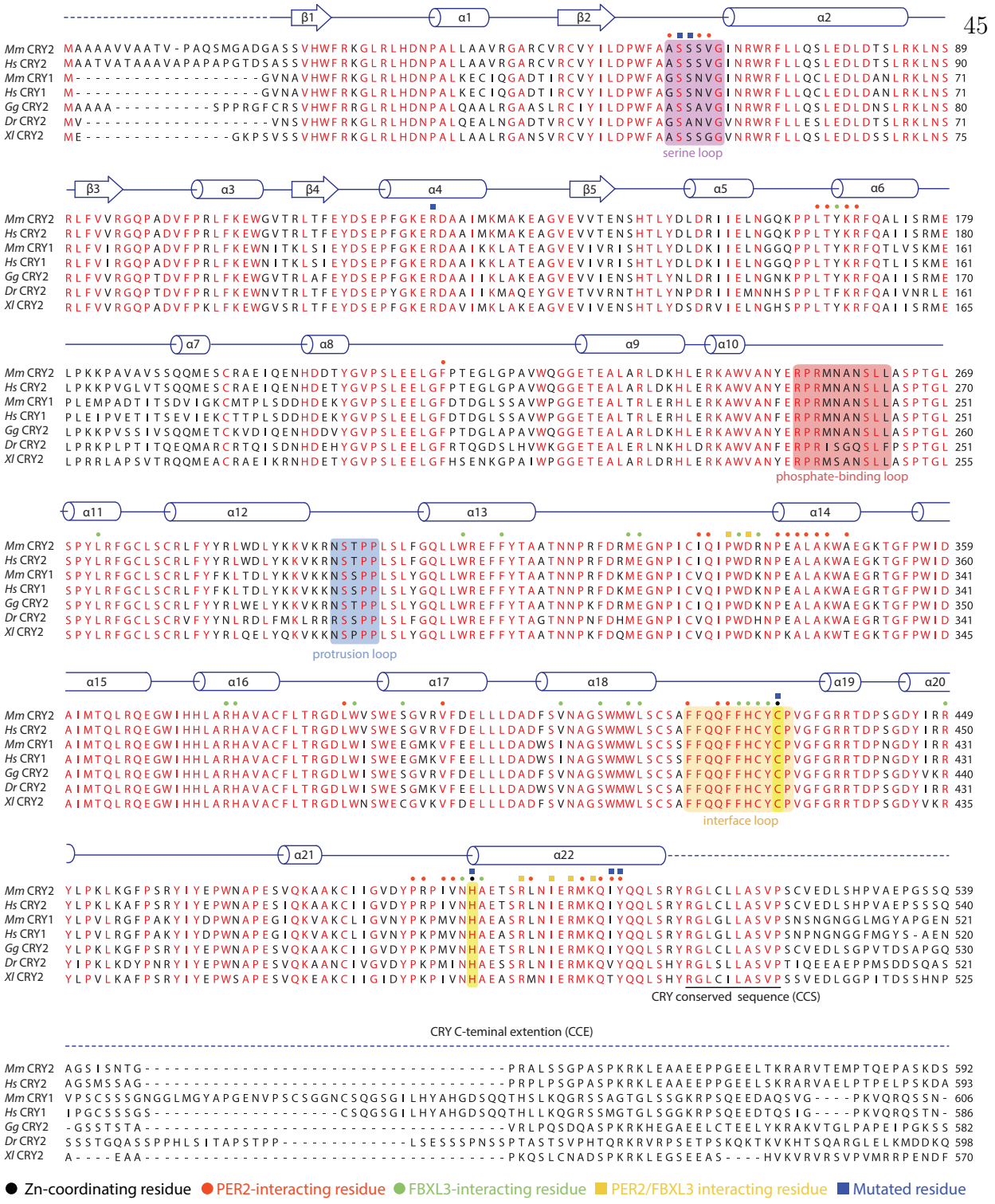


Figure 3.3: **Sequence Alignment and Secondary Structure of Vertebrate CRY.** Alignment and secondary structure assignments of CRY2 orthologs from Mus musculus (Mm), Homo sapiens (Hs), Gallus gallus (Gg), Danio rerio (Dr), and Xenopus laevis (Xl). Strictly conserved residues are colored in red. Blue and green dots indicate mPER2-CBD-, and hFBXL3-interacting residues, respectively. Yellow squares indicate residues that interact with both PER2 and FBXL3. Black dots indicate residues that are involved in zinc coordination. Colored boxes represent the boundaries of structurally dynamic loops. Dashed lines represents the regions outside the PHR.

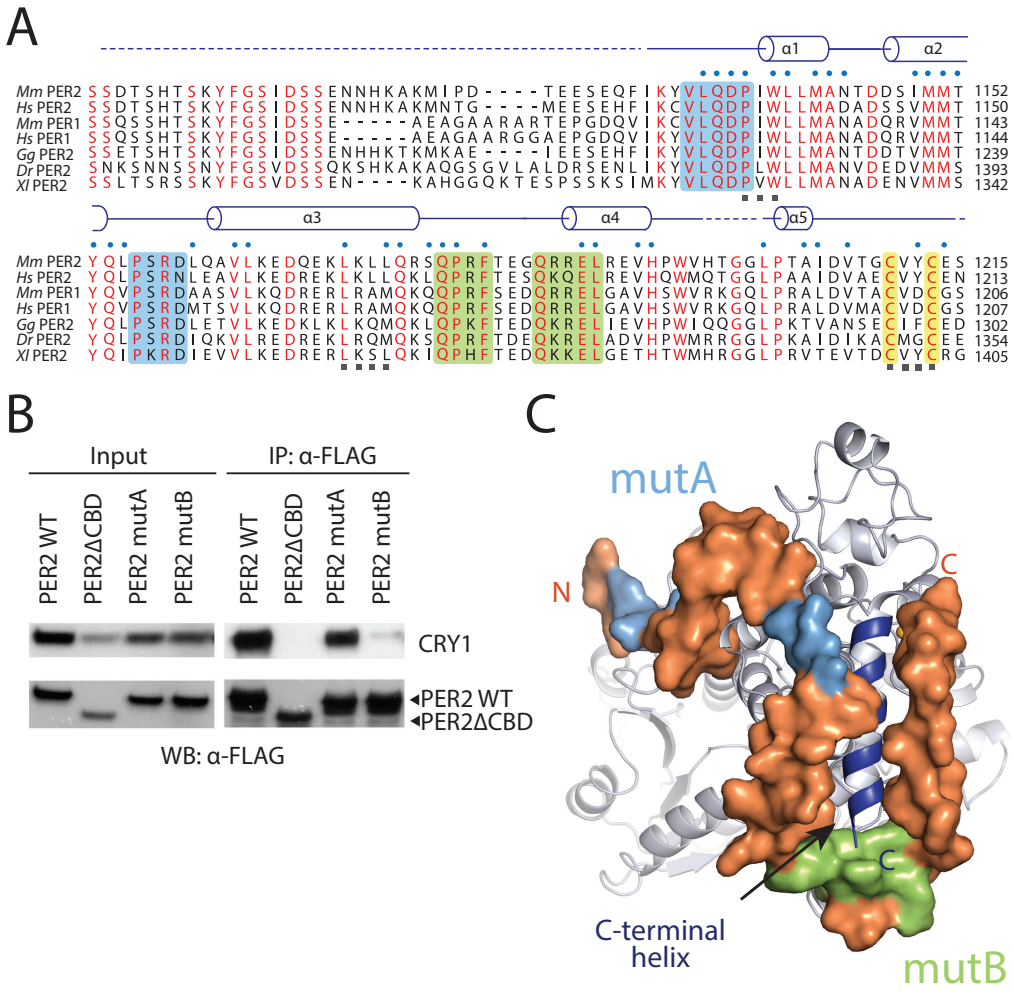


Figure 3.4: **The PER CRY-binding Domain.** A. PER2 CBD sequence alignment. 49% of PER2 CBD residues interact with CRY2 (blue dots). The zinc-coordinating residues are conserved throughout vertebrates (highlighted in yellow). Blue and green boxes correspond to the mutA and mutB constructs, respectively, and indicate regions of PER2-CBD that were mutated to alanines. Dashed lines indicate crystallographically disordered regions. Black squares indicate residues mutated under structure guidance. B. Co-immunoprecipitation of mutant PER2-CBD-FLAG constructs. Only mutB was able to abolish CRY1-MYC binding. Western blot of an immunoprecipitation of COS7 cells were transfected with PER2-NLS-FLAG and CRY1-MYC. Proteins were precipitated with α-FLAG and then analyzed by Western blots using α-MYC and α-FLAG. C. Crystallographic data identify the location of alanine scanning mutants. Importantly, the mutB construct is centered around the CRY2 C-terminal helix.

approximately 30° angle, while the region C-terminal to the loop locks onto the same CRY2 helix from the other side (Figure 3.4C). Together, these PER2-CBD structural elements encircle the CRY2 C-terminal helix like an U-shaped clamp. Arg501 and Lys503 in the CRY2 C-terminal helix have previously been documented to be important for PER2 binding (Ozber et al., 2010). In the crystal, these two positively charged residues of CRY2 project in opposite directions and latch onto the surrounding PER2 regions by forming salt bridges with Asp1167 and Asp1206, respectively (Figure 3.5B). To confirm the critical role of the CRY2 C-terminal helix in binding PERs, we mutated two hydrophobic residues, Ile505 and Tyr506, at the end of this CRY2 helix, which are involved in fixing the α-helix to the rest of the CRY2 α-helical domain (Figure 3.6A). As expected, mutating both residues to aspartate completely abolished the PER2-binding activity of CRY2 (Figure 3.5B). The same effect was also achieved when negative charges were introduced to the side chains of a stretch of four nearby residues (amino acids 1171–1174) in the α3 helix of PER2-CBD (Figure 3.5C). Based on these results, we conclude that the CRY2 C-terminal helix represents a key anchoring site for PER2 binding.

The close interaction between the C-terminal half of PER2-CBD and CRY2 C-terminal helix is immediately reminiscent of the docking mode between FBXL3 and CRY2. In the crystal structure of the FBXL3-CRY2 complex, the leucine-rich repeat (LRR) domain of FBXL3 engages CRY2 at the same site as PER2-CBD does in the PER2-CRY2 complex. The interface between FBXL3-LRR and CRY2 is also centered around the long C-terminal helix of the cryptochrome protein. In fact, the CRY2 surface regions involved in contacting FBXL3-LRR and PER2-CBD share extensive overlapping regions (Figure 3.6A). Superposition analysis reveals that FBXL3 and PER2 cannot be simultaneously engaged with CRY2 without clashing (Figure 3.7). PERs, therefore, have the capability of protecting CRYs from FBXL3-mediated ubiquitination and degradation by directly competing with the ubiquitin ligase for binding CRYs.

To functionally characterize the multiple interfaces on CRYs mapped by the crystal structures, we systematically assessed several representative CRY mutants for their abilities to

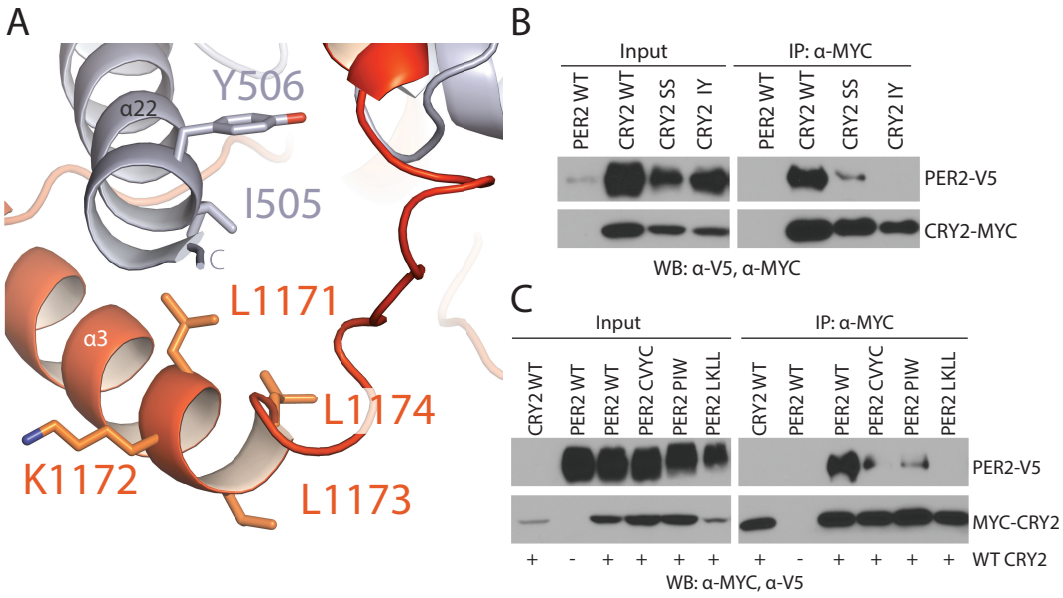


Figure 3.5: **Interacting Residues Around the CRY2 C-terminal Helix.** A. A close-up view of the PER2-CRY2 interface at the end of CRY2 C-terminal helix. While the upper portion of the CRY2 C-terminal helix maintains ionic interactions with PER2, the lower is predominantly mediated by hydrophobic interactions. CRY2 and PER2 residues chosen for subsequent mutational analysis are shown in sticks. B. Concurrent mutations of hydrophobic residues on the CRY C-terminal helix (I505D and Y506D) prevent PER-CRY complex formation. Similarly, the PER-CRY complex is compromised with a S44D and S45D (SS) mutation C. Diminished PER2-CRY2 interaction was replicated in a co-immunoprecipitation assay, in which the CXXC motif of the full-length FLAG-tagged PER2 protein was mutated to four alanines. Binding is also affected when the N-terminal PIW or the the hydrophobic LKLL sequence is mutated to alanines. Co-immunoprecipitations were performed with transfected full-length PER2-V5 and MYC-CRY2 in HEK293 cells with $\alpha$-MYC beads and analyzed by Western blotting using $\alpha$-V5 and $\alpha$-MYC.

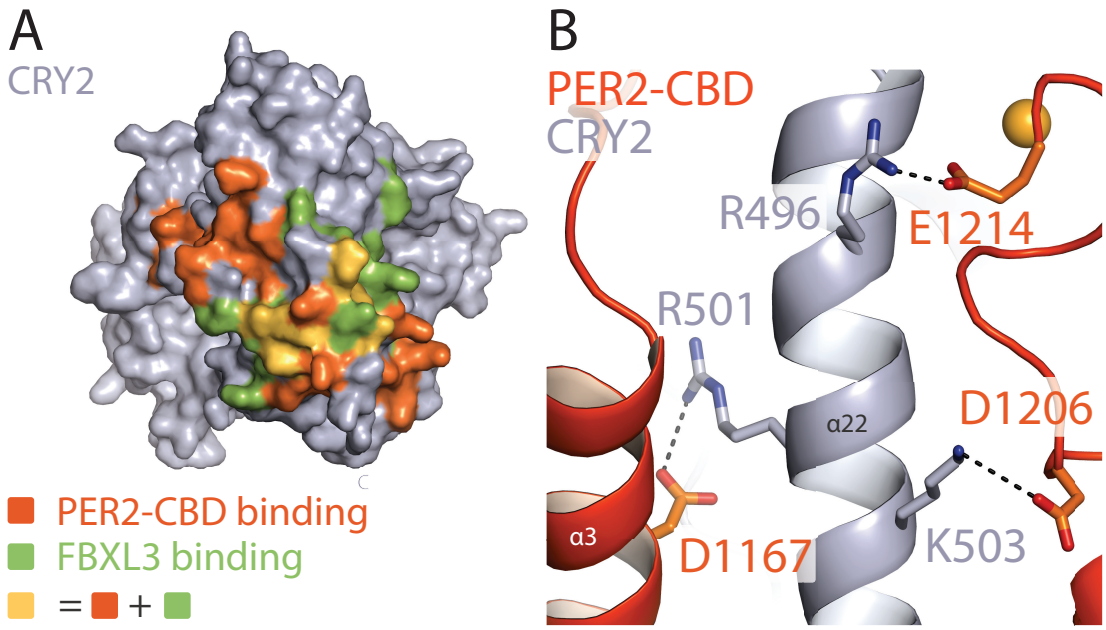


Figure 3.6: **CRY2 C-terminal Helix is the Central Locus of Both PER2 and FBXL3 Interactions.** A. Surface mapping of FBXL3- and PER2-binding sites on CRY2. Residues that share contacts with PER2 and FBXL3 are colored in yellow and are clustered along the C-terminal helix. Other residues involved in binding PER2 and FBXL3 are colored in orange and green, respectively. B. PER2 (orange) forms three salt-bridges along CRY2 C-terminus helix (gray) R501 and K503 have been previously reported as critical binding residues.

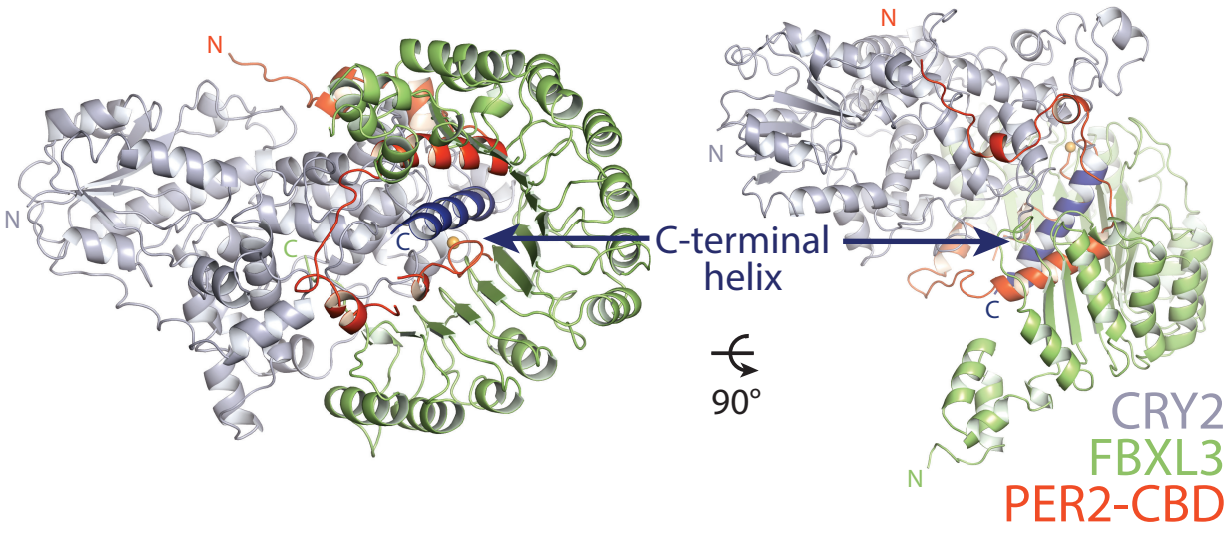


Figure 3.7: **Mutually Exclusive Binding of PER2 and FBXL3 on CRY.** Superimposition analysis demonstrates the direct competition of PER2-CBD (orange) and FBXL3 (green) binding to CRY (gray), which is centered around the CRY2 C-terminal helix (blue).

rescue rhythmicity in *Cry*-deficient MEF cells. Consistent with previous studies, wild-type CRY1 was able to repress the expression of the P(Per2)-dLuc reporter gene and produce robust bioluminescence rhythms. By contrast, the 'IY' mutant of CRY1, which confers severe structural disruption in the C-terminal helix, failed to restore any level of circadian rhythm, although it has the ability to repress CLOCK-BMAL1 as seen by the constitutively low luciferase signal (Figure 3.8). Because the C-terminal helix of CRY is a critical region for binding both FBXL3 and PERs, this result underscores the importance of CRY ubiquitination and degradation in establishing clock rhythmicity and suggests the ability of CRY1 to inhibit CLOCK-BMAL1 in a PER-independent manner.

### *3.5 Intermolecular Zinc Finger*

Amino acid sequence alignment of vertebrate PER1–2 orthologs reveals that their sequence conservation ends at a CXXC motif near the C-terminus (Figure 3.4A). In the complex structure, these two cysteine (C1210 and C1213) residues face a pair of cysteine and histidine residues in CRY2 (C432 and H491), which are also invariant among vertebrate CRY1/2 proteins (Figure 3.3). Together, these four residues sequester a strong density at the center, hinting at the coordination of a $Zn^{2+}$ ion at the end of the PER2-CRY2 interface (Figure 3.9). Indeed, we were able to validate the identity of the $Zn^{2+}$ ion by both anomalous dispersion measurements and inductively coupled plasma mass spectrometry (Figure 3.10). Although a $Zn^{2+}$ ion has been previously reported to mediate protein–protein interactions (Somers et al., 1994), to our knowledge, this is the first CCCH-type intermolecular zinc finger that has been identified in a protein complex. Interestingly, the electron density of the PER2 sequence preceding the CXXC motif is not as strong as other regions of PER2-CBD, suggesting that the intermolecular zinc finger might have evolved to stabilize a flexible region of the PER-CRY interaction by acting as a "molecular clasp".

To assess the role of the intermolecular zinc finger in mediating PER-CRY association, we first tested the CRY2-binding activity of a recombinant mutant PER2-CBD, which lacks the CXXC motif. In comparison to the wild-type polypeptide, the ability of the PER2-CBD

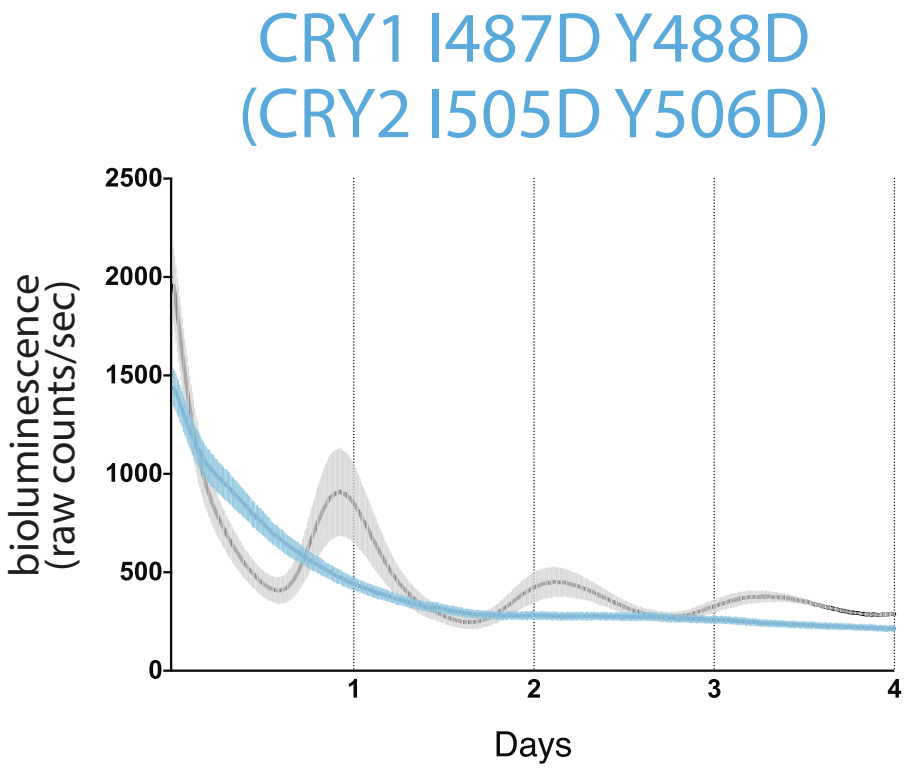


Figure 3.8: **Circadian Phenotype of CRY 'IY' Mutant.** CRY1 I487D Y488D (CRY2 I505 Y506) 'IY' (I505D and Y506D) mutant abolishes rhythmicity but maintains repression compared to WT, suggesting that PER is not required for transcriptional repression. Corresponding CRY2 residues are in parenthesis. Cry1:CRY2 DKO MEFs. Bioluminescence (raw counts/s) monitoring was performed continuously using a photomultiplier tube at 37°C. Traces are shown as mean ± SEM and are representative of triplicate samples. Mutants are shown in blue and WT control in black. Only CRY1, not CRY2 is able to reconstitute robust circadian rhythmicity.

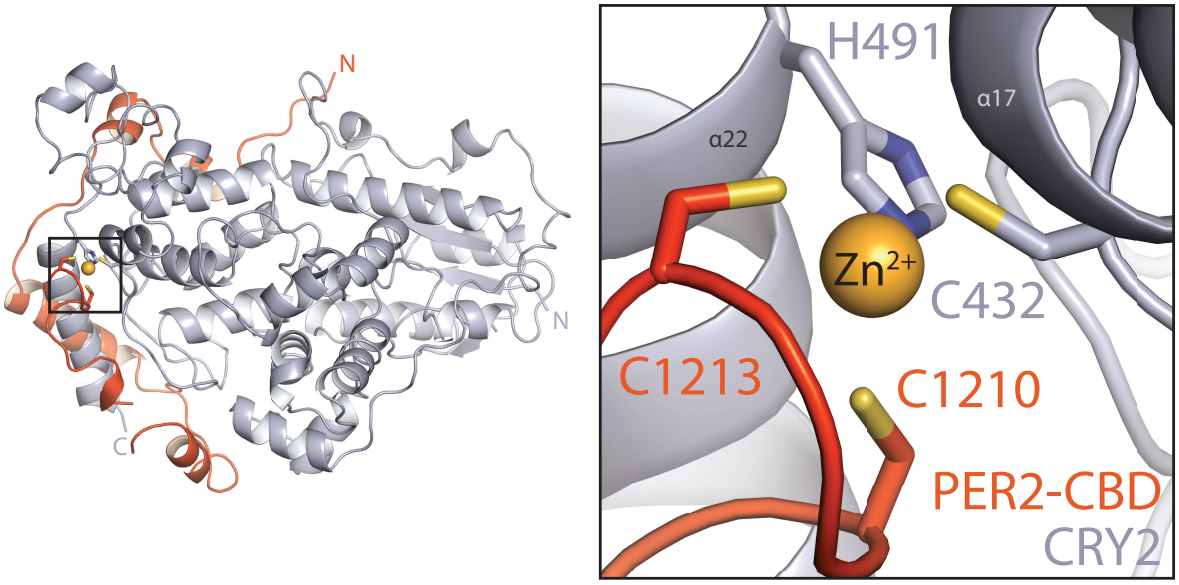


Figure 3.9: **Identification of Intermolecular Zinc Finger.** Four conserved, contributing residues from PER2 (C1210 and C1213) and CRY2 (C432 and H491) form a CCCH-type zinc finger.

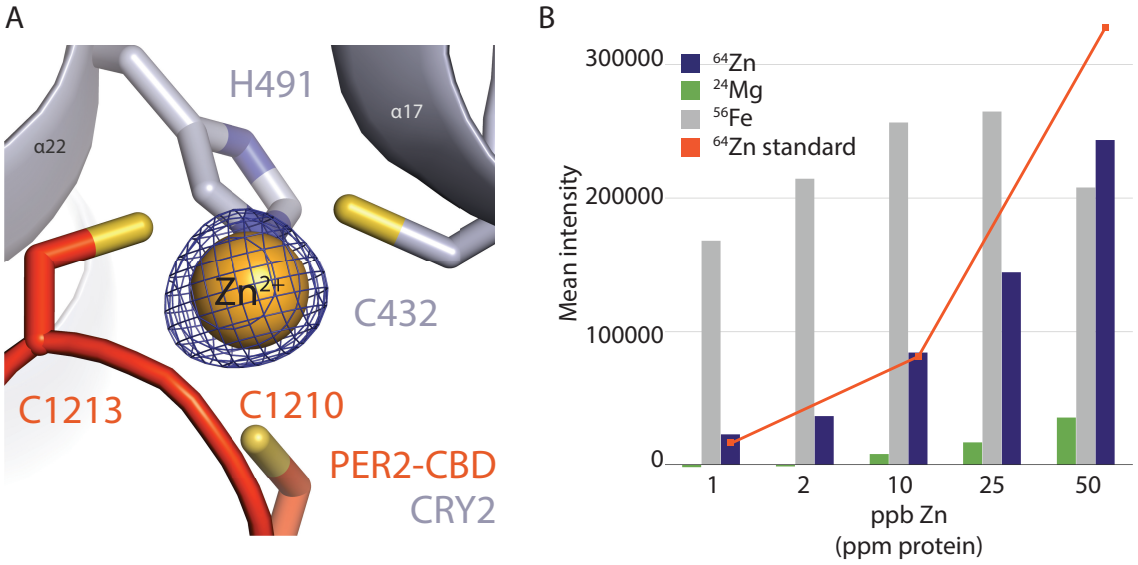


Figure 3.10: **Analysis of the Intermolecular Zinc Finger.** A. Zinc-coordinating residues of PER2-CBD (orange) and CRY2 (gray) with zinc anomalous signal ($\lambda = 1.284$ Å) contoured at 7 σ (blue mesh). B. Inductively-coupled plasma mass spectrometric analysis of metal isotopes. Purified PER2-CBD-CRY2 complex was dehydrated, dissolved in concentrated $HNO_3$ overnight, diluted to 1% vol/vol $HNO_3$, and titrated. Zn (purple) isotopes ($^{64}$Zn, $^{66}$Zn, $^{67}$Zn, $^{68}$Zn, $^{70}$Zn) were the only ones that showed a greater than sixfold increase in mean signal intensity above the blank, dose-dependent increase, and approximated the predicted intensity of the standard (orange line). $^{24}$Mg (green) and $^{56}$Fe (gray) are shown as controls.

mutant to bind CRY2 was substantially compromised (Figure 3.11A). Similarly weakened interaction was also observed in a co-immunoprecipitation assay, in which the CXXC motif of the full-length PER2 protein or the two zinc-coordinating residues of CRY2 were mutated to alanines (Figure 3.11B). Together, these results highlight the importance of the intermolecular zinc finger in strengthening the PER-CRY interface.

In agreement, two CRY1 mutants unable to coordinate zinc, C414A and H473A, were also capable of transcriptional repression, even though their PER-binding activities are largely compromised.

We noticed that the two zinc finger CRY1 mutants still sustained circadian rhythms. However, they showed defects in their bioluminescence oscillations (Figure 3.12). Such a phenotype was not observed for a mutant with a nearby residue, Cys412, mutated to alanine, which did not perturb PER or FBXL3 binding as previously documented (Figure 3.12C) (Xing et al., 2013). The contrast between the two zinc finger-defective mutants and the wild-type-like C412A mutant confirms the functional role of the zinc-coordinating residues in the negative arm of the feedback loop.

### *3.6 Identification and Characterization of a Repression Pocket*

Cryptochromes and DNA photolyases belong to the same family of flavoproteins, whose common PHR fold is characterized by two large surface pockets: the FAD-binding pocket and a photoantenna cofactor. Previously, we have identified the FAD-binding pocket as a regulatory "hot spot", which is targeted by FAD, the extreme carboxyl tail of FBXL3, and the clock-modulating small molecule, KL001 (Nangle et al., 2013; Xing et al., 2013). However, the functional significance of the antenna pocket remained unexplored Figure 3.13.

In the PER2-CRY2 crystal, the N-terminal half of PER2-CBD diverges from the FBXL3-binding site of CRY2 and reaches the rim of the repression pocket after traversing around the $\alpha$-helical domain (Figure 3.2). With a highly-conserved sequence, the N-terminal end of PER2-CBD is embedded in a V-shaped cleft formed between the two globular domains of CRY2-PHR, burying a PER2 tryptophan residue (Trp1139) at the junction (Figure 3.14A).

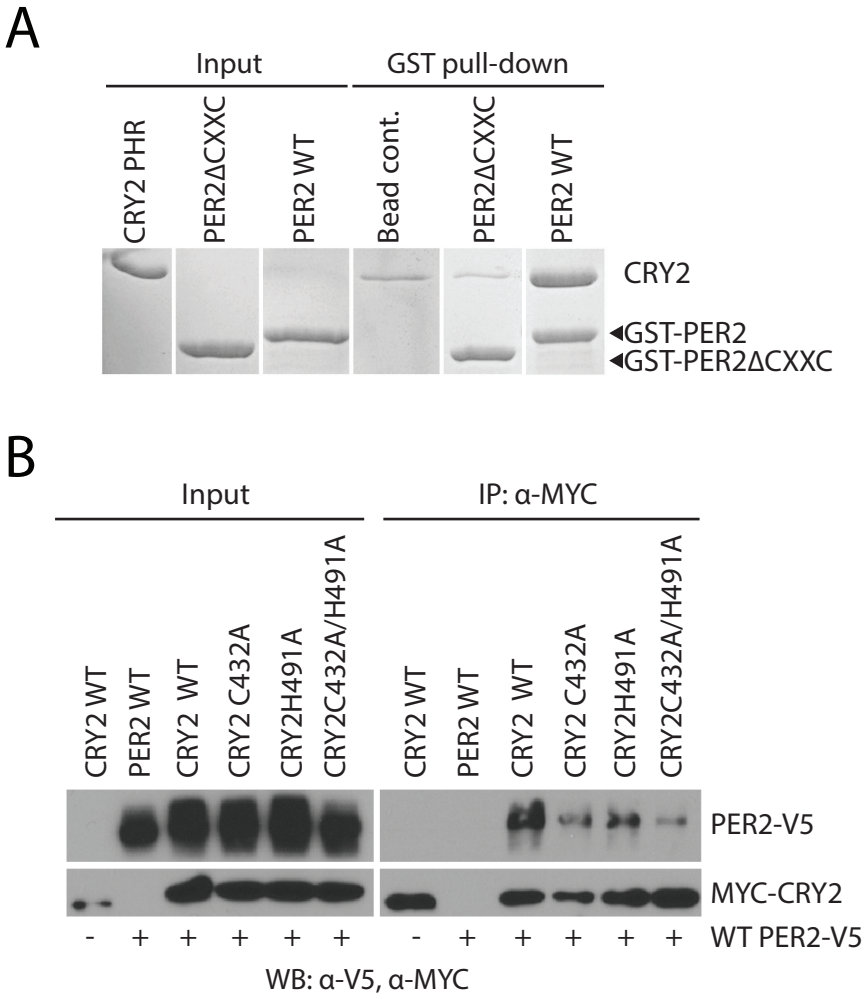


Figure 3.11: **Intermolecular Zinc Finger is an Important Structural Element.** A. GST-pull-down assay with recombinant GST-tagged PER2ΔCXXC CBD and untagged CRY2-PHR protein show compromised CRY binding in the zinc finger mutant compared to WT PER2-CBD. B. Similarly diminished interaction was replicated in a co-immunoprecipitation assay. Alanine mutations were introduced to CRY2 zinc-coordinating residues, C432 and H491, individually or in combination. Co-immunoprecipitations were performed with transfected full-length PER2 and CRY2 in HEK293 cells with $\alpha$-MYC beads.

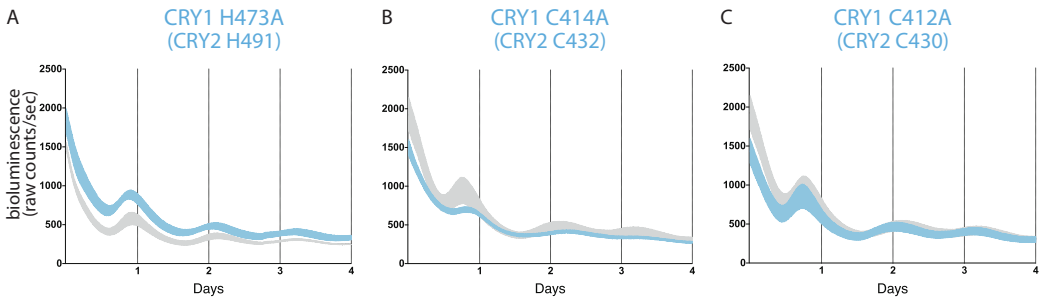


Figure 3.12: **Cell-based Circadian Perturbations of Zinc Finger Mutants.** A-B. Zinc-coordinating residues on CRY1 C414 and H473 (CRY2 C432 and H491) show blunted rhythm amplitude. C. A nearby cysteine residue, C412 (CRY2 430), when mutated to alanine, does not show a significantly different phenotype from the WT control. Corresponding CRY2 residues are in parenthesis. Mutants are shown in blue and WT control in black.

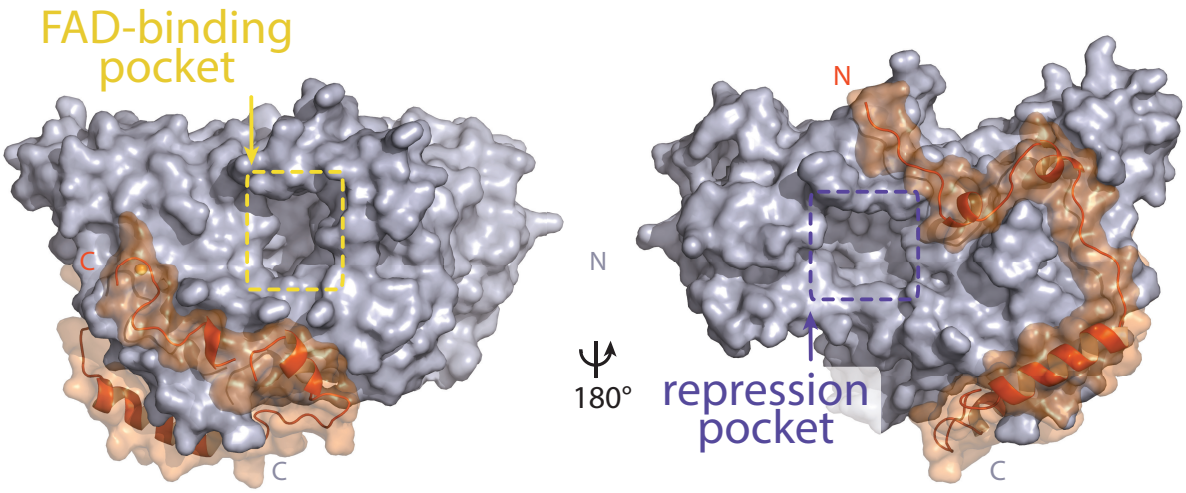


Figure 3.13: **Relative Positions of the Two Large Surface Pockets on CRY2.** Two cofactor pockets are situated opposite each other and are key sites of regulation.

One side of the cleft is constructed by a serine-rich loop in CRY2, which we name as "serine loop". Distinct from its surrounding regions, this loop adopts different conformations in several available crystal structures of CRY (Figure 3.18A). Remarkably, PER2 binding induces yet another distinct structural configuration of the loop, thereby, defining a unique structural state of the local area next to the back pocket.

Although CRYs are known to not engage a second cofactor (Zoltowski et al., 2011; Xing et al., 2013), our previous cell-based random mutagenesis screen has identified three residues within this back pocket (Gly106 and Arg109 in CRY1, Glu121 in CRY2) (Figure 3.14B), whose missense mutations effectively abolished the repressor activity of CRYs (McCarthy et al., 2009). Among these three residues, Arg109 is exposed to the solvent and decorates one side of the pocket. Co-immunoprecipitation analysis of the R109Q mutant showed that alteration of this single amino acid is sufficient to abrogate CLOCK-BMAL1, but not PER1 or PER2 binding (Figure 3.15). Thus, the repression pocket of CRYs represents an important docking site for the heterodimeric transcriptional activators. Anchoring of PER2 at the edge of this CRY pocket not only reinforces its function as a previously unrecognized locus for protein–protein interactions, but also suggests a possible role of PERs in modulating the repressor functions of CRYs.

Consistent with its impaired CLOCK-BMAL1 binding activity, the CRY1 R109Q mutant showed significant derepression in the rescue assay (Figure 3.16A) (McCarthy et al., 2009). This single amino acid mutation highlights the key role of the repression pocket of CRYs for repression. Intriguingly, double serine to aspartate mutations (S44D S45D) in the nearby serine loop at the opposite side of the CRY repression pocket completely rescued the circadian rhythm, although the period of the bioluminescence rhythms rescued by the mutant was reliably shorter than the wild-type CRY1 by about 1-hr (Figure 3.16B). In our co-immunoprecipitation experiments, this double serine mutation appeared weakened PER2 binding to a lesser degree than the zinc finger mutations, which did not elicit a similar period-shortening effect (Figure 3.5B). Therefore, the period-shortening effect induced by the double serine mutation is likely specific to the defects of the local PER-CRY interface

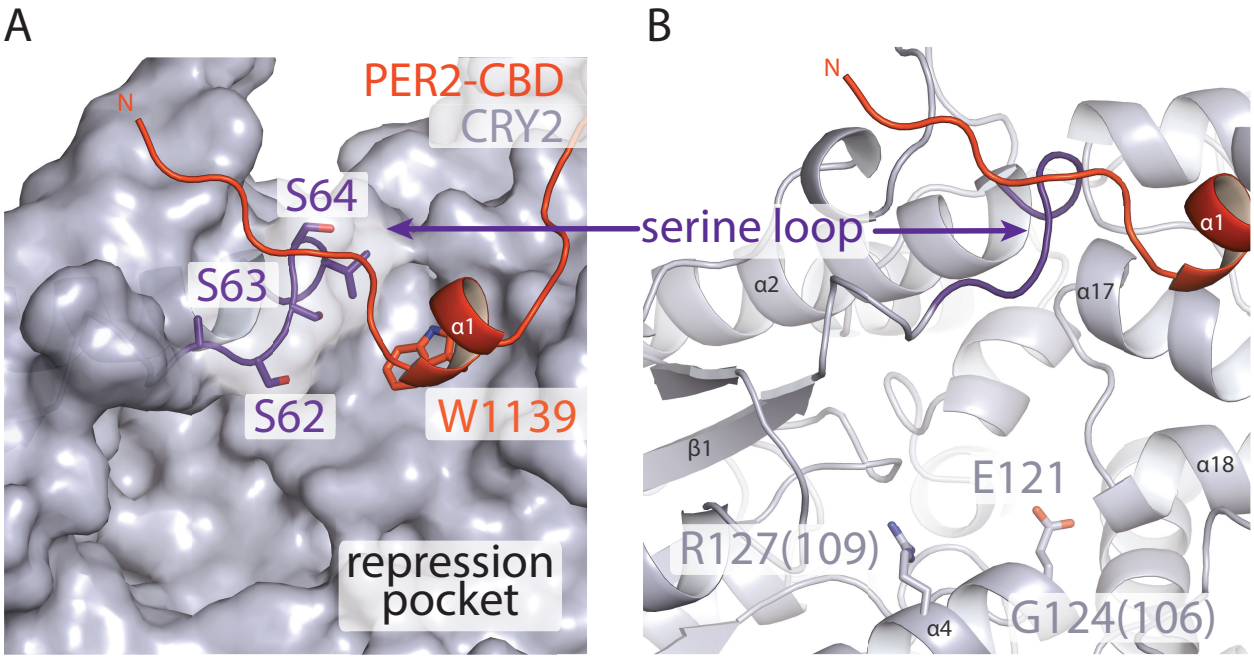


Figure 3.14: **Structural Plasticity of CRY Serine Loop.** A. Surface representation of CRY2 with side chains of the serine loop shown in sticks. PER2 $\alpha$1 helix inserts into a hydrophobic cleft. Compared to other CRY2 complexed forms, the serine loop flips up and engages PER2. B. The serine loop lies opposite to the CRY $\alpha$4 helix, which together frame the repression pocket. The $\alpha$4 helix contains three residues (CRY1 G106R and R109Q, CRY2 E121K), whose mutations result in a weak repression phenotype.

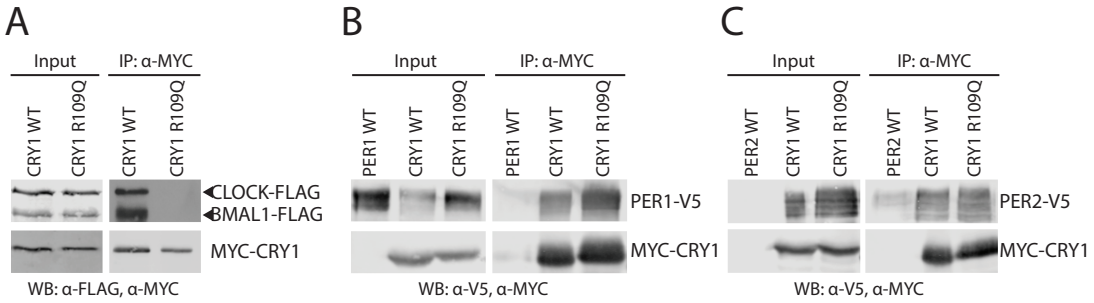


Figure 3.15: **Repression Pocket R109Q Disrupts CLOCK-BMAL1 Binding to CRY.** Co-immunoprecipitation assays show that the CRY1 R109Q mutant is A. unable to bind CLOCK-BMAL1, but B-C. retains PER1 and PER2 binding.

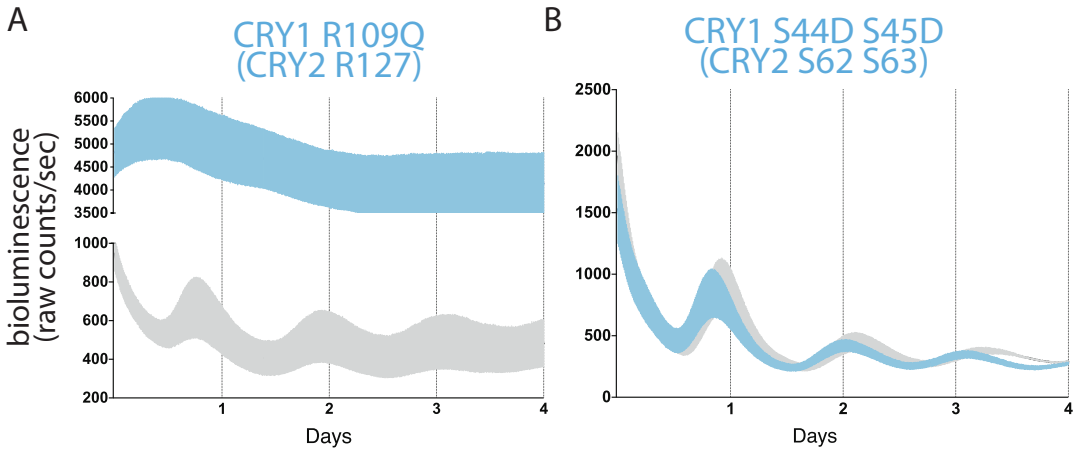


Figure 3.16: **Circadian Phenotypes of Repression Pocket Mutants.** A. A critical residue on the repression pocket, CRY1 R109 (CRY2 R127) shows a severely weakened repression phenotype when mutated to a glutamine. Traces are shown as mean ± SEM and are representative of duplicate samples. B. Mutations of two serine residues in the serine loop, CRY1 S44D S45D (CRY2 S62 S63), show near WT rhythmicity and repression but with a 1-hr shorter period. Corresponding CRY2 residues are in parenthesis. Mutants are shown in blue and WT control in black.

instead of their overall binding. It is conceivable that PERs might engage with CRYs near the CLOCK-BMAL1 docking site to control a periodicity-related step of negative feedback different from what they do at the predominant PER-CRY interface. Encouraged by these consistent *in vivo* data, we sought to clarify the results with recombinant proteins. Compared to wild-type CRY1-PHR, mutant R109Q CRY1-PHR is unable to form a high-affinity complex with a CLOCK-BMAL1 bHLH tandem PAS construct, indicating that this arginine is a key component in the CRY1-CLOCK-BMAL1 complex (Figure 3.17).

## *3.7 Discussion and Conclusions*

Previous studies have established a critical role of PERs in driving the rhythmic negative feedback loop (Reppert and Weaver, 2002). To fulfil this role, PERs have been suggested to act through multiple mechanisms, including mediating CRY nuclear entry, coupling CRYs to CLOCK-BMAL1, and competing with FBXL3 to stabilize CRYs. Our structural and mutagenic analyses of the PER2-CBD-CRY2 complex reveal a surprisingly robust binary assembly, which is resilient to mutational disruption. This stable complex is enabled by an extended binding mode of PER2-CBD, which spreads several distinct functional modules over a mostly linear interface. The hallmark of the PER-CRY interactions is its steric incompatibility with the FBXL3-CRY complex, which provides the structural basis for the competition of PERs and the FBXL3 ubiquitin ligase for controlling CRY stability. Interestingly, distant from the FBXL3-CRY interface, PERs also anchor themselves next to the putative CLOCK-BMAL1-binding pocket of CRYs, possibly regulating a specific step of transcriptional repression. Despite intensive genetic and cell-based studies, the precise spatial and temporal steps undertaken by PERs to coordinate transcriptional repression in the molecular clockwork remain unclear. On the one hand, PERs have been reported to be essential for CRYs to interact with CLOCK-BMAL1 (Chen et al., 2009). On the other hand, emerging evidence suggests that PERs binding might interfere with complex formation between CRYs and CLOCK-BMAL1 at certain steps during repression (Ye et al., 2011; Akashi et al., 2014). Conceivably, by interacting with the CRY C-terminal helix, PERs could com-

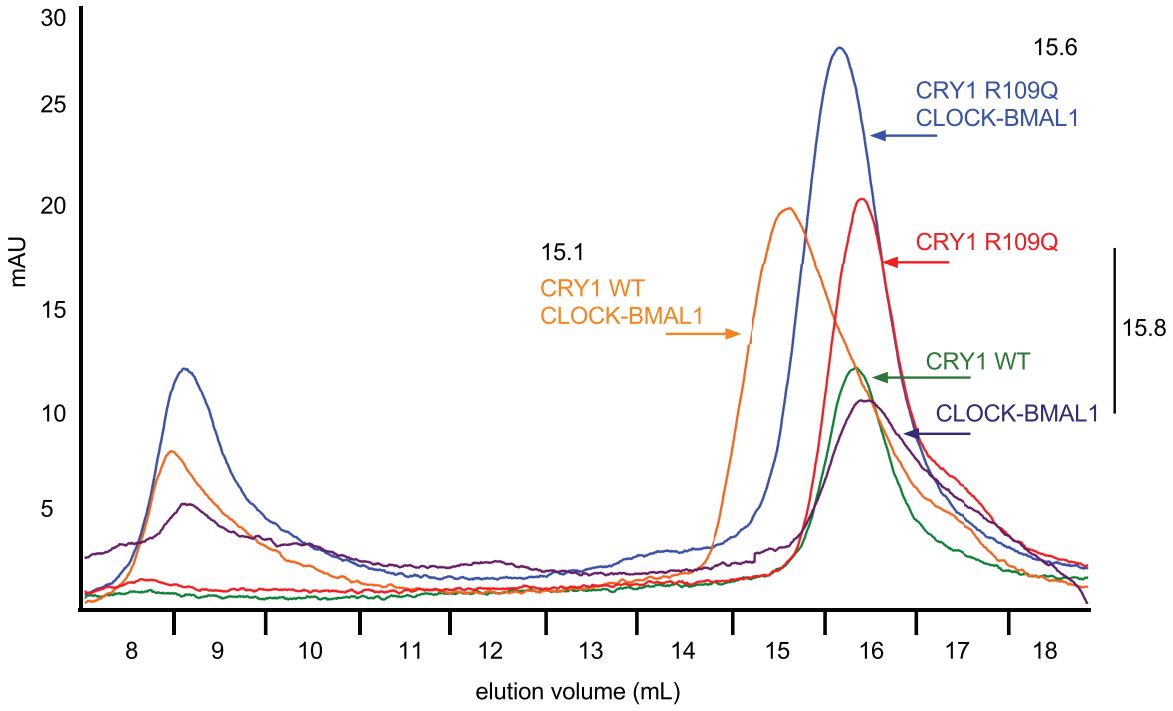


Figure 3.17: ***In Vitro* Analysis of Repression Pocket Mutants.** SEC binding assay with 1:1.2 CLOCK-BMAL1:CRY1 molar ratio. CRY1 WT (green), CRY1 R109Q (red), and CLOCK-BMAL1 (purple) all elute at identical positions (15.6 mL). CRY1 WT and CLOCK-BMAL1 are able to form a stable complex eluting 0.7 mL sooner than each individual component. Whereas, mutant CRY1 is unable to bind CLOCK-BMAL1 at high enough affinity to be resolved and elutes at an equivalent position of each alone (15.6 mL). All runs were performed back-to-back on a Superdex 200 10/300 Increase column in the same sample buffer (20 mM Tris-HCl pH 8, 200 mM NaCl, 2.5 mM DTT, 5% glycerol). mAU indicates the absorption at 280 nm.

pete with the C-terminus of the BMAL1 transactivation domain for CRY binding (Czarna et al., 2013). While detailed biochemical studies are necessary to resolve this controversy, our results offer the structural framework for in-depth mechanistic investigations.

Apart from the PER2-CBD-CRY2 complex, the crystal structures of CRY2 have been determined for four additional functional states, apo, FAD-, FBXL3-, and KL001-bound (Nangle et al., 2013; Xing et al., 2013). Together, these structures outline a rich landscape for the functional surfaces of mammalian CRYs, which distinguishes them from other members of the cryptochrome/photolyase family. In their C-terminal $\alpha$-helical domain, CRYs feature the conserved FAD-binding pocket, which is also targeted by the FBXL3 C-terminal tail and the clock-modulating drug, KL001. In their N-terminal $\alpha/\beta$ photolyase domain, CRYs have evolved the repression pocket into a critical site for CLOCK-BMAL1 binding. Importantly, both CRY surface pockets are demarcated by structural elements with noticeable structural plasticity (Figure 3.18). The FAD-binding pocket is framed by the phosphate-binding loop and the interface loop on opposite edges, whereas the repression pocket is guarded by the serine loop on one side. With the exception of the phosphate-binding loop, both the interface and serine loop have been shown to directly mediate protein–protein interactions. Lastly, the extreme C-terminal $\alpha$-helix of the mammalian CRYs presents yet another important surface area, which is responsible for the mutually exclusive binding of FBXL3 and PERs. Remarkably, all these molecular interacting sites likely represent an incomplete functional map of CRYs. Numerous mutants identified in our random mutagenesis screen of functionally deficient CRY1 and CRY2 bear mutations of amino acids located outside these sites (McCarthy et al., 2009). Future structural studies are needed to paint a complete picture of CRY functional surfaces.

Our crystal structure of the PER2-CBD-CRY2 complex unveils a structurally important intermolecular zinc finger, which might function as a stabilizing "molecular clasp". Although the evolutionary significance of the zinc-coordinating residues is apparent, as evidenced by their strict conservation across vertebrates, the functional significance of this unusual binding interface requires further investigation. On the one hand, the intermolecular zinc finger might

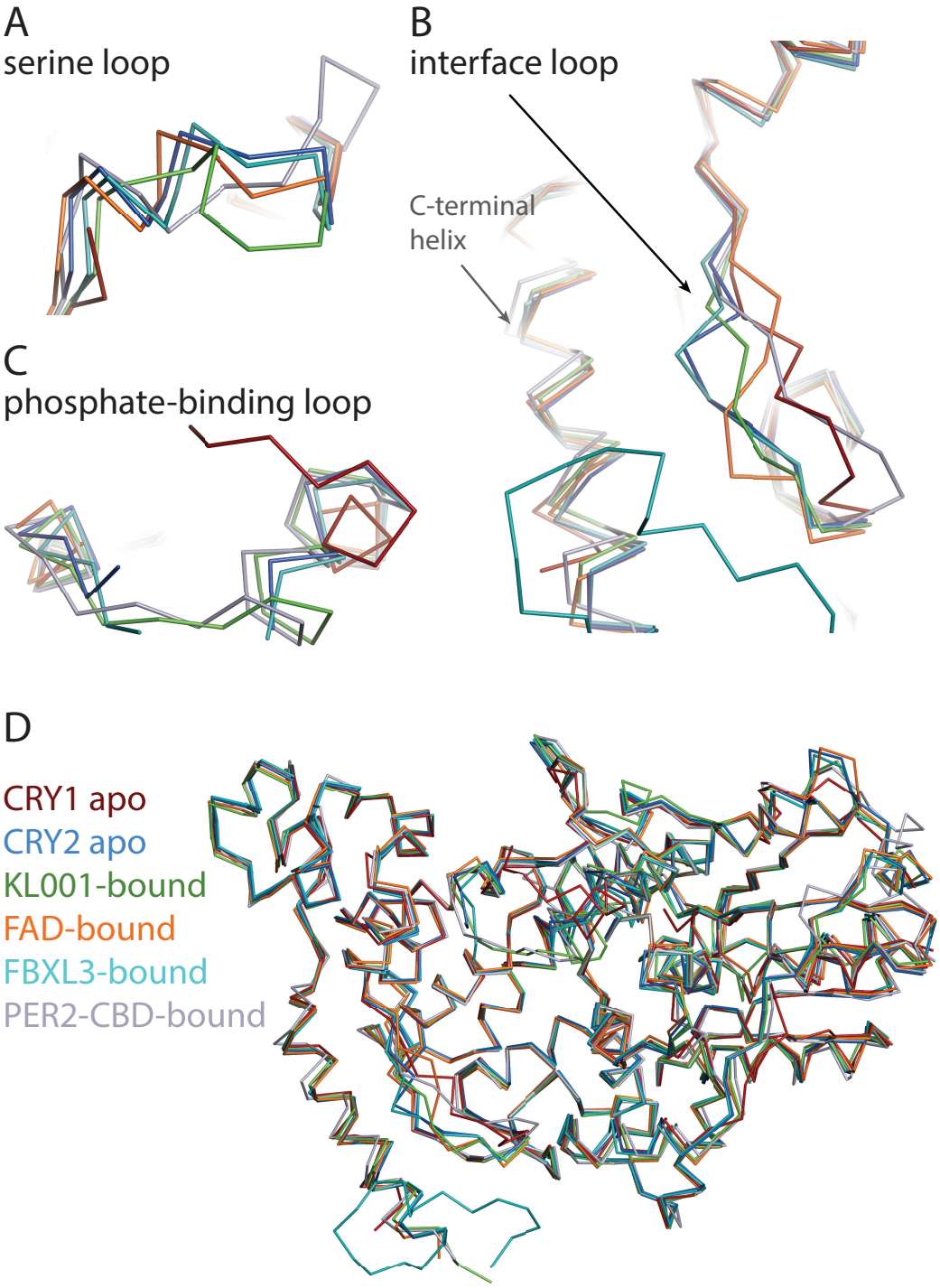


Figure 3.18: CRY1 apo (red), CRY2 apo (light blue), KL001-bound (green), FAD-bound (orange), FBXL3-bound (cyan), and PER2-CBD-bound (gray) CRY. A. Serine loop undergoes a large conformational change after PER2-CBD binding. (B and C) The interface loop and phosphate-binding loop are also sites of high structural plasticity. D. Overall CRY-PHR showing the global structure adopts a common fold.

be an intermediate product of the still evolving PER-CRY interface. On the other hand, it is plausible that this special protein interaction interface confers sensitivity to the fluctuating abundance of intracellular zinc (Wang et al., 2012), which might serve as a tissue-specific clock-modulating ion (Huang et al., 1993).

During the preparation of the manuscript for this complex, the structure of mammalian CRY1-PHR and PER2-CBD was reported (Schmalen et al., 2014). With high sequence conservation between CRY1 and CRY2, PER2-CBD adopts a similar CRY-binding mode with a tetrahedral coordination of a zinc ion by an intermolecular CCCH zinc-binding motif. The major structural difference lies at the interface of the N-terminal region of PER2-CBD and the CRY repression pocket. The CRY1-bound PER2-CBD fragment contains a residual fusion-protein sequence, which forms an artifactual β-hairpin with the first five amino acids of the PER2-CBD (Figure 3.19). In contrast to the PER2-bound CRY2 serine loop, but reminiscent of the *Drosophila* CRY antenna loop (Zoltowski et al., 2011), the otherwise disordered (Czarna et al., 2013) CRY1 serine loop adopts an inward conformation and occludes the repression pocket. This conformational difference reveals a substantial degree of structural plasticity, which might be necessary for differential binding and regulation at this site. Interestingly, Schmalen et al. (2014) identified a potential redox sensor involving a disulfide bond near the zinc finger between Cys412 and Cys363, which modulates CRY1-PER2 binding. However, in our circadian reporter assay, we did not detect any difference between the CRY1 wild type and C412A mutant (Figure 3.12C). More in-depth analyses can now exploit the specific structural differences between the two complexes to explain the non-redundant roles of the two cryptochrome proteins.

True to their name, Period proteins act as the master timekeepers in the circadian clock pathway, and likely use their multiple functional modules to simultaneously mediate the negative and positive phases of the clock through CRY stability and CRY-CLOCK-BMAL1 repression complex assembly.

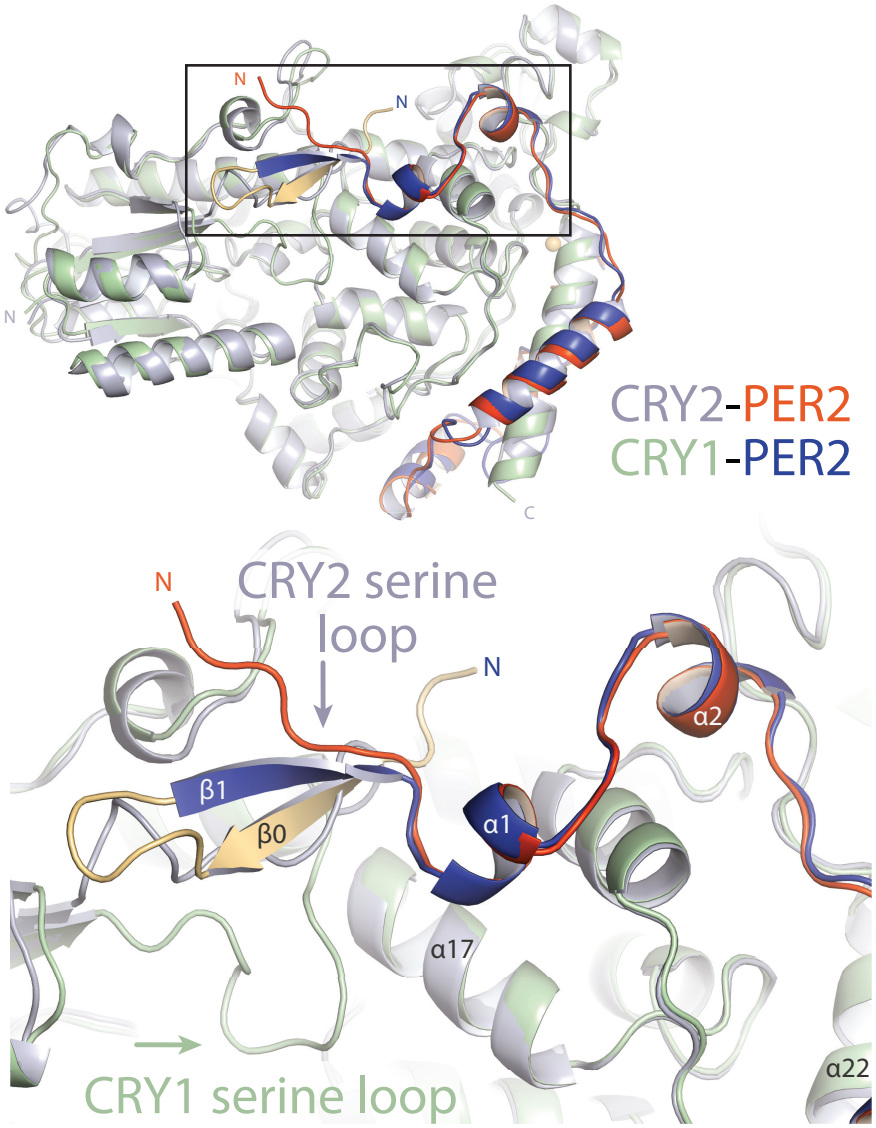


Figure 3.19: **Major Differences Between CRY1-PER2-CBD and CRY2-PER2-CBD Complex Structures.** Superposition of the two structures reveals major structural dissimilarities between the two paralogs at the CRY repression pocket and a residual fusion-protein sequence (yellow) in CRY1-bound PER2-CBD. The PER2-CBD (dark blue) N-terminus together with the artifactual sequence (AGLEVLFQGPDSM) forms a β-hairpin and induces an inward conformation of the CRY1 (light green) serine loop.

| | CRY2-PER2 |
|---|---|
| Data collection | |
| Space group | $P4_1$ |
| Cell dimensions: | |
| a, b, c (Å) | 97.67 97.67 163.21 |
| $\alpha$, $\beta$, $\gamma$ (°) | 90 90 90 |
| Resolution (Å) | 2.9 (2.8) |
| $R_{meas}$ | 0.06 (0.8) |
| I/$\sigma$I | 18.8 (2.1) |
| Completeness (%) | 99.6 (98.2) |
| Redundancy | 4.2 (4.2) |
| | |
| Refinement: | |
| Resolution (Å) | 42.7–2.8 |
| No. reflections | 37541 (3671) |
| $R_{work}$ / $R_{free}$ | 20.5/27.7 |
| No. atoms | 9342 |
| Protein | 9292 |
| Ligand/ion | 2 |
| Water | 48 |
| B-factors | 97.3 |
| Protein | 97.5 |
| Ligand/ion | 114.1 |
| Water | 66.3 |
| R.m.s. deviations | |
| Bond lengths (Å) | 0.009 |
| Bond angles (°) | 1.3 |

Table 3.1: Data collection and refinement statistics for CRY2-PER2. Values in parentheses are for highest-resolution shell

# Chapter 4

# BIOCHEMICAL ANALYSIS OF THE CRY-CLOCK-BMAL1 COMPLEX

## *4.1 Introduction*

BMAL1-CLOCK-dependent transcriptional regulation is formed by three temporally distinct phases: 1. the early repressive phase (CT 12–20, from mouse liver) when large multi-subunit complexes of CRYs and PERs form with CLOCK-BMAL1 on DNA, 2. the late repressive phase (CT 0–4) when CRY-CLOCK-BMAL1 is bound to DNA and transcription is inhibited, and 3. the active phase when CLOCK-BMAL1 is free to initiate transcription through the recruitment of coactivating proteins (e.g., p300-CBP) (Figure 3.1) (Koike et al., 2012). Because CBP and CRY1 compete for overlapping sites on BMAL1 CRY-binding region (CBR) of the TAD, nuclear concentrations of CRY are a critical factors in the transition mechanism (Kiyohara et al., 2006; Koike et al., 2012). The stoichiometry of these complexes *in vivo* have not yet been established and are likely extremely dynamic. Recombinant CRY1, but not PER2 is known to directly interact with CLOCK-BMAL1 on and off E-box elements (Ye et al., 2011) suggesting that if PERs bind to CLOCK-BMAL1, as they appear to *in vivo* (Lee et al., 2001; Ye et al., 2014; Chen et al., 2009; Koike et al., 2012), post-translation modifications and/or additional proteins are needed to facilitate the complex formation. Two putative sites of CRY binding to the heterodimeric transcription activation complex have been mapped: the final 43 amino acids in BMAL1 TAD (CBR) and the CLOCK HI loop (Zhao et al., 2007; Kiyohara et al., 2006; Xu et al., 2015) (Figure 4.1, Figure 4.2). Additionally, each core clock component has large (and in most cases, highly-conserved) flexible loops that may enable them to interact dynamically with each other and other regulatory subunits whose modifications fine-tune the assemblies in a time- and tissue-dependent manner.

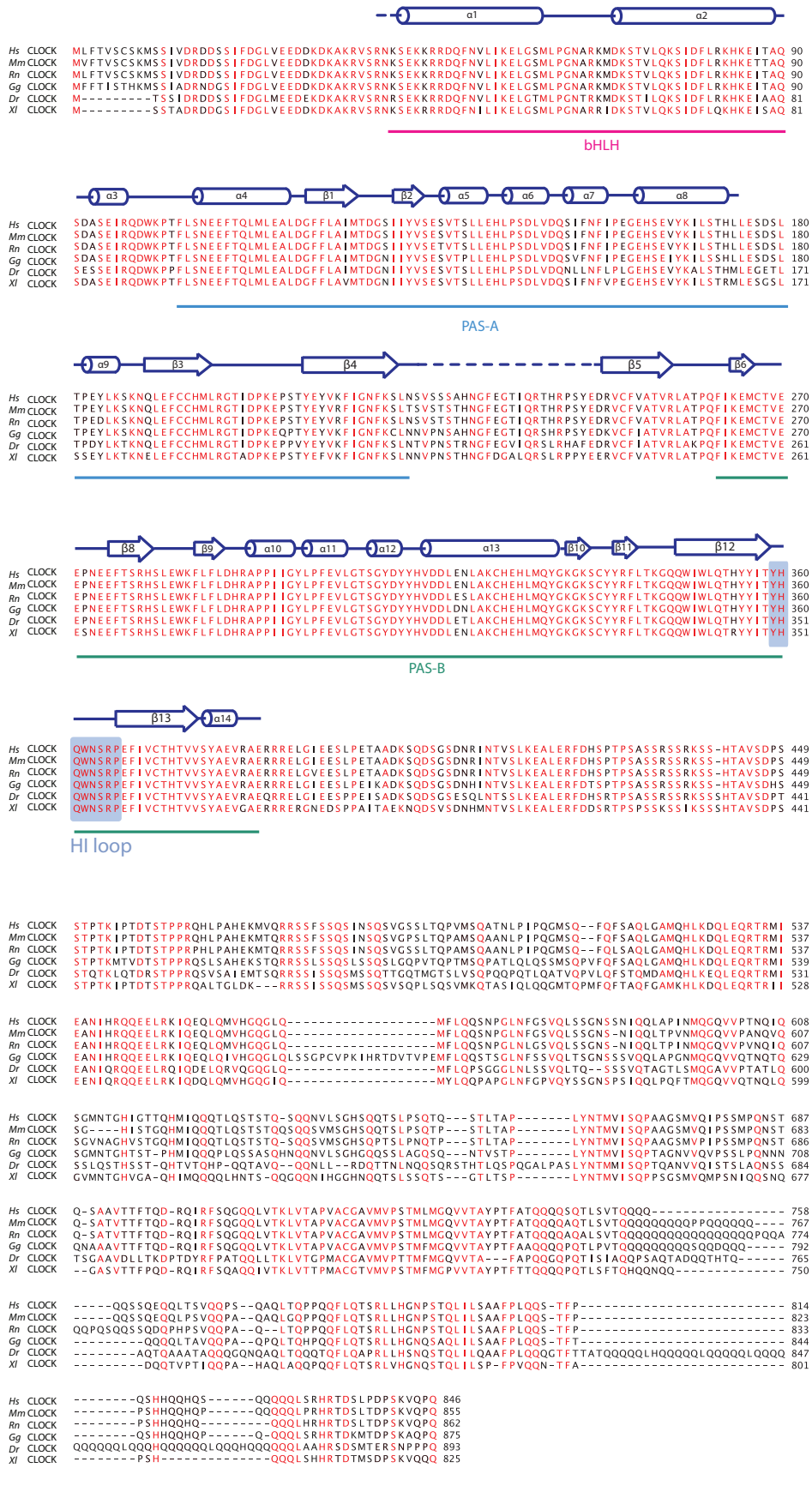


Figure 4.1: **Sequence Alignment and Secondary Structure of Vertebrate CLOCK.** Alignment and secondary structure assignments of CLOCK orthologs from Homo sapiens (Hs), Mus musculus (Mm), Rattus norvegicus (Rn), Gallus gallus (Gg), Danio rerio (Dr), and Xenopus laevis (Xl). Strictly-conserved residues are in red. Blue box represents the boundaries of the HI loop, a putative CLOCK-CRY interface. The CLOCK transactivation domain is not finely mapped but Dashed lines represent disordered regions.

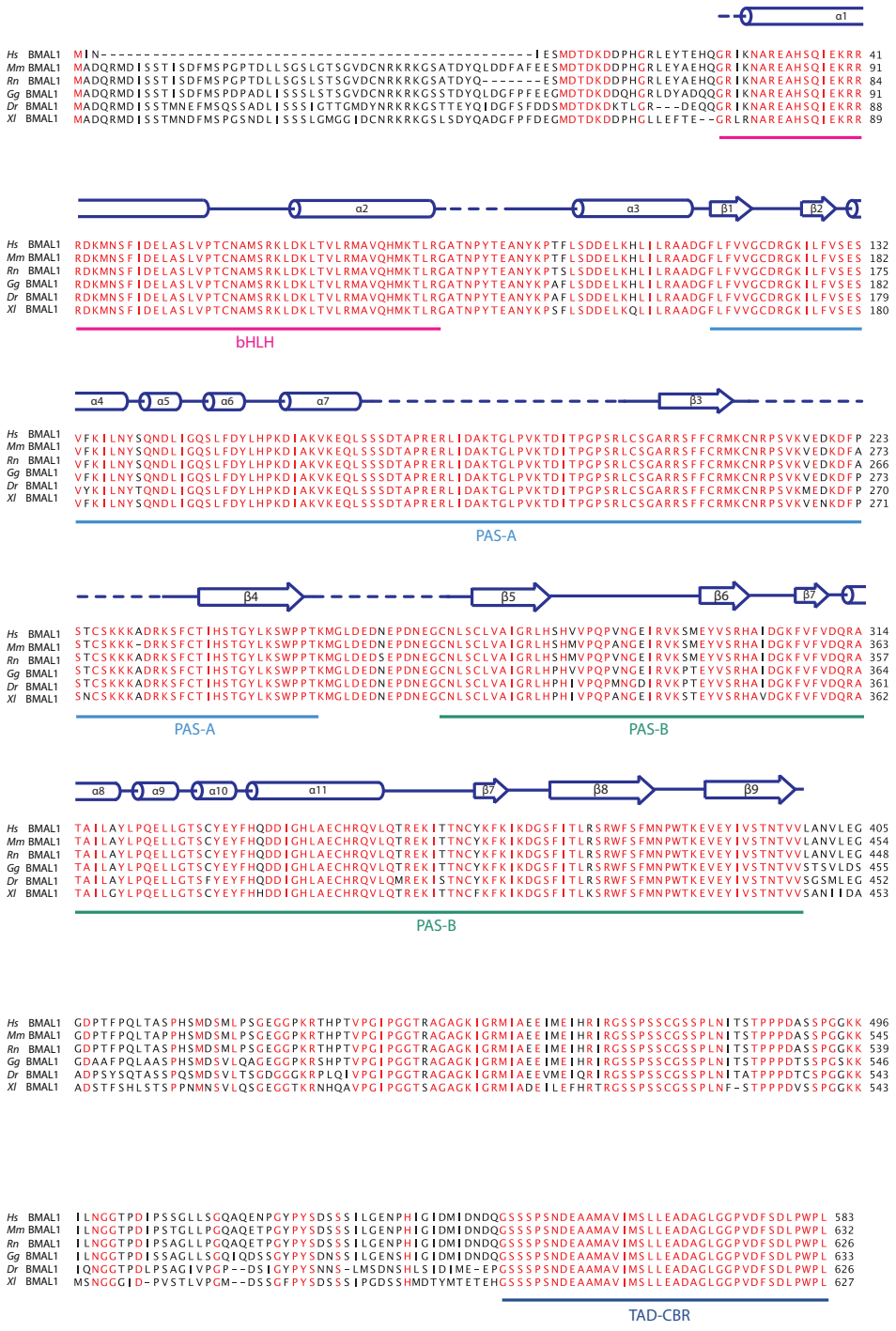


Figure 4.2: **Sequence Alignment and Secondary Structure of Vertebrate BMAL1.** Alignment and secondary structure assignments of BMAL1 orthologs from Homo sapiens (Hs), Mus musculus (Mm), Rattus norvegicus (Rn), Gallus gallus (Gg), Danio rerio (Dr), and Xenopus laevis (Xl). TAD-CBR, CRY-binding region of the transcriptional activation domain. Strictly-conserved residues are in red. Dashed lines represent disordered regions.

### *4.2 Formation of the Ternary Complex*

Although both CRY and CLOCK-BMAL1 structures have been determined, the binding mode of the ternary complex is not intuitive. Yeast two-hybrid data suggests that CRY binding is diminished when two amino acid substitutions are made on the solvent-exposed CLOCK HI loop in the PAS-B domain (Q361P and W362R) (Zhao et al., 2007) and nearby point mutations (G332E, E367K, and H360Y) show derepression phenotypes in a circadian transcriptional reporter assay (Sato et al., 2006). The Trp362 residue corresponds to the BMAL1 Trp427, which nestles into the a hydrophobic cleft of CLOCK PAS-B (Figure 1.5). The intriguing use of interfacial tryptophans suggest that the surface-exposed CLOCK W362 serves a functional role. Additional CRY interfaces on BMAL1 have been mapped to its C-terminal TAD, which are necessary for transcriptional repression by CRY1 (Kiyohara et al., 2006) (Figure 1.5). CRY1–2 C-terminal helix (isolated from the PHR) directly binds to the BMAL1 TAD-CBR at low μM affinity *in vitro* (Czarna et al., 2011).

*Cry1*$^{-/-}$ and *Cry2*$^{-/-}$ animals only experience a -1-hr and +1-hr period shift, respectively; however, *Cry1*$^{-/-}$/*Cry2*$^{-/-}$ mice are arrhythmic. Despite their high sequence homology (86%), only CRY1 is able to maintain robust circadian oscillations in isolated cell-lines (i.e., without input from the SCN) (Liu et al., 2007; Cho et al., 2012). CRY2 is unable to rescue rhythms in a *Cry1*$^{-/-}$/*Cry2*$^{-/-}$ fibroblast cell line even when expressed under the *Cry1* promoter (Khan et al., 2012). We hypothesize that it is biochemical, not genetic, variations that manifest these striking differences. The CRY paralogs, while having overlapping activity, are not functionally redundant. Apart from their highly-similar PHR, which is sufficient to maintain rhythms (Khan et al., 2012), CRYs have a non-conserved, disordered C-terminal extension (Figure 3.3) that fine-tunes the circadian period and amplitude (Chaves et al., 2006). Unfortunately, full-length CRYs have been impractical for large-scale purification and no structures have been determined containing this C-terminal extension. However, we believe that the PHR is sufficient for extrapolating CRY function *in vivo*. As a natural extension to revealing the structural mechanisms of the core clock, we attempted

to establish the CRY-CLOCK-BMAL1 ternary complex.

Because of our previous success with CRY2 and the sequence similarity between CRY1 and CRY2, our preliminary work focused on establishing the ternary complex with CRY2. Although CRY2 can bind CLOCK-BMAL1 (CLOCK bHLH tandem PAS (amino acids 26-384) and near full-length BMAL1 (67-626)) through initial affinity co-purification steps, the BMAL1 C-terminal tail is readily degraded. Even after optimization of the tail that is not susceptible to degradation, the complex does not withstand size-exclusion chromotography (SEC) purification. Likewise, co-crystallization attempts of individual components (with and without E-box oligos as well as a mixture of CRY2, bHLH PAS CLOCK-BMAL1, PER-CBD, and a peptide of the final 45 amino acids of BMAL1) were also unsuccessful. Inspired by these negative results and the aforementioned literature, we focused on CRY1 for complex formation. Although neither CRY1 nor CRY2 can co-purify with the bHLH-PAS (i.e., BMAL1 lacking the C-terminal tail and TAD-CBR) constructs, CRY1 but not CRY2 can bind to this construct on SEC (Figure 4.3). These results indicate that surfaces other than the BMAL1 TAD-CBR are sufficient for CRY1 binding, such as the CLOCK PAS-B HI loop interacting with the CRY repression pocket (Figure 3.17). Nevertheless, these constructs, while well-behaving on SEC, have not been able to crystallize.

## *4.3 Virtual Screening for CRY-CLOCK-BMAL1 Interfacial Inhibitor*

Disruption of the clock is implicated in many diseases including metabolic syndrome, obesity, sleep defects, cardiovascular disease, and cancer (Maury et al., 2010). And as our society continues to globalize and more individuals experience daily perturbations to their circadian rhythms, due to high-intensity light exposure and irregular sleeping and eating times; understanding the regulation of the clock from a pharmacological perspective becomes increasingly relevant. Motivated by the joint hypotheses that CRY1 can bind the PAS-B of CLOCK and the CRY repression pocket is required for CLOCK-BMAL1 binding, we designed a virtual ligand screen (VLS) to target this CRY pocket. The goal of these experiments is to probe the chemical and molecular mechanisms that fine-tune clock activity in hopes to treat and

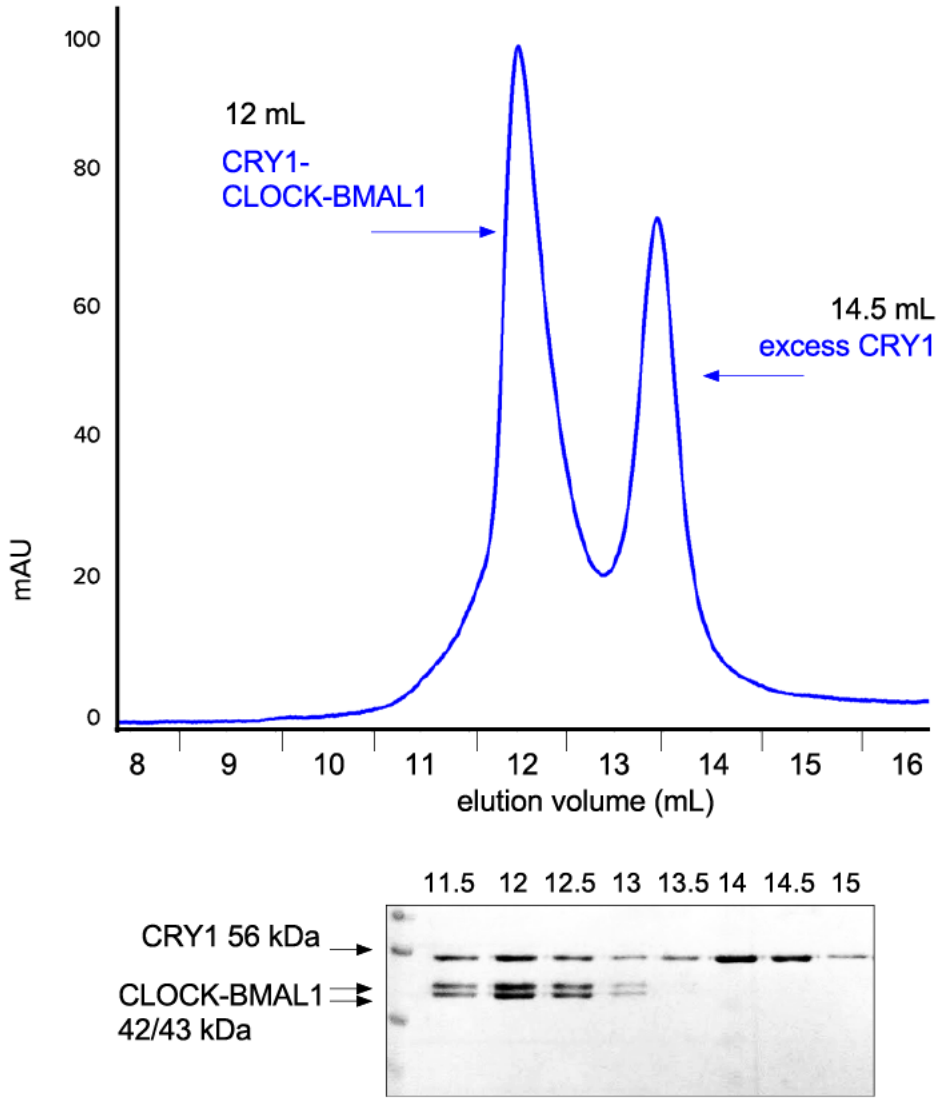


Figure 4.3: ***In Vitro* Ternary Complex Assembly on SEC.** SEC binding assay with 1:2 CLOCK-BMAL1:CRY1 molar ratio. Co-migration of CRY1 PHR with the CLOCK-BMAL1 bHLH tandem PAS indicates ternary complex formation. Binding was accomplished with a Superdex 200 10/300 Increase column in sample buffer (20 mM Tris-HCl pH 8, 400 mM NaCl, 2.5 mM DTT, 10% glycerol). mAU indicates the absorption at 280 nm.

prevent many common disorders.

We hypothesize that the small molecule would disrupt the CRY-CLOCK-BMAL1 repressor complex and exert control over the transcriptional clock program. Using ICM-VLS, we virtually screened a 450,000 compound library against a representative CRY2 crystal structure (CRY2-KL001 PBD:4MLP) and found a diverse set of drug-like molecules with favorable fit, logP values, and docking scores. Of the 20 of the high-scoring compounds we selected, half came in close proximity to the CRY2 Arg127 (CRY1 Arg109) side chain that is putatively in direct contact at the CRY-CLOCK-BMAL1 interface (Table 4.1, Figure 3.17, Figure 4.4). To evaluate their functional activity, initial hits were analyzed with a GST-pull-down assay with co-purified GST-CRY1-CLOCK-BMAL1 pre-formed complex. Although saturating concentrations of compound were incubated with the immobilized complex, we failed to detect any that were able to disrupt the ternary complex. While it is unknown whether the compounds maintained solubility at the working concentrations, it is possible that rather than separating the CLOCK-BMAL1 heterodimer from CRY1, they promote the interaction. It is with this revised hypothesis that we require more quantitative binding kinetics (e.g., AlphaScreen, biolayer interferometry).

Future work will explore the possibility that these compounds can facilitate the ternary complex formation and iteratively improve the chemistry of selected hits. Once several high-scoring compounds have been designed, we will attempt to crystallize the compounds with CRY to confirm and evaluate the binding mode, and use a cell-based circadian reporter assay to determine whether the compounds are able to manipulate CRY repressor activity.

### *4.4 Discussion and Conclusions*

CRY1-PHR stably binds CLOCK-BMAL1 bHLH PAS *in vitro*. CRY2 binds CLOCK-BMAL1 bHLH PAS only when the BMAL1 TAD is included in the construct, but the interaction is not robust and disassembles after affinity and ion-exchange chromatography. In the previous chapter we established that the repression pocket is biochemically and physiologically relevant in complex formation with CLOCK-BMAL1. Additionally, we hypothesize

| ID | Mol Weight | Mol Name |
|---|---|---|
| 63285467 | 276.4 | 2-{[6-amino-2-(benzylthio)pyrimidin-4-yl]amino}ethanol |
| 59070287 | 365.4 | 2-(3-{3-[5-(1-piperidinylcarbonyl)-2-furyl]phenyl}-1H-pyrazol-1-yl)ethanol |
| 66337080 | 324.4 | 2-{2-[1-(4-methoxybenzyl)-1H-imidazol-2-yl]phenoxy}ethanol |
| 37087092 | 371.5 | 3-{(3R*,4S*)-4-(dimethylamino)-1-[(4-methoxyquinolin-2-yl)carbonyl]piperidin-3-yl}propan-1-ol |
| 77725587 | 346.5 | (4aS*,8aR*)-6-[(1-allyl-1H-pyrazol-4-yl)methyl]-1-(4-hydroxybutyl)octahydro-1,6-naphthyridin-2(1H)-one |
| 45420236 | 381.5 | 2-[1-(4-biphenylylmethyl)-3-oxo-2-piperazinyl]-N-(3-hydroxypropyl)acetamide |
| 15121980 | 327.4 | 4-(3,6-dimethyl-2-pyrazinyl)-2-{[3-(hydroxymethyl)-1-piperidinyl]methyl}phenol |
| 20407746 | 352.4 | 2-{[7-(1-benzofuran-5-ylcarbonyl)-6,7,8,9-tetrahydro-5H-pyrimido[4,5-d]azepin-4-yl]amino}ethanol |
| 24740357 | 363.4 | N-{4-[5-(hydroxymethyl)-2-furyl]-2-oxo-1,2,3,4-tetrahydroquinolin-7-yl}nicotinamide |
| 11116900 | 353.4 | 2-[5-{[3-(3-methoxyphenyl)-1H-pyrazol-4-yl]carbonyl}-5,6-dihydropyrrolo[3,4-c]pyrazol-1(4H)-yl]ethanol |
| 77603875 | 355.4 | 4-[({[3-hydroxy-1-(4-methylphenyl)propyl]amino}carbonyl)amino]-N,3-dimethylbenzamide |
| 71519986 | 367.8 | 5-chloro-6-[8-(2-hydroxyethyl)-9-oxo-2,8-diazaspiro[5.5]undec-2-yl]nicotinic acid |
| 11567088 | 277.3 | 4-(5-{[(3-hydroxypropyl)amino]methyl}-1,2,4-oxadiazol-3-yl)benzoic acid |
| 55993794 | 302.4 | 2-{1-methyl-4-[4-(1-methyl-1H-pyrazol-4-yl)pyrimidin-2-yl]piperazin-2-yl}ethanol |
| 49793128 | 359.5 | (4aS*,8aR*)-6-[4-(aminomethyl)benzoyl]-1-(4-hydroxybutyl)octahydro-1,6-naphthyridin-2(1H)-one |
| 52780215 | 349.4 | (4-{[(1R*,3S*)-1-hydroxy-3-(2-hydroxyethoxy)-7-azaspiro[3.5]non-7-yl]methyl}phenyl)acetic acid |
| 98201379 | 322.4 | N-(3-hydroxypropyl)-1-[(3-propyl-1H-pyrazol-5-yl)carbonyl]piperidine-3-carboxamide |
| 54547375 | 387.6 | 1-(3-{[3-(2-hydroxyethyl)-4-(1-isopropyl-4-piperidinyl)-1-piperazinyl]methyl}phenyl)ethanone |
| 54231321 | 343.4 | N-(2,3-dihydro-1,4-benzodioxin-2-ylmethyl)-6-[(2-hydroxyethyl)amino]-N-methylnicotinamide |
| 60151652 | 442.5 | N-benzyl-1-(2-hydroxyethyl)-5-(5-quinoxalinylmethyl)-4,5,6,7-tetrahydro-1H-pyrazolo[4,3-c]pyridine-3-carboxamide |

Table 4.1: **Candidates Identified from Virtual Ligand Screen.** Top 20 hits from Chembridge that were tested in the GST-pull-down assay. Hit2Lead ID, molecular weight (Da), and name are listed.

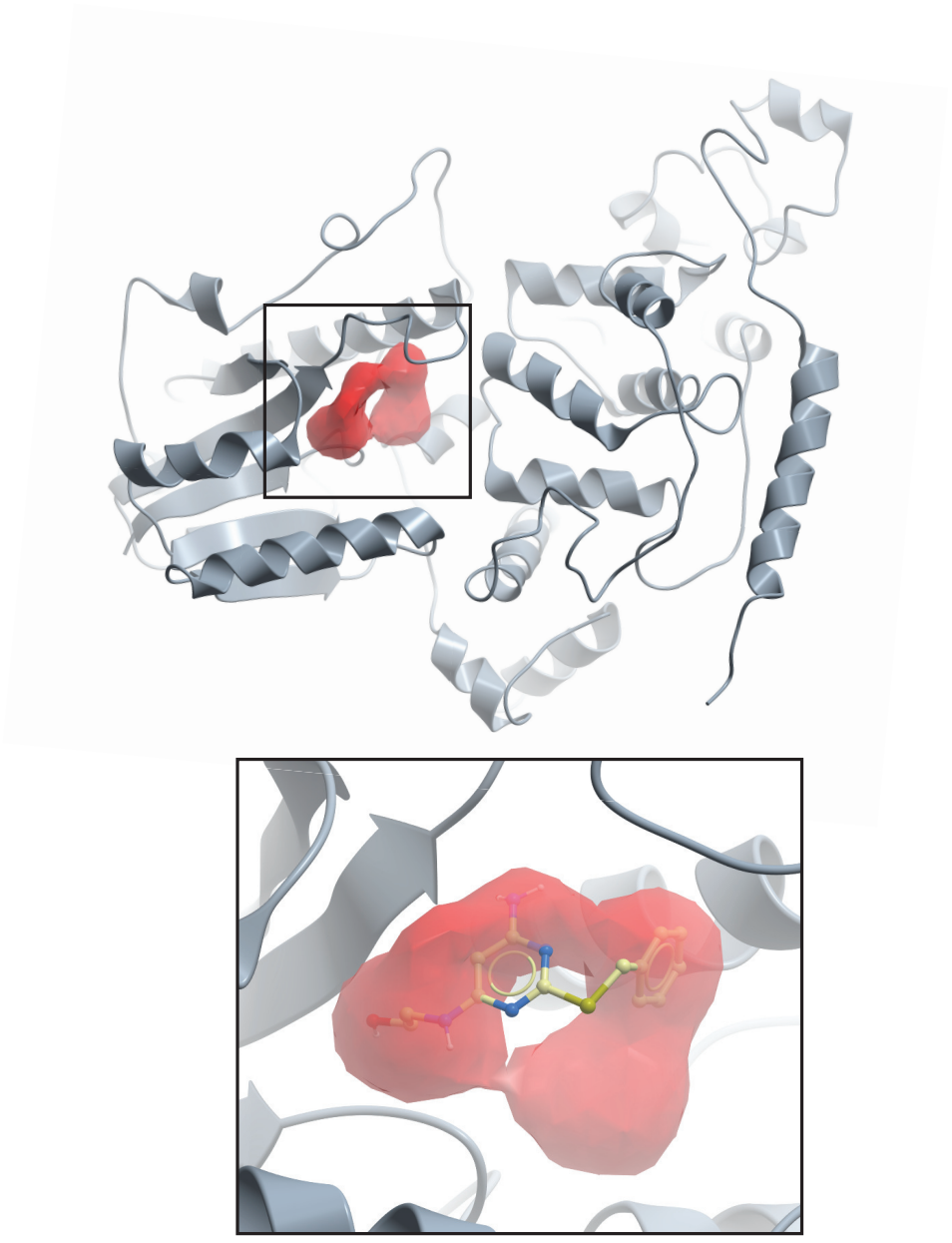

Figure 4.4: **VLS-derived Receptor Pocket on CRY.** Receptor map has been computationally determined to best fit the CRY repression pocket (upper), a representative virtual hit docked into the pocket (yellow) (lower).

that the CRY1 interface outside of the TAD is on the CLOCK PAS-B HI loop, and plan to mutate residues in this loop, particularly Trp362, to ascertain relevance of this binding surface to CRY1. Ongoing work seeks to identify stable, high-affinity constructs for crystallization studies of the ternary complex. Given the prevalence of large, flexible loops on both CLOCK and BMAL1, we are exploring both *in situ* limited-proteolytic digestion as well as constructs with loop deletions.

Although preliminary validation of the virtual hits has not conclusively resulted in any interfacial inhibitors, due to limitations of the assay, the compounds could be acting to promote complex stability. If this is the case, we could use these compounds as crystallization additives if the affinity of current CRY1 PHR CLOCK-BMAL1 bHLH PAS constructs is insufficient for crystal formation and cannot be overcome by construct optimization.

Together, these results indicate that the CRY1-CLOCK-BMAL1 complex is highly sensitive and requires in-depth biochemical analysis to design rational constructs capable of crystallization. If these attempts are exhausted, we will use the largest purifiable constructs (ideally, >170 kDa) for cryo-electron microscopy.

# Chapter 5

# CONCLUSIONS AND FUTURE WORK

Circadian clocks are evolutionarily conserved across all kingdoms of life and represent one of the most tractable systems for understanding the relationship between genes, physiology, and behavior (Reppert and Weaver, 2002). Chronobiology is a wide-spanning interdisciplinary field applicable to ostensibly all lifeforms on Earth. It has benefited greatly from the well-spring of genetics, however, structural biology has not yet been fully exploited in circadian biology. The work presented here couples key aspects of mammalian clock protein structure and function.

We have described the binding mode and mechanism of action of a first-in-class core clock-targeting circadian modulator and substrate-targeting ubiquitination antagonist. KL001 binds to the CRY flavin pocket and acts as a hybrid of FAD and the FBXL3 C-terminal tryptophan, which stabilizes CRY and dose-dependently lengthens the circadian period. KL001 has been shown to inhibit glucagon-induced gluconeogenesis in hepatocytes and offers a novel vector for studying and treating certain metabolic syndromes (Hirota et al., 2012). Not only have we described the structural mechanisms of KL001, we have provided a basis for further chemical optimization and structure-based drug design due to the high resolution of this complex structure (Nangle et al., 2013).

The collective crystal structures of CRY2 we have determined in recent years of apo, FAD-, FBXL3-, KL001- and PER2-bound (Nangle et al., 2014, 2013; Xing et al., 2013) outline a rich topography for the functional surfaces of mammalian CRYs: a level of detail that distinguishes them from other members of the cryptochrome/photolyase family. The PER2-CRY2 complex explains several known mechanisms of PER-CRY dynamics, such as the way in which PER stabilizes CRY from FBXL3-dependent ubiqutination, via the C-terminal he-

lix, which is the site of mutually exclusive binding of FBXL3 and PERs. As well as an explanation for the high-affinity interaction that is formed between a large globular protein and a comparatively small polypeptide sequence. But as is generally the case in structure determination, the complex unveiled more unexpected features. Most strikingly, a structurally important intermolecular zinc finger that clasps CRY and PER together. Although all four residues that coordinate zinc are highly conserved, the functional significance of this never-before-seen binding interface requires additional study. The intermolecular zinc finger might be an intermediate product of the ever-evolving PER-CRY interface or represents an additional aspects of complex formation and clock regulation. Another heretofore unexplored facet of CRY is the function of another large surface pocket opposite to the FAD-binding pocket and the homologous site of the photolyase antenna cofactor binding. We have characterized this pocket as a putative locus for CRY-dependent repression as well as a critical site of CLOCK-BMAL1 binding. Both CRY pockets are demarcated by structural elements with noticeable structural plasticity (Figure 3.18). The FAD-binding pocket is framed by the phosphate-binding loop and the interface loop on opposite edges, whereas the repression pocket is lined by the serine loop. Though only the interface and serine loop have been shown to directly mediate protein–protein interactions. Given these advances, we are only at the beginning stages of formulating a complete description of the CRY molecular landscape, and yet our knowledge of CRY far exceeds that of other clock proteins (Nangle et al., 2014).

The natural progression from the aforementioned work into the CRY-CLOCK-BMAL1 complex has been met with a manifold technical challenges that remain to be resolved. While we know the putative stoichiometry, the boundaries of stable constructs, and have identified crucial binding sites, the conditions necessary for crystal formation are unknown. We hope that with additional screening and construct design (e.g., removal and/or inclusion of loops and use of orthologs) we can form a higher-affinity interaction suitable for crystallization. Complementary studies on the novel CRY-binding compound may also aid in complex analysis, and crystallization particularly, if they act as "molecular adhesives" rather than an interfacial inhibitors.

These data present a foundation from which to build a nuanced and highly sophisticated depiction of the mammalian circadian clockwork, not only for the understanding of a ubiquitously important cellular process, but to reveal effective therapeutics and agents to optimize and fortify the human body.

# BIBLIOGRAPHY

Adams, P. D., Grosse-Kunstleve, R. W., Hung, L.-W., Ioerger, T. R., McCoy, A. J., Moriarty, N. W., Read, R. J., Sacchettini, J. C., Sauter, N. K., and Terwilliger, T. C. (2002). Phenix: building new software for automated crystallographic structure determination. *Acta Crystallographica Section D: Biological Crystallography*, 58(11):1948–1954.

Afonso, C., Tulman, E., Lu, Z., Oma, E., Kutish, G., and Rock, D. (1999). The genome of melanoplus sanguinipes entomopoxvirus. *Journal of virology*, 73(1):533–552.

Ahmad, M. and Cashmore, A. R. (1993). Hy4 gene of a. thaliana encodes a protein with characteristics of a blue-light photoreceptor. *Nature*.

Akashi, M., Okamoto, A., Tsuchiya, Y., Todo, T., Nishida, E., and Node, K. (2014). A positive role for period in mammalian circadian gene expression. *Cell reports*, 7(4):1056–1064.

Amores, A., Force, A., Yan, Y.-L., Joly, L., Amemiya, C., Fritz, A., Ho, R. K., Langeland, J., Prince, V., Wang, Y.-L., et al. (1998). Zebrafish hox clusters and vertebrate genome evolution. *Science*, 282(5394):1711–1714.

Archer, S. N., Robilliard, D. L., Skene, D. J., Smits, M., Williams, A., Arendt, J., and von Schantz, M. (2003). A length polymorphism in the circadian clock gene per3 is linked to delayed sleep phase syndrome and extreme diurnal preference. *Sleep*, 26(4):413–415.

Asher, G. and Schibler, U. (2011). Crosstalk between components of circadian and metabolic cycles in mammals. *Cell metabolism*, 13(2):125–137.

Balsalobre, A., Damiola, F., and Schibler, U. (1998). A serum shock induces circadian gene expression in mammalian tissue culture cells. *Cell*, 93(6):929–937.

Banerjee, R. and Batschauer, A. (2005). Plant blue-light receptors. *Planta*, 220(3):498–502.

Bass, J. and Takahashi, J. S. (2010). Circadian integration of metabolism and energetics. *Science*, 330(6009):1349–1354.

Brünger, A. T., Adams, P. D., Clore, G. M., DeLano, W. L., Gros, P., Grosse-Kunstleve, R. W., Jiang, J.-S., Kuszewski, J., Nilges, M., Pannu, N. S., et al. (1998). Crystallography & nmr system: A new software suite for macromolecular structure determination. *Acta Crystallographica Section D: Biological Crystallography*, 54(5):905–921.

Buhr, E. D., Yoo, S.-H., and Takahashi, J. S. (2010). Temperature as a universal resetting cue for mammalian circadian oscillators. *Science*, 330(6002):379–385.

Busino, L., Bassermann, F., Maiolica, A., Lee, C., Nolan, P. M., Godinho, S. I. H., Draetta, G. F., and Pagano, M. (2007). SCFFbxl3 controls the oscillation of the circadian clock by directing the degradation of cryptochrome proteins. *Science*, 316(5826):900–4.

Canfield, D. E. (2005). The early history of atmospheric oxygen: homage to robert m. garrels. *Annu. Rev. Earth Planet. Sci.*, 33:1–36.

Cashmore, A. R., Jarillo, J. A., Wu, Y.-J., and Liu, D. (1999). Cryptochromes: blue light receptors for plants and animals. *Science*, 284(5415):760–765.

Cavallari, N., Frigato, E., Vallone, D., Fröhlich, N., Fernando Lopez-Olmeda, J., Foà, A., Berti, R., Javier Sánchez-Vázquez, F., Bertolucci, C., and Foulkes, N. S. (2011). A blind circadian clock in cavefish reveals that opsins mediate peripheral clock photoreception. *PLoS-Biology*, 9(9):1872.

Chaves, I., Yagita, K., Barnhoorn, S., Okamura, H., van der Horst, G. T., and Tamanini, F. (2006). Functional evolution of the photolyase/cryptochrome protein family: importance of the c terminus of mammalian cry1 for circadian core oscillator performance. *Molecular and cellular biology*, 26(5):1743–1753.

Chen, R., Schirmer, A., Lee, Y., Lee, H., Kumar, V., Yoo, S.-H., Takahashi, J. S., and Lee, C. (2009). Rhythmic per abundance defines a critical nodal point for negative feedback within the circadian clock mechanism. *Molecular cell*, 36(3):417–430.

Cho, H., Zhao, X., Hatori, M., Ruth, T. Y., Barish, G. D., Lam, M. T., Chong, L.-W., DiTacchio, L., Atkins, A. R., Glass, C. K., et al. (2012). Regulation of circadian behaviour and metabolism by rev-erb-[agr] and rev-erb-[bgr]. *Nature*, 485(7396):123–127.

Chothia, C., Levitt, M., and Richardson, D. (1977). Structure of proteins: packing of alpha-helices and pleated sheets. *Proceedings of the National Academy of Sciences*, 74(10):4130–4134.

Cockell, C. S. and Raven, J. A. (2007). Ozone and life on the archaean earth. *Philosophical Transactions of the Royal Society of London A: Mathematical, Physical and Engineering Sciences*, 365(1856):1889–1901.

Cortese, M. S., Uversky, V. N., and Dunker, A. K. (2008). Intrinsic disorder in scaffold proteins: getting more from less. *Progress in biophysics and molecular biology*, 98(1):85–106.

Craigie, W., Murray, J., and Simpson, J. (2015). *The Oxford English Dictionary*. Oxford University Press.

Cushing, D. (1951). The vertical migration of planktonic crustacea. *Biological reviews*, 26(2):158–192.

Czarna, A., Berndt, A., Singh, H. R., Grudziecki, A., Ladurner, A. G., Timinszky, G., Kramer, A., and Wolf, E. (2013). Structures of Drosophila Cryptochrome and Mouse Cryptochrome1 Provide Insight into Circadian Function. *Cell*, 153(6):1394–1405.

Czarna, A., Breitkreuz, H., Mahrenholz, C. C., Arens, J., Strauss, H. M., and Wolf, E. (2011). Quantitative analyses of cryptochrome-mbmal1 interactions mechanistic insights

into the transcriptional regulation of the mammalian circadian clock. *Journal of Biological Chemistry*, 286(25):22414–22425.

Darwin, C. and Darwin, F. (1880). *The power of movement in plants*. John Murray.

Duong, H. a., Robles, M. S., Knutti, D., and Weitz, C. J. (2011). A molecular mechanism for circadian clock negative feedback. *Science*, 332(6036):1436–9.

Ebisawa, T., Uchiyama, M., Kajimura, N., Mishima, K., Kamei, Y., Katoh, M., Watanabe, T., Sekimoto, M., Shibui, K., Kim, K., et al. (2001). Association of structural polymorphisms in the human period3 gene with delayed sleep phase syndrome. *EMBO reports*, 2(4):342–346.

Eker, A., Hessels, J., and Van de Velde, J. (1988). Photoreactivating enzyme from the green alga scenedesmus acutus. evidence for the presence of two different flavin chromophores. *Biochemistry*, 27(5):1758–1765.

Emsley, P., Lohkamp, B., Scott, W. G., and Cowtan, K. (2010). Features and development of coot. *Acta Crystallographica Section D: Biological Crystallography*, 66(4):486–501.

Etchegaray, J.-P., Lee, C., Wade, P. A., and Reppert, S. M. (2003). Rhythmic histone acetylation underlies transcription in the mammalian circadian clock. *Nature*, 421(6919):177–182.

Fujihashi, M., Numoto, N., Kobayashi, Y., Mizushima, A., Tsujimura, M., Nakamura, A., Kawarabayasi, Y., and Miki, K. (2007). Crystal structure of archaeal photolyase from sulfolobus tokodaii with two fad molecules: implication of a novel light-harvesting cofactor. *Journal of molecular biology*, 365(4):903–910.

Fuxreiter, M., Tompa, P., Simon, I., Uversky, V. N., Hansen, J. C., and Asturias, F. J. (2008). Malleable machines take shape in eukaryotic transcriptional regulation. *Nature chemical biology*, 4(12):728–737.

Gao, P., Yoo, S.-H., Lee, K.-J., Rosensweig, C., Takahashi, J. S., Chen, B. P., and Green, C. B. (2013). Phosphorylation of the cryptochrome 1 c-terminal tail regulates circadian period length. *Journal of Biological Chemistry*, 288(49):35277–35286.

Gehring, W. and Rosbash, M. (2003). The coevolution of blue-light photoreception and circadian rhythms. *Journal of molecular evolution*, 57(1):S286–S289.

Gerber, A., Esnault, C., Aubert, G., Treisman, R., Pralong, F., and Schibler, U. (2013). Blood-borne circadian signal stimulates daily oscillations in actin dynamics and srf activity. *Cell*, 152(3):492–503.

Glas, A. F., Schneider, S., Maul, M. J., Hennecke, U., and Carell, T. (2009). Crystal structure of the t (6-4) c lesion in complex with a (6-4) dna photolyase and repair of uv-induced (6-4) and dewar photolesions. *Chemistry-A European Journal*, 15(40):10387–10396.

Glasauer, S. M. and Neuhauss, S. C. (2014). Whole-genome duplication in teleost fishes and its evolutionary consequences. *Molecular Genetics and Genomics*, 289(6):1045–1060.

Godinho, S. I., Maywood, E. S., Shaw, L., Tucci, V., Barnard, A. R., Busino, L., Pagano, M., Kendall, R., Quwailid, M. M., Romero, M. R., et al. (2007). The after-hours mutant reveals a role for fbxl3 in determining mammalian circadian period. *Science*, 316(5826):897–900.

Green, C. B., Takahashi, J. S., and Bass, J. (2008). The meter of metabolism. *Cell*, 134(5):728–742.

Griffin, E. A., Staknis, D., and Weitz, C. J. (1999). Light-independent role of cry1 and cry2 in the mammalian circadian clock. *Science*, 286(5440):768–771.

Hastings, J. W. and Sweeney, B. M. (1957). On the mechanism of temperature independence in a biological clock. *Proceedings of the National Academy of Sciences of the United States of America*, 43(9):804.

Hirano, A., Yumimoto, K., Tsunematsu, R., Matsumoto, M., Oyama, M., Kozuka-Hata, H., Nakagawa, T., Lanjakornsiripan, D., Nakayama, K. I., and Fukada, Y. (2013). FBXL21 Regulates Oscillation of the Circadian Clock through Ubiquitination and Stabilization of Cryptochromes. *Cell*, 152(5):1106–18.

Hirota, T., Lee, J. W., St John, P. C., Sawa, M., Iwaisako, K., Noguchi, T., Pongsawakul, P. Y., Sonntag, T., Welsh, D. K., Brenner, D. a., Doyle, F. J., Schultz, P. G., and Kay, S. a. (2012). Identification of small molecule activators of cryptochrome. *Science*, 337(6098):1094–7.

Huang, N., Chelliah, Y., Shan, Y., Taylor, C. a., Yoo, S.-H., Partch, C., Green, C. B., Zhang, H., and Takahashi, J. S. (2012). Crystal structure of the heterodimeric CLOCK:BMAL1 transcriptional activator complex. *Science*, 337(6091):189–94.

Huang, R.-C., Peng, Y.-W., and Yau, K.-W. (1993). Zinc modulation of a transient potassium current and histochemical localization of the metal in neurons of the suprachiasmatic nucleus. *Proceedings of the National Academy of Sciences*, 90(24):11806–11810.

John, P. C. S., Hirota, T., Kay, S. A., and Doyle, F. J. (2014). Spatiotemporal separation of per and cry posttranslational regulation in the mammalian circadian clock. *Proceedings of the National Academy of Sciences*, 111(5):2040–2045.

Johnson, J. L., Hamm-Alvarez, S., Payne, G., Sancar, G. B., Rajagopalan, K., and Sancar, A. (1988). Identification of the second chromophore of escherichia coli and yeast dna photolyases as 5, 10-methenyltetrahydrofolate. *Proceedings of the National Academy of Sciences*, 85(7):2046–2050.

Jorns, M. S., Sancar, G. B., and Sancar, A. (1984). Identification of a neutral flavin radical and characterization of a second chromophore in escherichia coli dna photolyase. *Biochemistry*, 23(12):2673–2679.

Kelner, A. (1949). Photoreactivation of ultraviolet-irradiated escherichia coli, with special reference to the dose-reduction principle and to ultraviolet-induced mutation. *Journal of bacteriology*, 58(4):511.

Khan, S. K., Xu, H., Ukai-Tadenuma, M., Burton, B., Wang, Y., Ueda, H. R., and Liu, A. C. (2012). Identification of a novel cryptochrome differentiating domain required for feedback repression in circadian clock function. *Journal of Biological Chemistry*, 287(31):25917–25926.

Kiyohara, Y. B., Tagao, S., Tamanini, F., Morita, A., Sugisawa, Y., Yasuda, M., Yamanaka, I., Ueda, H. R., van der Horst, G. T., Kondo, T., et al. (2006). The bmal1 c terminus regulates the circadian transcription feedback loop. *Proceedings of the National Academy of Sciences*, 103(26):10074–10079.

Klugh, A. B. (1930). The effect of the ultra-violet component of the sun's radiation upon some aquatic organisms. *Canadian Journal of Research*, 2(5):312–317.

Koh, K., Zheng, X., and Sehgal, A. (2006). Jetlag resets the drosophila circadian clock by promoting light-induced degradation of timeless. *Science*, 312(5781):1809–1812.

Koike, N., Yoo, S.-H., Huang, H.-C., Kumar, V., Lee, C., Kim, T.-K., and Takahashi, J. S. (2012). Transcriptional architecture and chromatin landscape of the core circadian clock in mammals. *Science*, 338(6105):349–354.

Koornneef, M., Rolff, E., and Spruit, C. (1980). Genetic control of light-inhibited hypocotyl elongation in arabidopsis thaliana (l.) heynh. *Zeitschrift für Pflanzenphysiologie*, 100(2):147–160.

Kucera, N., Schmalen, I., Hennig, S., Öllinger, R., Strauss, H. M., Grudziecki, A., Wieczorek, C., Kramer, A., and Wolf, E. (2012). Unwinding the differences of the mammalian period clock proteins from crystal structure to cellular function. *Proceedings of the National Academy of Sciences*, 109(9):3311–3316.

Kume, K., Zylka, M. J., Sriram, S., Shearman, L. P., Weaver, D. R., Jin, X., Maywood, E. S., Hastings, M. H., and Reppert, S. M. (1999). mCRY1 and mCRY2 are essential components of the negative limb of the circadian clock feedback loop. *Cell*, 98(2):193–205.

Kurabayashi, N., Hirota, T., Sakai, M., Sanada, K., and Fukada, Y. (2010). Dyrk1a and glycogen synthase kinase 3$\beta$, a dual-kinase mechanism directing proteasomal degradation of cry2 for circadian timekeeping. *Molecular and cellular biology*, 30(7):1757–1768.

Lakin-Thomas, P. L. and Brody, S. (2004). Circadian rhythms in microorganisms: new complexities. *Annu. Rev. Microbiol.*, 58:489–519.

Lamia, K. a., Sachdeva, U. M., DiTacchio, L., Williams, E. C., Alvarez, J. G., Egan, D. F., Vasquez, D. S., Juguilon, H., Panda, S., Shaw, R. J., Thompson, C. B., and Evans, R. M. (2009). AMPK regulates the circadian clock by cryptochrome phosphorylation and degradation. *Science*, 326(5951):437–40.

Lee, C., Etchegaray, J. P., Cagampang, F. R., Loudon, a. S., and Reppert, S. M. (2001). Posttranslational mechanisms regulate the mammalian circadian clock. *Cell*, 107(7):855–67.

Li, Y. F., Kim, S.-T., and Sancar, A. (1993). Evidence for lack of dna photoreactivating enzyme in humans. *Proceedings of the National Academy of Sciences*, 90(10):4389–4393.

Lin, C. and Todo, T. (2005). The cryptochromes. *Genome biology*, 6(5):220.

Liu, A. C., Welsh, D. K., Ko, C. H., Tran, H. G., Zhang, E. E., Priest, A. A., Buhr, E. D., Singer, O., Meeker, K., Verma, I. M., et al. (2007). Intercellular coupling confers robustness against mutations in the scn circadian clock network. *Cell*, 129(3):605–616.

Lowrey, P. L., Shimomura, K., Antoch, M. P., Yamazaki, S., Zemenides, P. D., Ralph, M. R., Menaker, M., and Takahashi, J. S. (2000). Positional syntenic cloning and functional characterization of the mammalian circadian mutation tau. *Science*, 288(5465):483–491.

Lowrey, P. L. and Takahashi, J. S. (2011). Genetics of circadian rhythms in mammalian model organisms. *Advances in genetics*, 74:175.

Maul, M. J., Barends, T. R., Glas, A. F., Cryle, M. J., Domratcheva, T., Schneider, S., Schlichting, I., and Carell, T. (2008). Crystal structure and mechanism of a dna (6-4) photolyase. *Angewandte Chemie International Edition*, 47(52):10076–10080.

Maury, E., Ramsey, K. M., and Bass, J. (2010). Circadian rhythms and metabolic syndrome from experimental genetics to human disease. *Circulation research*, 106(3):447–462.

McCarthy, E. V., Baggs, J. E., Geskes, J. M., Hogenesch, J. B., and Green, C. B. (2009). Generation of a novel allelic series of cryptochrome mutants via mutagenesis reveals residues involved in protein-protein interaction and cry2-specific repression. *Molecular and cellular biology*, 29(20):5465–5476.

Mei, Q. and Dvornyk, V. (2015). Evolutionary history of the photolyase/cryptochrome superfamily in eukaryotes. *PloS one*, 10(9):e0135940.

Nangle, S., Xing, W., and Zheng, N. (2013). Crystal structure of mammalian cryptochrome in complex with a small molecule competitor of its ubiquitin ligase. *Cell research*, 23(12):1417.

Nangle, S. N., Rosensweig, C., Koike, N., Tei, H., Takahashi, J. S., Green, C. B., and Zheng, N. (2014). Molecular assembly of the period-cryptochrome circadian transcriptional repressor complex. *Elife*, 3:e03674.

Öllinger, R., Korge, S., Korte, T., Koller, B., Herrmann, A., and Kramer, A. (2014). Dynamics of the circadian clock protein period2 in living cells. *Journal of cell science*, 127(19):4322–4328.

Otwinowski, Z., Minor, W., and W Jr, C. C. (1997). Processing of x-ray diffraction data collected in oscillation mode. *Methods in Enzymology*.

Ozber, N., Baris, I., Tatlici, G., Gur, I., Kilinc, S., Unal, E. B., and Kavakli, I. H. (2010). Identification of two amino acids in the c-terminal domain of mouse cry2 essential for per2 interaction. *BMC molecular biology*, 11(1):69.

Padmanabhan, K., Robles, M. S., Westerling, T., and Weitz, C. J. (2012). Feedback regulation of transcriptional termination by the mammalian circadian clock period complex. *Science*, 337(6094):599–602.

Panda, S., Antoch, M. P., Miller, B. H., Su, A. I., Schook, A. B., Straume, M., Schultz, P. G., Kay, S. A., Takahashi, J. S., and Hogenesch, J. B. (2002). Coordinated transcription of key pathways in the mouse by the circadian clock. *Cell*, 109(3):307–320.

Pando, M. P., Morse, D., Cermakian, N., and Sassone-Corsi, P. (2002). Phenotypic rescue of a peripheral clock genetic defect via scn hierarchical dominance. *Cell*, 110(1):107–117.

Partch, C. L., Clarkson, M. W., Özgür, S., Lee, A. L., and Sancar, A. (2005). Role of structural plasticity in signal transduction by the cryptochrome blue-light photoreceptor. *Biochemistry*, 44(10):3795–3805.

Partch, C. L., Green, C. B., and Takahashi, J. S. (2014). Molecular architecture of the mammalian circadian clock. *Trends in cell biology*, 24(2):90–99.

Pittendrigh, C. S. (1993). TEMPORAL ORGANIZATION : Reflections of a Darwinian. pages 17–54.

Plikus, M. V., Vollmers, C., de la Cruz, D., Chaix, A., Ramos, R., Panda, S., and Chuong, C.-M. (2013). Local circadian clock gates cell cycle progression of transient amplifying cells during regenerative hair cycling. *Proceedings of the National Academy of Sciences*, 110(23):E2106–E2115.

Project, C. C. (1994). The ccp4 suite: programs for protein crystallography. *Acta crystallographica. Section D, Biological crystallography*, 50(Pt 5):760.

Reischl, S., Vanselow, K., Westermark, P. O., Thierfelder, N., Maier, B., Herzel, H., and Kramer, A. (2007). $\beta$-trcp1-mediated degradation of period2 is essential for circadian dynamics. *Journal of biological rhythms*, 22(5):375–386.

Reppert, S. M. and Weaver, D. R. (2002). Coordination of circadian timing in mammals. *Nature*, 418(6901):935–41.

Rupert, C. S., Goodgal, S. H., and Herriott, R. M. (1958). Photoreactivation in vitro of ultraviolet inactivated hemophilus influenzae transforming factor. *The Journal of general physiology*, 41(3):451.

Sack, R. L., Auckley, D., Auger, R. R., Carskadon, M. A., Wright Jr, K. P., Vitiello, M. V., and Zhdanova, I. V. (2007). Circadian rhythm sleep disorders: part ii, advanced sleep phase disorder, delayed sleep phase disorder, free-running disorder, and irregular sleep-wake rhythm: an american academy of sleep medicine review. *Sleep*, 30(11):1484.

Sancar, A. (1994). Structure and function of dna photolyase. *Biochemistry*, 33(1):2–9.

Sancar, A. (1996). Dna excision repair. *Annual review of biochemistry*, 65(1):43–81.

Sancar, A. (2003). Structure and function of dna photolyase and cryptochrome blue-light photoreceptors. *Chemical reviews*, 103(6):2203–2238.

Sancar, A. (2008). Structure and function of photolyase and in vivo enzymology: 50th anniversary. *Journal of Biological Chemistry*, 283(47):32153–32157.

Sato, T. K., Yamada, R. G., Ukai, H., Baggs, J. E., Miraglia, L. J., Kobayashi, T. J., Welsh, D. K., Kay, S. A., Ueda, H. R., and Hogenesch, J. B. (2006). Feedback repression is required for mammalian circadian clock function. *Nature genetics*, 38(3):312–319.

Schmalen, I., Reischl, S., Wallach, T., Klemz, R., Grudziecki, A., Prabu, J. R., Benda, C., Kramer, A., and Wolf, E. (2014). Interaction of circadian clock proteins cry1 and per2 is modulated by zinc binding and disulfide bond formation. *Cell*, 157(5):1203–1215.

Shanware, N. P., Hutchinson, J. A., Kim, S. H., Zhan, L., Bowler, M. J., and Tibbetts, R. S. (2011). Casein kinase 1-dependent phosphorylation of familial advanced sleep phase syndrome-associated residues controls period 2 stability. *Journal of Biological Chemistry*, 286(14):12766–12774.

Shearman, L. P., Sriram, S., Weaver, D. R., Maywood, E. S., Chaves, I., Zheng, B., Kume, K., Lee, C. C., Hastings, M. H., Reppert, S. M., et al. (2000). Interacting molecular loops in the mammalian circadian clock. *Science*, 288(5468):1013–1019.

Shirogane, T., Jin, J., Ang, X. L., and Harper, J. W. (2005). Scf$\beta$-trcp controls clock-dependent transcription via casein kinase 1-dependent degradation of the mammalian period-1 (per1) proteinm. *Journal of Biological Chemistry*, 280(29):26863–26872.

Siepka, S. M., Yoo, S.-H., Park, J., Song, W., Kumar, V., Hu, Y., Lee, C., and Takahashi, J. S. (2007). Circadian mutant Overtime reveals F-box protein FBXL3 regulation of cryptochrome and period gene expression. *Cell*, 129(5):1011–23.

Smolensky, M. H. and Peppas, N. A. (2007). Chronobiology, drug delivery, and chronotherapeutics. *Advanced drug delivery reviews*, 59(9):828–851.

Somers, W., Ultsch, M., De Vos, A. M., and Kossiakoff, A. A. (1994). The x-ray structure of a growth hormone prolactin receptor complex. *Nature*.

Storch, K.-F., Lipan, O., Leykin, I., Viswanathan, N., Davis, F. C., Wong, W. H., and Weitz, C. J. (2002). Extensive and divergent circadian gene expression in liver and heart. *Nature*, 417(6884):78–83.

Takano, A., Uchiyama, M., Kajimura, N., Mishima, K., Inoue, Y., Kamei, Y., Kitajima, T., Shibui, K., Katoh, M., Watanabe, T., et al. (2004). A missense variation in human casein kinase i epsilon gene that induces functional alteration and shows an inverse association with circadian rhythm sleep disorders. *Neuropsychopharmacology: official publication of the American College of Neuropsychopharmacology*, 29(10):1901–1909.

Toh, K. L., Jones, C. R., He, Y., Eide, E. J., Hinz, W. A., Virshup, D. M., Ptáček, L. J., and Fu, Y.-H. (2001). An hper2 phosphorylation site mutation in familial advanced sleep phase syndrome. *Science*, 291(5506):1040–1043.

Tu, B. P. and Weissman, J. S. (2002). The fad-and o 2-dependent reaction cycle of ero1-mediated oxidative protein folding in the endoplasmic reticulum. *Molecular cell*, 10(5):983–994.

Ueda, H. R., Chen, W., Adachi, A., Wakamatsu, H., Hayashi, S., Takasugi, T., Nagano, M., Nakahama, K.-i., Suzuki, Y., Sugano, S., et al. (2002). A transcription factor response element for gene expression during circadian night. *Nature*, 418(6897):534–539.

Ueda, T., Kato, A., Kuramitsu, S., Terasawa, H., and Shimada, I. (2005). Identification and characterization of a second chromophore of dna photolyase from thermus thermophilus hb27. *Journal of Biological Chemistry*, 280(43):36237–36243.

Ukai-Tadenuma, M., Yamada, R. G., Xu, H., Ripperger, J. A., Liu, A. C., and Ueda, H. R. (2011). Delay in feedback repression by cryptochrome 1 is required for circadian clock function. *Cell*, 144(2):268–281.

Van Der Horst, G. T., Muijtjens, M., Kobayashi, K., Takano, R., Kanno, S.-i., Takao, M., de Wit, J., Verkerk, A., Eker, A. P., van Leenen, D., et al. (1999). Mammalian cry1 and cry2 are essential for maintenance of circadian rhythms. *Nature*, 398(6728):627–630.

Vanselow, K. and Kramer, A. (2007). Role of phosphorylation in the mammalian circadian clock. In *Cold Spring Harbor symposia on quantitative biology*, volume 72, pages 167–176. Cold Spring Harbor Laboratory Press.

Wang, D., Hosteen, O., and Fierke, C. A. (2012). Zntr-mediated transcription of znta responds to nanomolar intracellular free zinc. *Journal of inorganic biochemistry*, 111:173–181.

Wang, H., Ma, L.-G., Li, J.-M., Zhao, H.-Y., and Deng, X. W. (2001). Direct interaction of arabidopsis cryptochromes with cop1 in light control development. *Science*, 294(5540):154–158.

Willer, D. O., McFadden, G., and Evans, D. H. (1999). The complete genome sequence of shope (rabbit) fibroma virus. *Virology*, 264(2):319–343.

Willich, S., Klatt, S., and Arntz, H. (1998). Circadian variation and triggers of acute coronary syndromes. *European heart journal*, 19:C12–23.

Woelfle, M. A., Ouyang, Y., Phanvijhitsiri, K., and Johnson, C. H. (2004). The adaptive value of circadian clocks: an experimental assessment in cyanobacteria. *Current Biology*, 14(16):1481–1486.

Wood, R. D. (1997). Nucleotide excision repair in mammalian cells. *Journal of Biological Chemistry*, 272(38):23465–23468.

Xing, W., Busino, L., Hinds, T. R., Marionni, S. T., Saifee, N. H., Bush, M. F., Pagano, M., and Zheng, N. (2013). SCFFBXL3 ubiquitin ligase targets cryptochromes at their cofactor pocket. *Nature*, pages 5–10.

Xu, H., Gustafson, C. L., Sammons, P. J., Khan, S. K., Parsley, N. C., Ramanathan, C., Lee, H.-W., Liu, A. C., and Partch, C. L. (2015). Cryptochrome 1 regulates the circadian clock through dynamic interactions with the bmal1 c terminus. *Nature structural & molecular biology*.

Xu, Y., Padiath, Q. S., Shapiro, R. E., Jones, C. R., Wu, S. C., Saigoh, N., Saigoh, K., Ptáček, L. J., and Fu, Y.-H. (2005). Functional consequences of a ck$i\delta$ mutation causing familial advanced sleep phase syndrome. *Nature*, 434(7033):640–644.

Yagita, K., Tamanini, F., Yasuda, M., Hoeijmakers, J. H. J., van der Horst, G. T. J., and Okamura, H. (2002). Nucleocytoplasmic shuttling and mCRY-dependent inhibition of ubiquitylation of the mPER2 clock protein. *EMBO J.*, 21(6):1301–14.

Yagita, K., Yamaguchi, S., Tamanini, F., van der Horst, G. T., Hoeijmakers, J. H., Yasui, A., Loros, J. J., Dunlap, J. C., and Okamura, H. (2000). Dimerization and nuclear entry of mper proteins in mammalian cells. *Genes & development*, 14(11):1353–1363.

Yamazaki, S., Numano, R., Abe, M., Hida, A., Takahashi, R.-i., Ueda, M., Block, G. D., Sakaki, Y., Menaker, M., and Tei, H. (2000). Resetting central and peripheral circadian oscillators in transgenic rats. *Science*, 288(5466):682–685.

Ye, R., Selby, C. P., Chiou, Y.-Y., Ozkan-Dagliyan, I., Gaddameedhi, S., and Sancar, A. (2014). Dual modes of clock: Bmal1 inhibition mediated by cryptochrome and period proteins in the mammalian circadian clock. *Genes & development*, 28(18):1989–1998.

Ye, R., Selby, C. P., Ozturk, N., Annayev, Y., and Sancar, A. (2011). Biochemical analysis of the canonical model for the mammalian circadian clock. *J. Biol. Chem.*, 286(29):25891–902.

Yildiz, O., Doi, M., Yujnovsky, I., Cardone, L., Berndt, A., Hennig, S., Schulze, S., Urbanke, C., Sassone-Corsi, P., and Wolf, E. (2005). Crystal structure and interactions of the PAS repeat region of the Drosophila clock protein PERIOD. *Mol. Cell*, 17(1):69–82.

Yoo, S.-H., Mohawk, J. A., Siepka, S. M., Shan, Y., Huh, S. K., Hong, H.-K., Kornblum, I., Kumar, V., Koike, N., Xu, M., Nussbaum, J., Liu, X., Chen, Z., Chen, Z. J., Green, C. B., and Takahashi, J. S. (2013). Competing E3 Ubiquitin Ligases Govern Circadian Periodicity by Degradation of CRY in Nucleus and Cytoplasm. *Cell*, 152(5):1091–1105.

Zhao, W.-N., Malinin, N., Yang, F.-C., Staknis, D., Gekakis, N., Maier, B., Reischl, S., Kramer, A., and Weitz, C. J. (2007). Cipc is a mammalian circadian clock protein without invertebrate homologues. *Nature cell biology*, 9(3):268–275.

Zhou, M., Kim, J. K., Eng, G. W. L., Forger, D. B., and Virshup, D. M. (2015). A period2 phosphoswitch regulates and temperature compensates circadian period. *Molecular cell*, 60(1):77–88.

Zhu, H., Conte, F., and Green, C. B. (2003). Nuclear localization and transcriptional repression are confined to separable domains in the circadian protein cryptochrome. *Current biology*, 13(18):1653–1658.

Zoltowski, B. D., Vaidya, A. T., Top, D., Widom, J., Young, M. W., and Crane, B. R. (2011). Structure of full-length Drosophila cryptochrome. *Nature*, 480(7377):396–9.

# Appendix A

# MATERIALS AND METHODS

## *A.1 Recombinant Protein Purification*

### *A.1.1 CRY2-KL001*

The mouse CRY2 (amino acids 1-512) was expressed as a glutathione S-transferase (GST) fusion protein in High Five (Invitrogen) suspension insect cells and isolated by glutathione affinity chromatography using buffer containing 20mM Tris-HCl, pH8, 300mM NaCl, 10% glycerol, 5mM DTT (dithiothreitol). The protein was cleaved on-column by tobacco etch virus (TEV) protease then purified further by cation- exchange chromatography. Concentrated CRY2 protein (10 mg/ml) was mixed with 50 mM KL001 dissolved in DMSO and further purified by gel-filtration chromatography using buffer containing 10 mM Tris pH 7.5, 50 mM NaCl, 50 mM KCl, 10 mM DTT, 10% glycerol.

### *A.1.2 CRY2-PER2*

The mouse CRY2 (amino acids 1-512) was expressed as a glutathione S-transferase (GST) fusion protein in High Five (Invitrogen, Carlsbad, CA) suspension insect cells and isolated by glutathione affinity chromatography using buffer containing 20 mM Tris-HCl pH 8, 200 mM NaCl, 10% glycerol, 5 mM DTT. The protein was cleaved on-column by TEV protease then purified further by cation-exchange chromatography. Proteolytically stable murine PER2 (amino acids 1095-1215) was expressed as a GST-fusion protein in Escherichia coli expression system and isolated through glutathione affinity chromatography using buffer containing 20 mM Tris-HCl pH 8, 300 mM NaCl, 5 mM DTT. The protein was cleaved on-column by TEV protease then purified further by anion-exchange and size-exclusion chromatography. Both

proteins were combined, concentrated, and further purified by size-exclusion chromatography using buffer containing 20 mM Tris-HCl pH 8, 300 mM NaCl, 5 mM DTT, 10% glycerol to establish stoichiometric binding.

### *A.1.3 CRY-CLOCK-BMAL1*

Significant effort was made to create readily purifiable CLOCK-BMAL1 constructs. Initially, I used the boundaries reported in Huang et al. (2012) human untagged CLOCK (amino acids 26-384) and GST-BMAL1 (67-447) which is composed of the N-terminal bHLH DNA binding domain and the tandem PAS domains. These constructs were co-expressed in High Five suspension insect cell culture and purified using buffer containing 20 mM Tris-HCl pH 8, 400 mM NaCl, 10% glycerol, 5 mM DTT by glutathione affinity chromatography, followed by heparin and size-exclusion chromatography. Purified CLOCK-BMAL1 was then mixed at a 1:1.2 molar ratio with CRY1 PHR to establish a 1:1 stoichiometric complex on SEC. While this construct could be concentrated up to 5 mg/mL no crystal hits were observed after multiple high-throughput screens. Subsequent constructs were designed for co-expression with CRY2 and varied the length of the BMAL1 C-terminal loop and TAD. While a number of these constructs could co-purify with CRY, degradation and complex instability on SEC lead to the abandonment of the CRY2 co-expression approach.

## *A.2 Crystallization, Data Collection, and Structure Determination*

### *A.2.1 CRY2-KL001*

The crystals of the CRY2-KL001 complex were grown at 4°Cby the hanging-drop vapor diffusion method, using 1.5µl protein complex sample mixed with an equal volume of reservoir solution containing 0.1 M MES, pH 6.5, and 4-5% PEG8K. Diffraction-quality crystals were subjected to a post- crystallization cryo-protectant procedure by gradually increasing the concentration of ethylene glycol to 30% and then directly frozen in liquid nitrogen. The data sets were collected at the 19ID beamline at the Advanced Photon Source of the Argonne Na-

tional Laboratory as well as BL8.2.1 beamline at the Advanced Light Source of the Lawrence Berkeley National Laboratory. Reflection data were indexed, integrated, and scaled with the HKL2000 Otwinowski et al. (1997). The CRY2-KL001 complex was determined by molecular replacement using CRY2 from the murine CRY2-FBXL3 complex structure (PDB:4I6J) as the search model. The structural models were manually built, refined, and rebuilt with the programs COOT Emsley et al. (2010) and PHENIX Adams et al. (2002). KL001 was built in and included in the refinement after the R-free value dropped below 0.24. The crystals contain four KL001-bound CRY2 molecules in the asymmetric unit with minor conformational differences in select loop regions (Supplementary Figure1a). All figures were made using PyMOL (Schrdinger, LLC).

### *A.2.2 CRY2-PER2*

The crystals of the CRY2-PER2 complex were grown at 4°Cby the hanging-drop vapor diffusion method, using 2 µl protein complex sample mixed 2:1 with reservoir solution containing 100 mM HEPES pH 7.5, 200 mM NaCl, 15% PEG 3350. Diffraction-quality crystals were subjected to a cryo-protectant procedure by gradually increasing the concentration of ethylene glycol to 25% (vol/vol) and then frozen in liquid nitrogen. The native and zinc anomalous data sets were collected at the BL8.2.1 beamline at the Advanced Light Source of the Lawrence Berkeley National Laboratory. Reflection data were indexed, integrated, and scaled with the HKL2000. The CRY2-PER2 complex was determined by molecular replacement using CRY2 from the CRY2-KL001 complex structure (PDB:4MLP) as the search model. The structural models were manually built, refined, and rebuilt with the programs COOT, PHENIX, and CCP4 Project (1994). PER2 was built in following density modification. All figures were made using PyMOL. Buried surface area was calculated using CNS Brünger et al. (1998).

### *A.3 In Vitro GST Pull Down*

GST-tagged mCRY2 (amino acids 1-512) was over-expressed in High Five insect cells suspension culture. GST-tagged mPER2 WT (amino acids 1095-1215) and GST-tagged mPER2ΔCXXC (amino acids 1095-1209) were over-expressed in E. coli and purified as previously described. Equal volumes CRY2-PHR was incubated with immobilized PER2 at 4°Cfor 1 hr. Glutathione beads were rigorously washed, and GST-PER2-CRY2 was released from the beads with SDS sample buffer, analyzed by SDS-PAGE and detected by Coomasssie stain.

### *A.4 Inductively-coupled Plasma Mass Spectrometry*

For quantitatively determining the identity of the heavy atom seen in the electron density map we used inductively-coupled plasma mass spectrometry for analysis of specific metal isotopes. Purified, concentrated PER2-CBD-CRY2 complex (8 mg/ml) in standard buffer (20 mM Tris-HCl pH 8, 100 mM NaCl (low salt is needed for increased sensitivity), 5 mM DTT, 10% glycerol) was dehydrated for 3-4 hours in a SpeedVac, dissolved in concentrated $HNO_3$ overnight at room temperature, diluted to a stock solution of 1% v/v HNO3, and titrated to 1, 2, 10, 25, 50 ppm protein. We took an unbiased approach looking at all biologically relevant isotopes of: Zn, Fe, Co, Cu, Mo, Mg. However Zn isotopes were the only that followed a dose-dependent increase and more than six-fold mean signal intensity above the blank. Because zinc isotopes are approximately 64 Da and the PER-CRY complex is 72 kDa, we estimated approximately $1{:}10^3$ zinc:protein ratio for our sample and standards calculations. Iron and Magnesium were used as controls. All measurements were subtracted by the buffer blank solution and were analyzed on the same sample. Repeated twice.

### *A.5 Co-immunoprecipitation*

N-terminal Myc-tagged Cry2 (0.25 g) and a C-terminal V5-tagged Per2 (0.5 g) were transfected (Fugene 6, Madison, WI) into HEK293 cells. After 48 hr, cells were harvested and lysed by centrifugation. α-MYC-conjugated beads were used to immobilize MYC-CRY2.

Beads were washed with buffer containing 50 mM Tris-HCl pH 7.5, 100 mM NaCl, 5% glycerol, 0.5 mM DTT, 0.5% Triton X-100, protease inhibitor (1:50). Protein was released from beads with SDS sample buffer and analyzed by Western blot using α-MYC and α-V5 for CRY2 and PER2, respectively.

### *A.6 Real-time Circadian Rescue Assays*

In collaboration with the Green lab at UT Southwestern, real-time circadian rescue assays performed as described in Ukai-Tadenuma et al. (2011) Ukai-Tadenuma et al. (2011). Cry1$^{/}$/Cry2$^{/}$ MEFs were plated in 35-mm dishes at a density of 5  105 cells per dish. 24 hr later, cells were transfected with FuGene6 with 4 g of pGL3-P(Per2)-dLuc reporter plasmid and 150 ng of the pMU2-mCry1 expression vector (Ukai-Tadenuma et al., 2011) or mutant forms of this vector. 72 hr after transfection, the cells were synchronized by a 2-hr incubation in medium (DMEM/10% FBS/antibiotics) with dexamethasone (1 μM). The medium was then replaced with medium prepared from powdered DMEM without phenol red (Corning 90-013-PB) containing 4.5 g/l glucose and supplemented with 10 mM HEPES pH 7.2, 100 μM luciferin, 1 mM sodium pyruvate, 0.035% sodium bicarbonate, 10% FBS, antibiotics, and 2 mM L-glutamine. Bioluminescence monitoring was performed using a LumiCycle (Actimetrics, Inc. Wilmette, IL) to record from each dish continuously for ∼70 s every 10 min using a photomultiplier tube at 37°C.

### *A.7 Virtual Ligand Screen of Repression Inhibitors*

In collaboration with the Cardozo lab at NYU we have virtually screened a 450,000 compound library against a representative CRY2 crystal structure (PDB:4MLP) using ICM-VLS (MolSoft LLC) and found a diverse set of drug-like molecules with favorable fit, logP values, and docking scores. The top 20 hits were purchased from Hit2Lead and dissolved in 100% DMSO to a final concentration of 10 mM compound, aliquoted, and stored at -20°C. Initial hits were analyzed with a GST pull down assay (as described above) co-purified GST-CRY1 his-BMAL1 and untagged CLOCK was immobilized on glutathione beads and incubated

with 400 μM compound overnight at 4°C. Beads were washed with 100 μM compound with 10 column volumes. Protein was released from beads with SDS sample buffer and analyzed by SDS-PAGE and detected by Coomasssie stain.

### *A.8 Idiosyncrasies in CRY Purification*

N-terminal GST-tagged CRY1 and CRY2 PHR can be expressed in suspension insect cell culture with average yields of 1-2 mg/L and 2-4 mg/L, respectively. Despite reasonable expression, CRYs have a fondness for sepharose and agarose affinity resins. During a project not mentioned here, we attempted to complex CRY1 with $G_{\alpha s}$. Despite numerous attempts with individual and co-expression of GST-$G_{\alpha s}$ and hexahis-CRY1, GST-CRY1 and hexahis-Gαs, GST-CRY2 and hexahis-Gαs, not complex was seen in either SEC or GST pull-down assay (with and without GDP or GTPγS. Other purification protocols include for co-expression of GST-CRY1 and hexahis-Gαs: NiNTA agarose, $Co^{2+}$ sepharose, Sepharose Q followed by NiNTA sepharose, Sepharose S followed by NiNTA sepharose appeared to pulldown the complex but was sub-stoichiometric. Curiously, the only strategy that appeared to form a complex was co-expression of GST-CRY1 and hexahis-Gαs followed by a NiNTA sepharose pull-down of hexahis-Gαs, the eluate (300 mM imidazole) was passed through a glutathione sepharose column to capture GST-CRY1. The captured complex could then be eluted with glutathione (10 mM) or cleaved on column in what appeared to be 1:1 stoichiometry. However, when GST-CRY1 alone was purified by NiNTA sepharose first, it was able to not only bind, but elute at high concentrations of imidazole (and not the wash, 25 mM). This negative control demonstrates that CRY-Gαs binding is an artifact of CRY sticking to the NiNTA resin through an unknown mechanism.

# VITA

Shannon is an ugly bag of mostly water that originated in south Florida. She attended the University of Florida and graduated with a B.S. in Neurobiology and Behavior with the naïve belief that she could maybe understand consciousness (she couldn't). She was then accepted into the Department of Pharmacology at the University of Washington to become a pharmacomancer and complete her Ph.D. work on the world's best protein, cryptochrome. Her lifelong ambition has been to facilitate a permanent human presence in space and plans to grow plant-human hybrids on Mars.

Publications:

Nangle, S.N., Rosensweig, C., Koike, N., Tei, H., Takahashi, J. S., Green, C. B., & Zheng, N. (2014) Molecular Assembly of the Period-Cryptochrome Circadian Transcriptional Repressor Complex. *eLife*.

Nangle, S.N., Xing, W., & Zheng, N. (2013) Crystal Structure of Mammalian Cryptochrome in Complex with a Small Molecule Competitor of its Ubiquitin Ligase. *Cell Research*.

Tsai, L., Chan, G., Nangle, S.N., Shimizu-Albergine, M., Jones, G., Storm, D., Beavo, J., & Zweifel, L. (2012) Inactivation of *Pde8b* Enhances Memory, Motor Performance, and Protects Against Age-induced Motor Coordination Decay. *Genes, Brain, and Behavior*.